PL-TR-97-2136

DEVELOPMENT OF A LITHOSPHERIC MODEL AND GEOPHYSICAL DATA BASE FOR NORTH AFRICA

D. I. Doser
G. R. Keller
S. Harder
K. C. Miller
P. J. Dial

University of Texas/El Paso
Department of Geological Sciences
El Paso, TX 79968-0555

20 October 1997

19980324 028

Final Report
(May, 1995-September, 1997)

This technical report has been reviewed and is approved for publication.

Katharine Kadinsky-Cade

KATHARINE KADINSKY-CADE
Contract Manager

Charles P. Pike

CHARLES P. PIKE, Director
Business Management Division

This report has been reviewed by the ESD Public Affairs Office (PA) and is releasable to the National Technical Information Service (NTIS).

Qualified requestors may obtain copies from the Defense Technical Information Center. All others should apply to the National Technical Information Service.

If your address has changed, or you wish to be removed from the mailing list, or if the addressee is no longer employed by your organization, please notify PL/IM, 29 Randolph Road, Hanscom AFB, MA 01731-3010. This will assist us in maintaining a current mailing list.

Do not return copies of the report unless contractual obligations or notices on a specific document requires that it be returned.

REPORT DOCUMENTATION PAGE

1. AGENCY USE ONLY (Leave blank)	2. REPORT DATE October 20, 1997	3. REPORT TYPE AND DATES COVERED Final Report (May 1995-Sept. 1997)

4. TITLE AND SUBTITLE

Development of a Lithospheric Model and Geophysical Data Base for North Africa

5. FUNDING NUMBERS

F 19638-95-C-0104
PE 69120H
PRDENN
TA GM
WU AI

6. AUTHOR(S)

D.I. Doser, G.R. Keller, S. Harder, K.C. Miller, and P. Dial

7. PERFORMING ORGANIZATION NAME(S) AND ADDRESS(ES)

Department of Geological Sciences
University of Texas at El Paso
El Paso, TX 79968-0555

8. PERFORMING ORGANIZATION REPORT NUMBER

9. SPONSORING/MONITORING AGENCY NAME(S) AND ADDRESS(ES)

Phillips Laboratory
29 Randolph Rd.
Hanscom AFB, MA 01731-3010
Contact Manager: Katharine Kadinsky-Cade/VSBS

10. SPONSORING/MONITORING AGENCY REPORT NUMBER

PL-TR-97-2136

11. SUPPLEMENTARY NOTES

12a. DISTRIBUTION/AVAILABILITY STATEMENT

Approved for Public Release, Distribution unlimited

12b. DISTRIBUTION CODE

13. ABSTRACT (Maximum 200 words)

We have collected seismic, geologic gravity and other potential data to develop a model of North African lithosphere via an integrated approach. We have generated a Bouguer gravity map and modeled gravity data along 3 transects. Seismograms from Worldwide Standardized Seismograph Network Stations of magnitude greater than 4.9 earthquakes occurring within North Africa (1963-1988) have also been collected and digitized. The regional waveforms of these seismograms have been used to construct 1-D velocity models across several regions of North Africa. We have collected delay time, travel time, focal mechanism, focal depth and magnitude information for these earthquakes. The data bases and results of our studies may be found at the web site: http://www.geo.utep.edu/nafr/nafr.html

14. SUBJECT TERMS

North Africa
Lithospheric Data Base

15. NUMBER OF PAGES
84

16. PRICE CODE

17. SECURITY CLASSIFICATION OF REPORT	18. SECURITY CLASSIFICATION OF THIS PAGE	19. SECURITY CLASSIFICATION OF ABSTRACT	20. LIMITATION OF ABSTRACT
Unclassified	Unclassified	Unclassified	SAR

Contents

List of Figures

List of Tables

Acknowledgements

Summary

We have collected seismic, geologic, gravity and potential field data to develop a model of the North African lithosphere via an integrated approach. We have modeled the gravity data along three transects across North Africa: 1) from north central Egypt across Libya to the Hoggar Uplift, 2) from central Tunisia across northern Algeria to the Atlantic coast of Morocco, 3) from north central Algeria across the Hoggar Uplift to northern Chad. These transects represent the major propagation paths between earthquakes and nuclear explosions and seismograph stations located within North Africa. The gravity models are constrained wherever possible by geologic and other geophysical information. Crustal thicknesses we have obtained for the Hoggar Uplift (38 km) agree well with preliminary results of seismological studies by other research groups. Our modeling results also suggest that the mantle anomaly under the Hoggar Uplift is relatively small (200 km wide, less than 20 km in vertical extent) compared to mantle anomalies associated with other hot spots and rift zones.

We have used our modeling results in conjunction with other geophysical studies to construct a map of crustal thickness for Africa. In most places away from the continental margin, the crust in North Africa is 35-40 km thick. Crustal thinning is associated with the Sirt Basin and the West and Central African rift system. Moderate crustal thickening (~41 km) is associated with the Atlas Mountains.

In addition to our gravity studies, we have compiled a collection of seismograms from Worldwide Standardized Seismograph Network (WWSSN) stations located at regional distances for magnitude $\geq$ 5.0 earthquakes occurring within North Africa (between 1963 and 1988) and their associated aftershocks. We have selected these earthquake sequences for study since many of the mainshocks have known focal mechanisms determined from teleseismic waveform modeling or first motion studies of regional, teleseismic and/or local network data. Many of the events produced numerous aftershocks of varying magnitudes. We have digitized over 200 regional waveforms from these aftershock sequences. Using the lithospheric models obtained from the gravity modeling as first approximations of the velocity structure, we have modeled the regional waveforms of these earthquake sequences. We have also collected delay time, travel time, source parameter and magnitude information for these sequences for our seismic data base. The entire geophysical and geological data base is available at the web site: http://www.geo.utep.edu/nafr/nafr.html

Introduction

North Africa has been the object of considerable oil exploration and a fair number of papers containing geological interpretations of upper crustal structure have been published. However, very few papers contain basic data which are relevant on the scale of a lithospheric investigation. Our task has been to develop a model of North African lithosphere via an integrated analysis of seismic, potential field, and geologic data. In particular, we have concentrated on constructing detailed 2-D models from known earthquake source regions to key seismic monitoring stations in the region. An outgrowth of this effort is a data base of geological and geophysical information which is available to the scientific community through electronic access.

Although data are sparse in many regions, it is clear that North Africa has experienced a complex evolution (Figure 1). The structure of the lithosphere presently must bear the signature of these tectonic events, and seismic waves propagating through it must be affected. The Pan-African orogeny (750-500 Ma) may represent the time at which the shield areas formed by terrane accretion (Black et al. 1994). This could be similar to the formation of the China region in the Paleozoic and Mesozoic. During the Paleozoic, the Caledonian and Hercynian orogenies affected the region and formed a series of basins and uplifts in a manner similar to the evolution of the midcontinent region of the U.S. during this same period. In the Cretaceous, Africa was subjected to widespread rifting and nearly split apart (Fairhead, 1992). During the Tertiary, the Alpine orogeny affected North Africa, most notably forming the Atlas Mountains. Volcanic centers such as Hoggar and Tibesti formed on topographic uplifts which are believed to related to mantle plumes (Figure 1).

Our approach to constructing a lithospheric model and data base for North Africa has been to integrate information such as well logs, gravity measurements, aeromagnetic surveys, heat flow measurements, and geologic maps to first develop lithospheric models along key profiles in North Africa. We then used these models as a starting point for modeling seismograms at regional distances, refining the models as the seismic data required. In following subsections we describe our data collection process. We then discuss the results of our gravity modeling and analysis. We also present preliminary results of regional seismic waveform modeling and a crustal thickness map for Africa. The appendices describe the data bases we have collected and how they can be accessed electronically.

Methods, Assumptions and Procedures

Geological Data Base

We have digitized the locations of numerous geological features within the North African region to aid in our interpretation of gravity and seismic data. Most of the digitized data comes from about six different geologic/tectonic maps we have collected for North Africa. Other features have been digitized from figures found in professional journals. These features include: surface exposures of Precambrian rocks in the major uplifts, depth to Paleozoic and Mesozoic basement within the Sirt Basin of Libya, surface faults within the Sirt Basin, the location of Pan-African suture zones and Cretaceous and Cenozoic age rifts, and the boundaries of West and Central African rift basins. Maps of these features are shown in Appendix A, along with details on how these outlines can be accessed electronically.
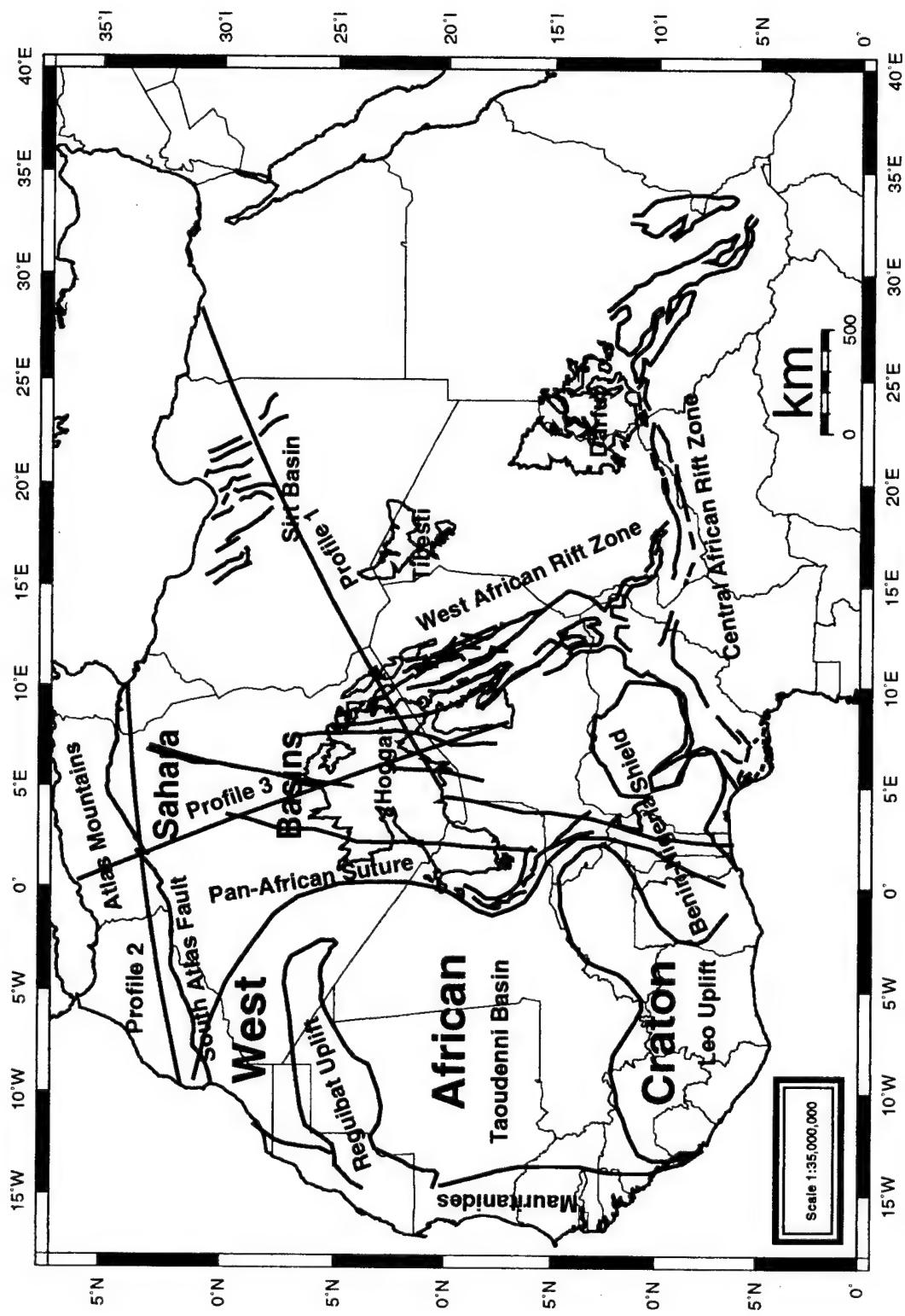
Figure 1. Generalized tectonic map of northern Africa

2

Gravity Data Base

We have collected gravity data from a number of sources. First we began with the unclassified data from the global data base maintained by the Defense Mapping Agency. For these data, we have complete information including elevation and there are over 36,000 data points. To this we have added data from Libya which were compiled by one of our graduate students (Suleiman, 1993). These data (over 5000 points) come from a variety of industrial sources, and thus, complete information is lacking. We do have latitude, longitude, and Bouguer anomaly value (density - 2.67 gm/cc). Details concerning these data are available in Appendix B.

A third and very important set of data was obtained in the form of a 5'x5' Bouguer gravity anomaly grid from GETECH, which is associated with Leeds University. These data are for the region between 0° and 37°N and 12°W and 40°E. We are only free to use these data in the form of maps which are contoured at intervals of 10 mGal or greater. Gravity station locations were also provided so that we can clearly see the constraints that these data provide. In addition, the station elevations were used by GETECH to correct errors in the ETOPO5 topographic data base, and we are using this commercial product in our study. The ETOPO5 data base is available from the National Geophysical Data Center, and the corrected data are directly available from GETECH. We have also obtained a global topographic data base from GETECH called DMT5, which has 5'x5' resolution.

All three data sets have been merged to produce the Bouguer gravity map of Northern Africa (Figure 2). Details on the availability of these data can be found in Appendix B.

Seismic Data Base

We selected a series of magnitude ≥ 5.0 earthquakes and their associated aftershocks occurring between 1963 and 1988 (the major years of operation of the WWSSN) for study (Figure 3, Table 1). Many of the mainshocks have focal mechanisms determined from teleseismic waveform modeling or first motion studies (Table 2). Some sequences produced numerous aftershocks, and we collected data for all events above magnitude 3.5. The data we collected consisted of: 1) location, origin time, arrival time, delay time, magnitude, and first motion information from listings of the International Seismological Centre or the U.S. Geological Survey's Earthquake Data Report, 2) published focal mechanisms, focal depth and other source parameter information determined from teleseismic or local network information, and 3) waveform data copied from microfiche for WWSSN stations located at regional distances from the events of interest.

The event locations, depths, station azimuths and distances, P and S arrival times, P and S delay times, and magnitudes were entered both into a PC based version of the EXCEL spreadsheet/data base software and to an ORACLE data base that is accessible from our North Africa web site. Examples of spreadsheets and other details related to this information are given in Appendix C. Figure 4 shows an example of how we have compared P-wave delay times versus azimuth for events within different regions of North Africa. Figure 4a shows a fairly standard means of depicting the delays for a magnitude 4.5 aftershock of the 1969 northern Red Sea earthquake sequence. Figure 4b shows a plane parallel coordinates plot of the same information, which we believe provides a more "user friendly" approach to viewing delay time and magnitude information. More examples of plane-parallel coordinate plots are found in Appendix C.

We have conducted an extensive search of the literature for focal mechanism information and believe we have collected all available focal mechanisms (Table 2).

3

Figure 2. Bouguer gravity map of North Africa. Contour interval: 20 mGal. Precambrian outline of Hoggar (Algeria), Tibesti (S. Libya), and Darfur (E. Chad and W. Sudan) domal uplifts shown in dark black. Locations of three crustal-scale gravity profiles also shown in white.

4
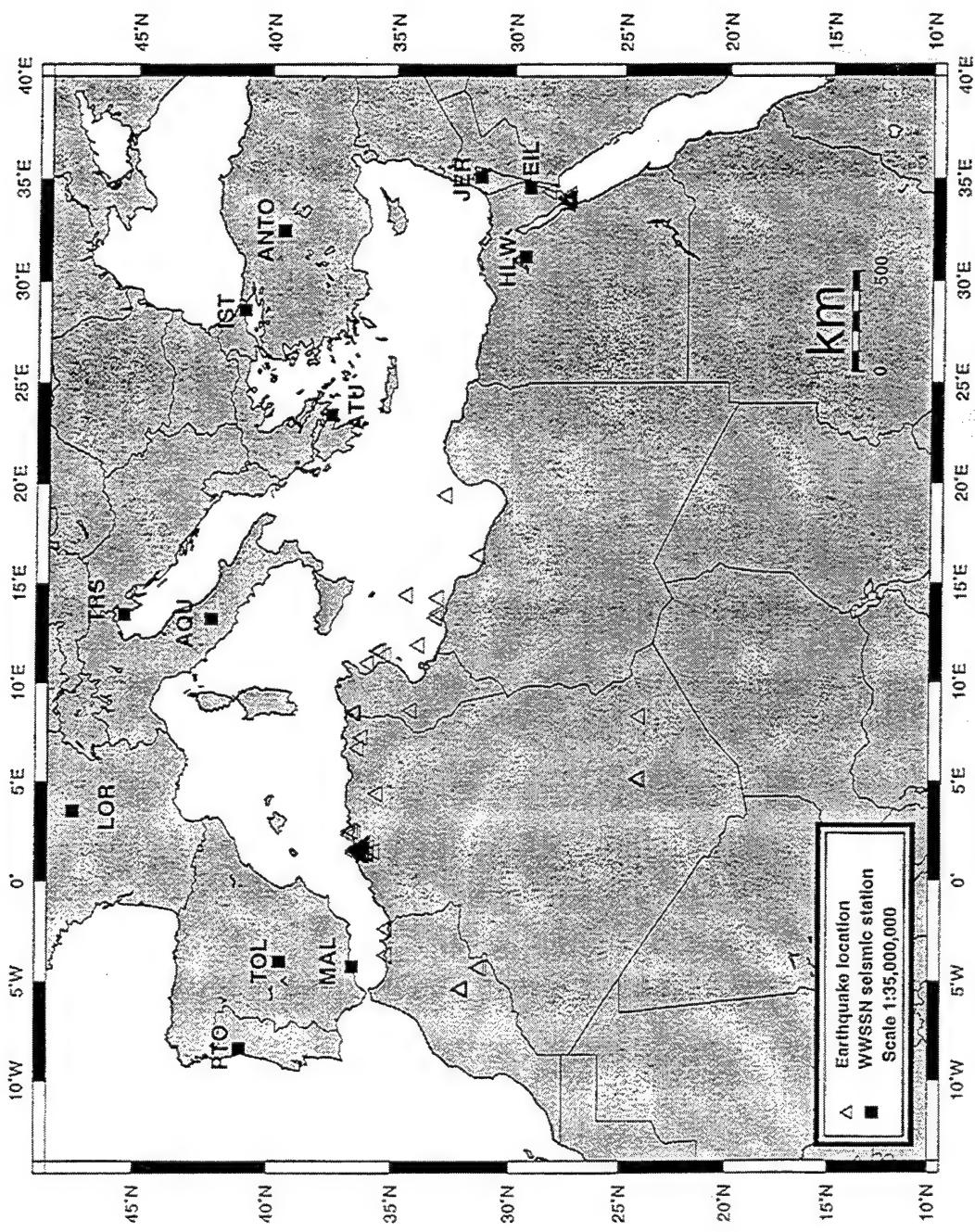
Figure 3. Magnitude ≥ 5.0 earthquakes (triangles) of North Africa (1963-1988). Labeled squares represent locations of WWSSN stations operating during the period of interest.

5

Table 1. Seismic Events (1963-1988) in North Africa of Interest to This Study

Date		Time	Magnitude	Location
Feb. 21,	1963	1724	5.0	Gulf of Sidra
May 11,	1963	0110	5.8	Gulf of Sidra
Oct. 20,	1963*	1259	5.6	French nuclear test
Jan. 1,	1965*	2138	5.0	M'Sila, Algeria
Jan. 26,	1967	1611	5.1	Tunisia
July 13,	1967	0210	5.0	Algeria
Apr. 17,	1968*	0912	5.1	Boudinar, Morocco
Mar. 24,	1969*	1154	5.2	N. Red Sea, Egypt
Mar. 31,	1969	0715	6.0	N. Red Sea, Egypt
Mar. 31,	1969	2142	5.0	N. Red Sea, Egypt
Apr. 8,	1969*	1031	5.2	N. Red Sea, Egypt
Apr. 16,	1969*	0812	5.0	N. Red Sea, Egypt
Apr. 23,	1969*	1337	5.0	N. Red Sea, Egypt
Dec. 1,	1970	0102	5.2	Tunisia
Jan. 12,	1970	0815	5.1	N. Red Sea, Egypt
Sept. 2,	1972	1453	5.3	Gulf of Sidra
June 28,	1972	0949	5.5	N. Red Sea, Egypt
Nov. 24,	1973	1405	5.1	Algeria
Nov. 24,	1973	1522	5.3	Algeria
April 29,	1974	2004	5.0	Nile Delta, Egypt
Sept. 4,	1974	0629	5.5	Tripoli, Libya
Dec. 9,	1976	2121	5.2	Tripoli, Libya
Jan. 1,	1977	2046	5.7	A'in Soltane, Tunisia
Dec. 9,	1978	0713	5.3	W. Egypt
Oct. 10,	1980	1539	6.1	El Asnam, Algeria
Oct. 10,	1980+	1733	5.2	El Asnam, Algeria
Oct. 10,	1980+	1908	5.0	El Asnam, Algeria
Oct. 13,	1980+	0637	5.0	El Asnam, Algeria
Oct. 14,	1980+	1734	5.0	El Asnam, Algeria
Oct. 30,	1980+	2338	5.1	El Asnam, Algeria
Nov. 8,	1980+	0754	5.1	El Asnam, Algeria
Dec. 7,	1980	1737	5.1	El Asnam, Algeria
Dec. 12,	1980	1332	4.8	El Asnam, Algeria
Jan. 15,	1981	0425	5.1	El Asnam, Algeria
Feb. 1,	1981	1320	5.2	El Asnam, Algeria
Oct. 27,	1985+	1934	5.7	Constantine, Algeria
Mar. 26,	1988+	1207	5.1	Gulf of Sirt, Libya

*Seismograms for this event have been digitized.
+Seismograms for this event have been digitized and modeled. See Appendix D.

Table 2. Focal Mechanisms for M≥5.0 North African Earthquakes (1963-1988)

Date	Mechanism strike,dip,rake	Data Used	Reference
Feb. 21, 1963	243,75,90	first motion	McKenzie (1972)
Jan. 1, 1965	70,65,68	first motion	McKenzie (1972)
July 13, 1967	167,30,90	first motion	McKenzie (1972)
Mar. 31, 1969	330,50,5	waveforms	Ben-Menahem et al. (1976)
	325,50,-40	first motion	McKenzie et al. (1970)
Jan. 12, 1972	8,86,-10	waveforms	Pearce (1980)
June 28, 1972	350,80,10	waveforms	Pearce (1977)
Apr. 29, 1974	310,47,-17	waveforms	Ben-Menahem et al. (1976)
Sept. 4, 1974	297,37,-141	waveforms	Westaway (1990)
Oct. 10, 1980	225,54,83	waveforms	Deschamps et al. (1982)
Oct. 30, 1980	42,40,72	first motion	Yielding et al. (1989)
Nov. 8, 1980	41,64,75	first motion	Yielding et al. (1989)
	50,30,97	first motion	Ouyed et al. (1983)

7
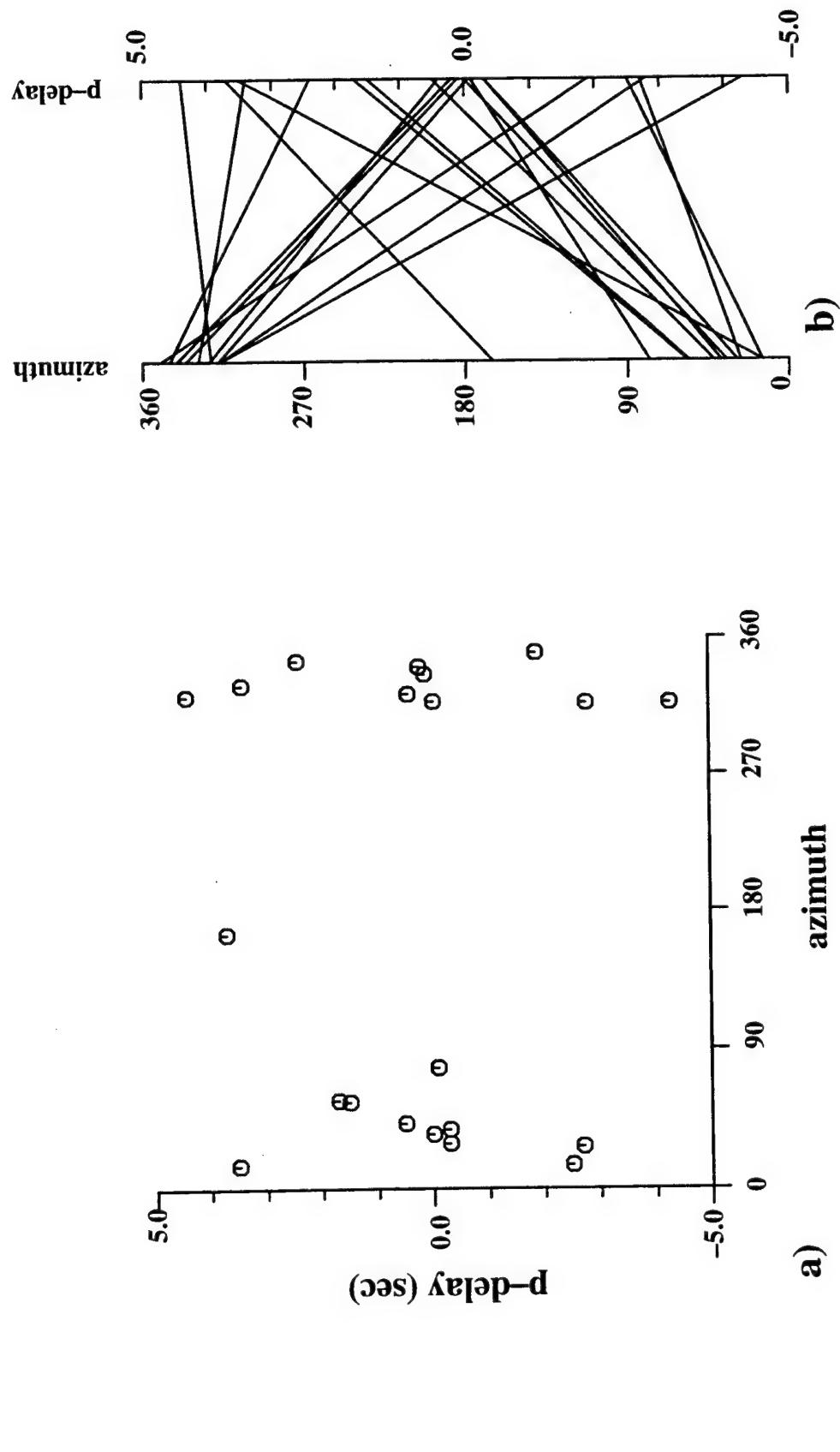
Figure 4. a) Plot of P-wave delay time (observed minus predicted arrival time from listings of the International Seismological Centre) versus azimuth from event to station for an aftershock of the 1969 northern Red Sea earthquake sequence. b) Plane parallel coordinate plot of same information.

All regional waveform data that were available have been collected. We have digitized 204 acceptable seismograms (Appendix D). Figure 5 shows an example of an M=5.0 aftershock of the October 1980 El Asnam sequence recorded at Toledo, Spain (TOL) located at 625 km from the event. During the second year of the research we have been modeling these waveforms to validate and update the preliminary lithospheric models obtained from the gravity data. To date, we have modeled 88 waveforms recorded at WWSSN seismic stations PTO, TOL and MAL (all located on the Iberian Peninsula) from aftershocks of the 1980 El Asnam, Algeria earthquake sequence. We have employed reflectivity techniques (Randall and Taylor, written comm., 1993) in this modeling process.

Results and Discussion

Gravity Modeling

Once we had merged the GETECH data into our existing database, we selected three profiles across the region to model (Figure 2). These profiles represent important propagation paths between earthquakes and seismograph stations located within North Africa. Profile 1 extends from central Egypt, the site of several recent earthquakes and seismograph stations (such as HLW), across central Libya, where we have good geological and geophysical control on crustal structure (e.g. Suleiman, 1993; Nyblade et al., 1996), to the Hoggar Uplift of southern Algeria (site of station TAM, Tamanrasset, and several French nuclear tests in the early 1960's). Profile 2 extends across the Atlas Mountains from the Atlantic coast of Morocco to central Tunisia. Seismograph stations are located along this profile in Morocco, Algeria and Tunisia, and earthquakes occur throughout the region. Profile 3 extends from north central Algeria across the Atlas Mountains to the Hoggar uplift. This profile is along the propagation path between northern Algerian earthquakes and TAM. A preliminary velocity model has been obtained by McNamara et al. (1996) from regional seismograms whose waves propagate along paths that parallel Profile 3.

The density model we have obtained for Profile 1 is shown in Figure 6. The upper part of our model reflects the basin structure of Egypt, Libya and Algeria obtained from published geological and geophysical studies of these basins (e.g. Goudarzi, 1980; van der Meer and Cloetingh, 1993; Guirard and Maurin, 1992; Exxon, 1985), primarily related to their petroleum potential. Since our knowledge of the upper crust below the sedimentary basins and the lower crust is poor, we have treated these units as having uniform densities. We have chosen to model the lower crust with density of 3.0 g/cc, upper crust with density 2.70 g/cc, and mantle with density 3.30 g/cc. These densities were chosen as average continental density values where we have little velocity constraint on the crust. We varied thicknesses of these units only as required to match the long wavelength features of the observed gravity data. Note that we have not attempted to match every short wavelength feature of the profile, since our knowledge of the shallow geology is incomplete. Geologic knowledge in these regions below about 3 km is sparse, and below 5 km is vague or completely lacking. We have used information from detailed regional studies, where available (Hoggar, Sirt Basin), and continental-scaled geologic/tectonic maps and resources elsewhere. The shallow geology also should influence regional waveform propagation less than the deeper crustal structure.

Profile 1 shows a relatively uniform boundary between the upper and lower crust. There is a gradual shallowing of the crust/mantle boundary between the Hoggar Uplift (38 km) and the Egyptian coast of the Mediterranean (26 km) (Sweeney, 1995). A similar eastward shallowing of the crust/mantle boundary is observed in northern

9
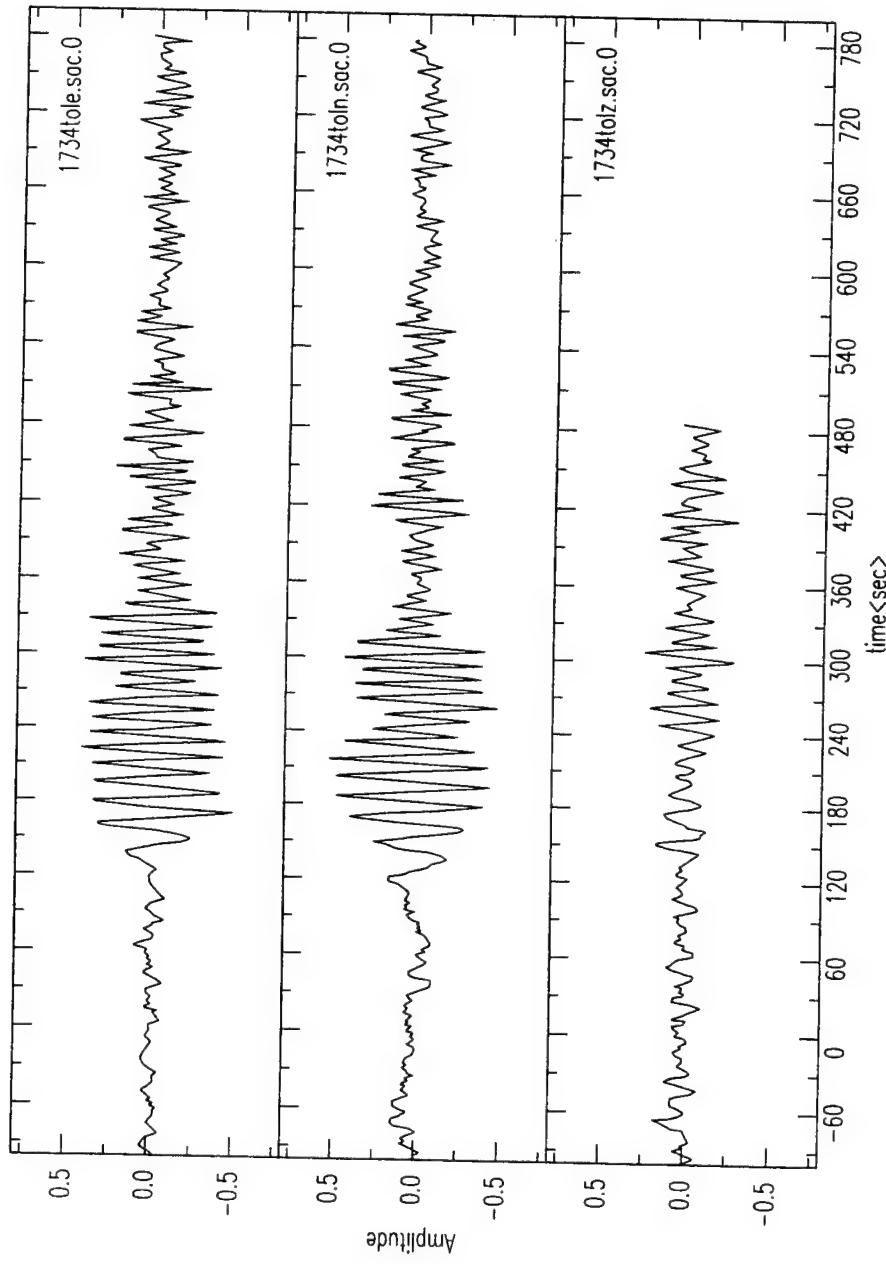
Figure 5. Seismograms of magnitude 5.0 aftershock of the October 1980 El Asnam, Algeria, earthquake sequence. Seismograms was recorded on the long-period vertical instrument operating at Toledo, Spain (TOL). Top trace is eat-west, middel trace is north-south, bottom trace is vertical.

10
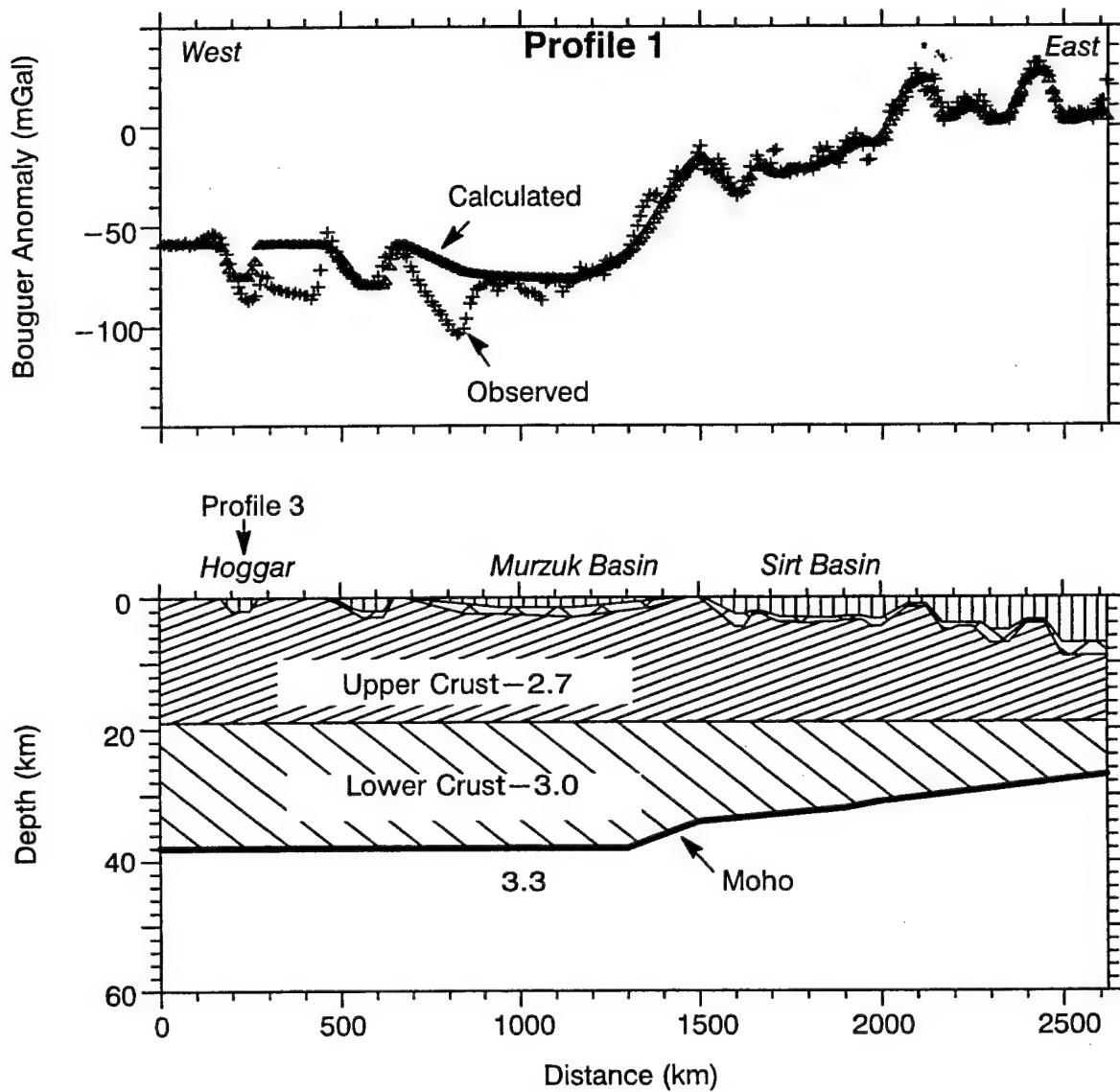
Figure 6. Interpretation of gravity data along Profile 1 trending West-East from Hoggar domal uplift (Algeria) to Mediterranean coastline (Egypt) (total length=2620 km). Above: Observed and calculated gravity values for each station along profile. Below: Crustal model used to generate calculated gravity values. Moho discontinuity shown in bold. Numbers are densities for the bodies (g/cc). Upper two units which are not labeled are Mesozoic and Paleozoic sedimentary rocks with densities of 2.5 g/cc and 2.6 g/cc, respectively.

11

Libya (Suleiman, 1993). The crustal thickness of the Hoggar Uplift is in good agreement with the velocity model of McNamara et al. (1996) and recent receiver function studies at TAM (E. Sandoval, pers. comm., 1996).

The zone between approximately 280 - 400 km shows a very poor match between the observed and calculated gravity values. We have not tried to model the observed anomaly because no gravity stations exist in this area of the gravity data set. The same holds true between 600 - 820 km and 1220 - 1350 km along Profile 1. These areas correspond to the least well modeled anomalies. The shallow geologic structure (<5 km) in the Hoggar, Murzuk and Sirt Basins is very well constrained. In these regions we feel that the local anomaly is best accounted for and that we can reasonably test the response of our model to deeper structure.

Profile 1 (Figure 6) intersects Profile 3 (Figure 7) at a distance of 250 km. Both profiles have a total crustal thickness of 38 km at this point and all layers are of the same thickness. The profiles cross in the northern section of the Illumeden Basin where the thickness of Mesozoic and Cenozoic sediments are well constrained (Tectonic Map of the World, 1985). Within the Sirt Basin and the Mediterranean platform (2150-2620 km, Profile 1) we have modeled a series of horsts and grabens. The horst and graben structure resulting from Cretaceous rifting is well known in the Sirt Basin (Goudarzi, 1980; Suleiman, 1993). This type of structure appears to occur on the Mediterranean platform as well, as suggested by the series of gravity highs and lows seen in this region.

Figures 7 and 8 show interpretations of Profile 3. The shallow upper crustal structure is constrained from knowledge of basin geometries and thicknesses (e.g. Schurmann, 1974; UNESCO, 1971; Lesquer et al., 1988). The Moho depth at the northern end of the profile is constrained by the results of the European Geotraverse (Ansorge et al., 1992). The crust appears to rapidly thicken beneath the Atlas Mountains, then gradually thicken to the south. Recent seismic refraction studies (e.g. Wigger et al., 1992) have modeled the Atlas Mountains with an asymmetric root extending only to 38 km depth in the north. The discrepancy between our results and the refraction studies may results from low mantle velocities (7.7 - 7.8 km/sec) detected in the refraction studies. These low mantle velocities suggest that the mantle density may be less than 3.30 g/cc. Again, the Hoggar Uplift can be modeled with a 38 km thick crust. This is much smaller than observed under the Ethiopian and Kenya domes.

Figure 7 is a density model without an upwelling mantle plume beneath the Hoggar, while Figure 8 shows the same density model with an upwelling mantle plume added. Note that there are zones along the profile with poor matches between observed and calculated anomalies. The zones between 950 - 1050 km , 1055 - 1200 km, and 1525 - 1775 km contain no gravity stations. Thus, we have not tried to model the observed anomalies in these areas. Profile 3 intersects both Profile 1 in the south and Profile 2 in the north (Figure 2). Where the profiles intersect, the layer thicknesses have been kept constant. Figure 8 shows that a mantle plume with a density of 3.20 g/cc extending horizontally for only 200 km and vertically from 38 to 58 km depth is all that is necessary to model the observed gravity anomaly of the Hoggar.

Between 1000 and 1900 km lie the Sahara Basins which include the Illizi and Mouydir Basins along with the interbasin divides. Depth to the Precambrian bedrock is well constrained within this area of Algeria (Schurmann, 1974). At 1900 km lies the South Atlas fault, separating the Atlas Mountains to the north from the Sahara platform to the south. The structure of the fault is not well studied. It is believed to be either a near-vertical reverse fault reactivated in the Alpine Orogeny or a complex boundary zone where lower angle thin-skinned thrust faulting penetrates into the Saharan domain (Outtani et al., 1995). The former view is more widely accepted and we have chosen to model the fault in this manner.

12
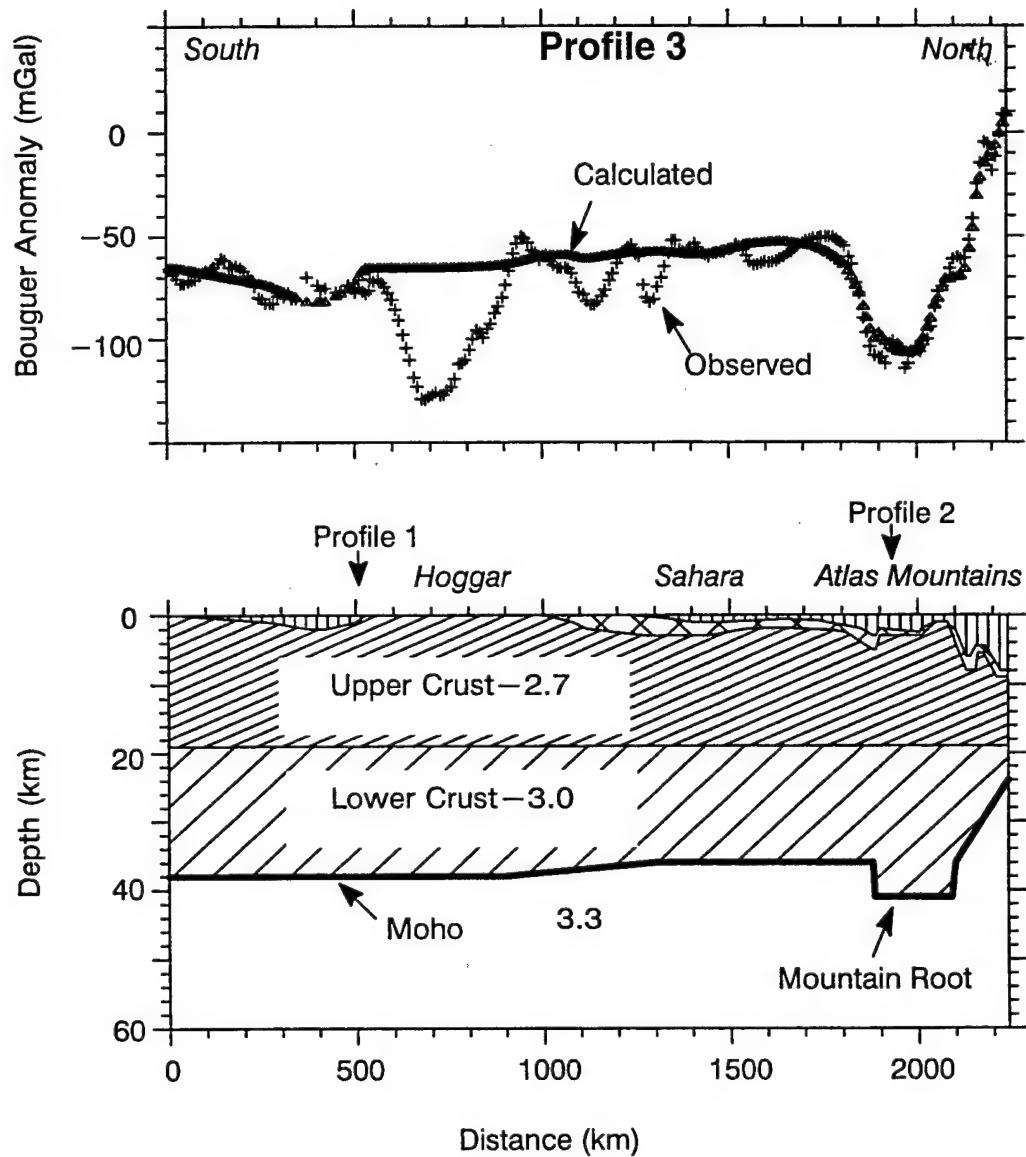
Figure 7. Interpretation of gravity data along Profile 3 trending South-North from Air massif (Niger) to Mediterranean coastline (Algeria) (total length=2240 km). Above: as in Figure 6. Below: as in Figure 6, with no mantle upwelling beneath Hoggar uplift.
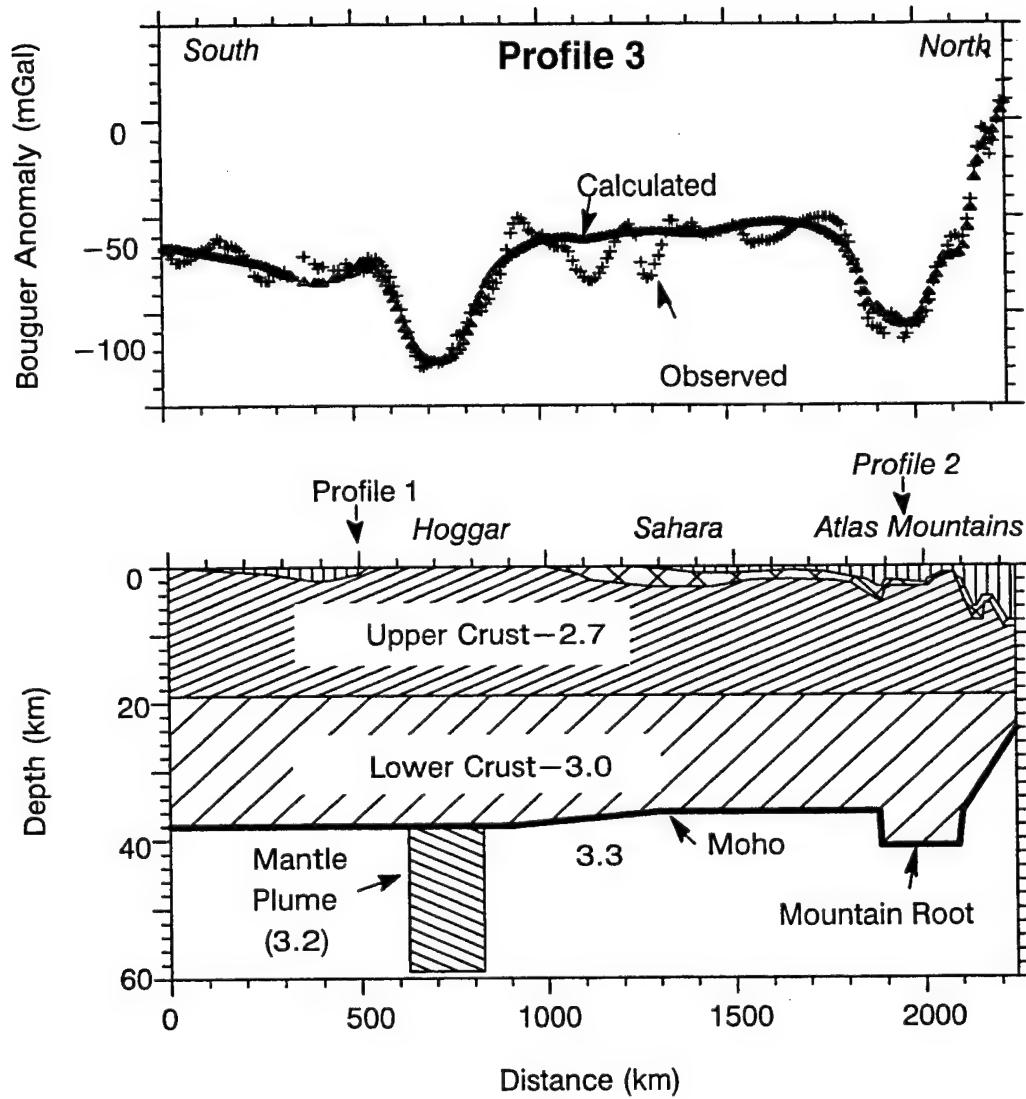
Figure 8. Interpretation of gravity data along Profile 3 trending South-North from Air massif (Niger) to Mediterranean coastline (Algeria) (total length=2240 km). Above: as in Figure 6. Below: as in Figure 6, with mantle plume beneath the Hoggar uplift.

14

The Atlas Mountains are a Tertiary feature which contains Precambrian basement uplift as modeled. We have modeled the mountain root to be 41 km in depth to match the observed gravity low. Previous seismic studies have modeled the crust of the High Atlas Mountains in Morocco to be 38 km thick. Profile 3 crosses the Atlas Mountains in north central Algeria where the range is about 2 km lower in elevation. The apparent discrepancy in crustal thickness values between our gravity models and the seismic studies may be the result of low mantle velocities which are not accounted for with our mantle density of 3.3 g/cc. We may choose to model this area in the future with a lower mantle density value to examine the effects. North of the Atlas Mountains are thrust nappes emplaced in the Tellian Atlas during the Alpine orogeny. One thrust nappe is modeled in Profile 3 between 2150 and 2240 km. The gravity high produced by the model matches the observed anomaly well.

Profile 2 (Figure 9) extends for 1840 km in an east-west direction across the approximate center of the Atlas Mountains. The profile stretches from the Atlantic coast of Morocco to the Mediterranean shoreline of Tunisia. Crustal thickness is only 31 km along the west coast of Morocco near the Atlantic, but quickly thickens to 41 km beneath the High Atlas of Morocco beginning at about 275 km and extending to a distance of 1125 km. Here, the crust begins to thin as the Mediterranean platform is crossed, where Paleozoic and younger sediments reach thicknesses of 9 km at 1840 km. In the High Atlas Paleozoic strata outcrop from 75-200 km along the profile. The crust thins from 36 km at 1150 km to 34 km at 1450 km across this part of the Saharan Atlas. Crustal thickness remains at 34 km to 1750 km along the profile, after which it quickly thins to a minimum of 28 km entering into the Mediterranean platform. Profile 3 is intersected at 1150 km where the crust is 36 km thick beneath the eastern margin of the Saharan Atlas. No gravity stations are present between 775 and 830 km, thus this portion of the profile was not modeled. The isolated gravity high between 1450 and 1600 km is likely due to a shallow intrusive body that has not been documented in the geological/geophysical literature available for this region.

Gravity Filtering

Along with the construction of three lithospheric gravity profiles, we have undertaken wavelength filtering of the gravity data. In gravity data the longer wavelength anomalies are caused by deeper, regional structure, while the shorter wavelength anomalies are caused by shallower, localized geologic structure. Figure 9 and 10 show the gravity data filtered to retain only wavelengths longer than 100 km (Figure 9) and 200 km (Figure 10). In Figure 9 the distinct anomalies associated with the rifted basins of the Central and West African Rift System (CWARS) are still evident. Another distinct feature on the figure is an anomaly which approximately follows the trace of the Pan-African sutures where the WAC and Sahara craton are joined. In Figure 10, sharp anomalies can no longer be associated with the individual aspects of the CWARS system, although higher gravity values still exist beneath the central arm of the CWARS, suggesting that the mantle is likely less dense. The anomaly associated with the Pan-Africa suture is no longer evident and the gravity lows associated with the main domal uplifts are subdued.

Crustal Thickness Map

Figure 11 shows a map of crustal thickness based on an integrated analysis of the limited seismic constraints and Bouguer gravity data. Note that the crust is generally 35-40 km thick away from the continental margins. There is a moderate amount of crustal thickening associated with the Atlas Mountains. Crustal thinning is associated with the
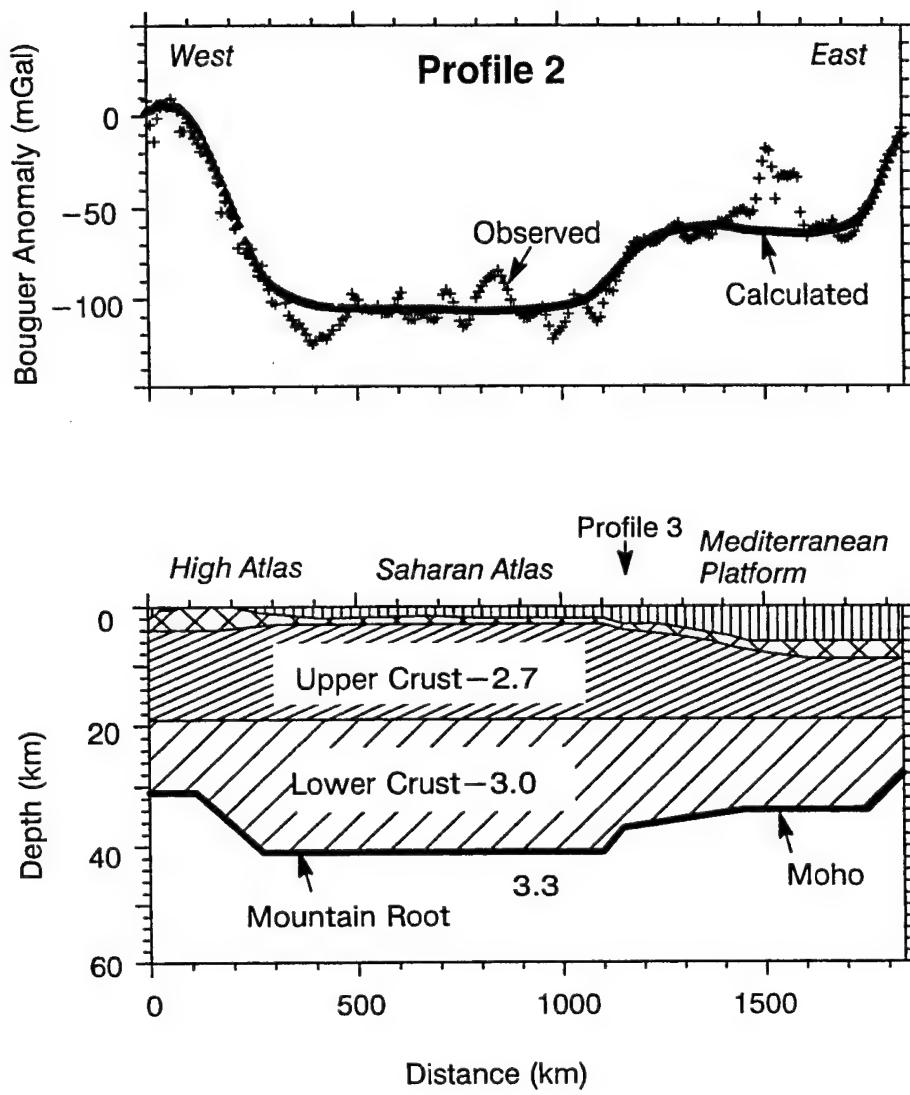
Figure 9. Lithospheric model for Profile 2 (western Morocco to northern Algeria). Numbers are densities in g/cc. Upper two units are as in Figure 6.

16
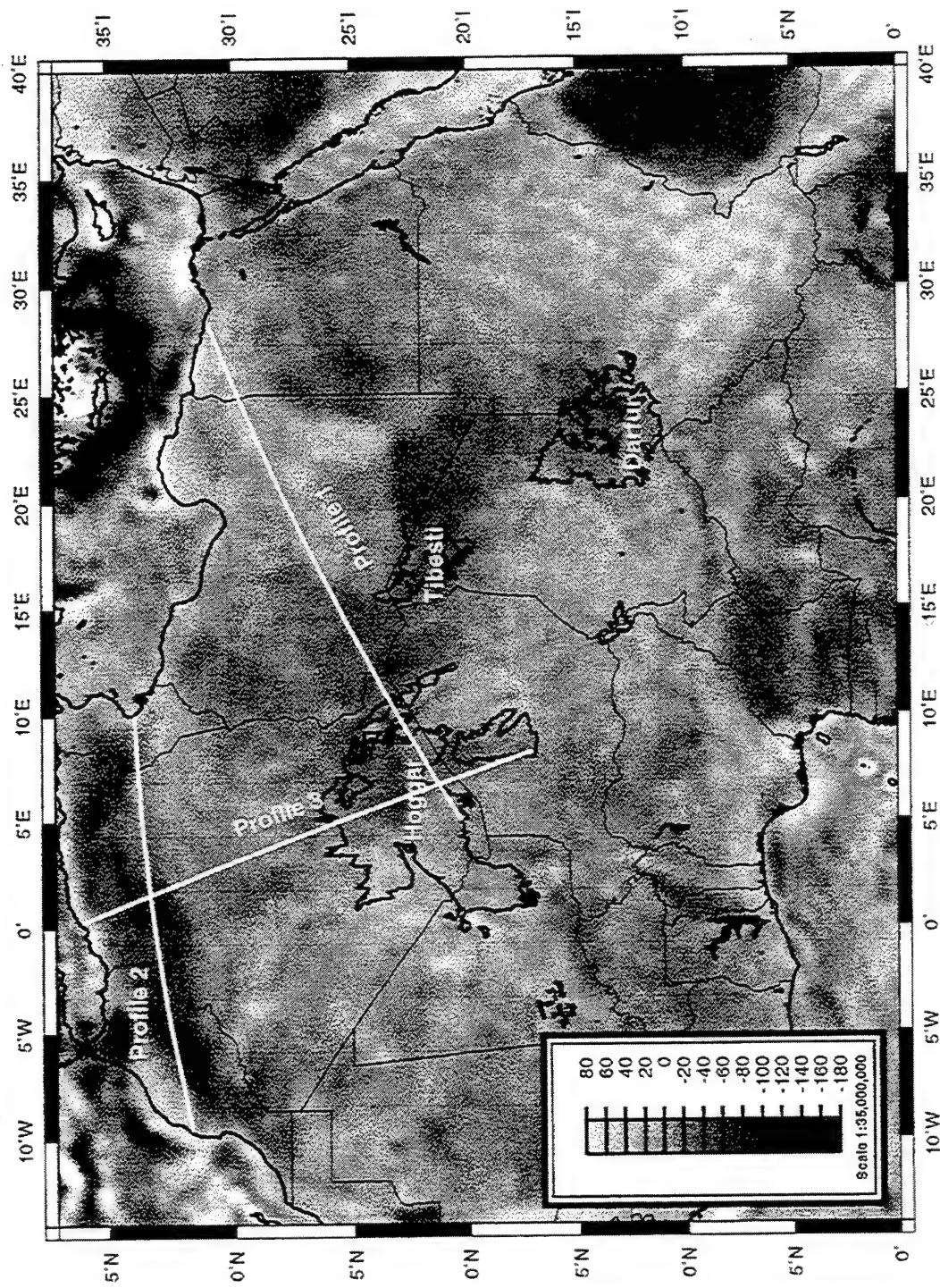
Figure 10. Filtered Bouguer gravity map of northern Africa. Wavelengths > 100 km passed.

17
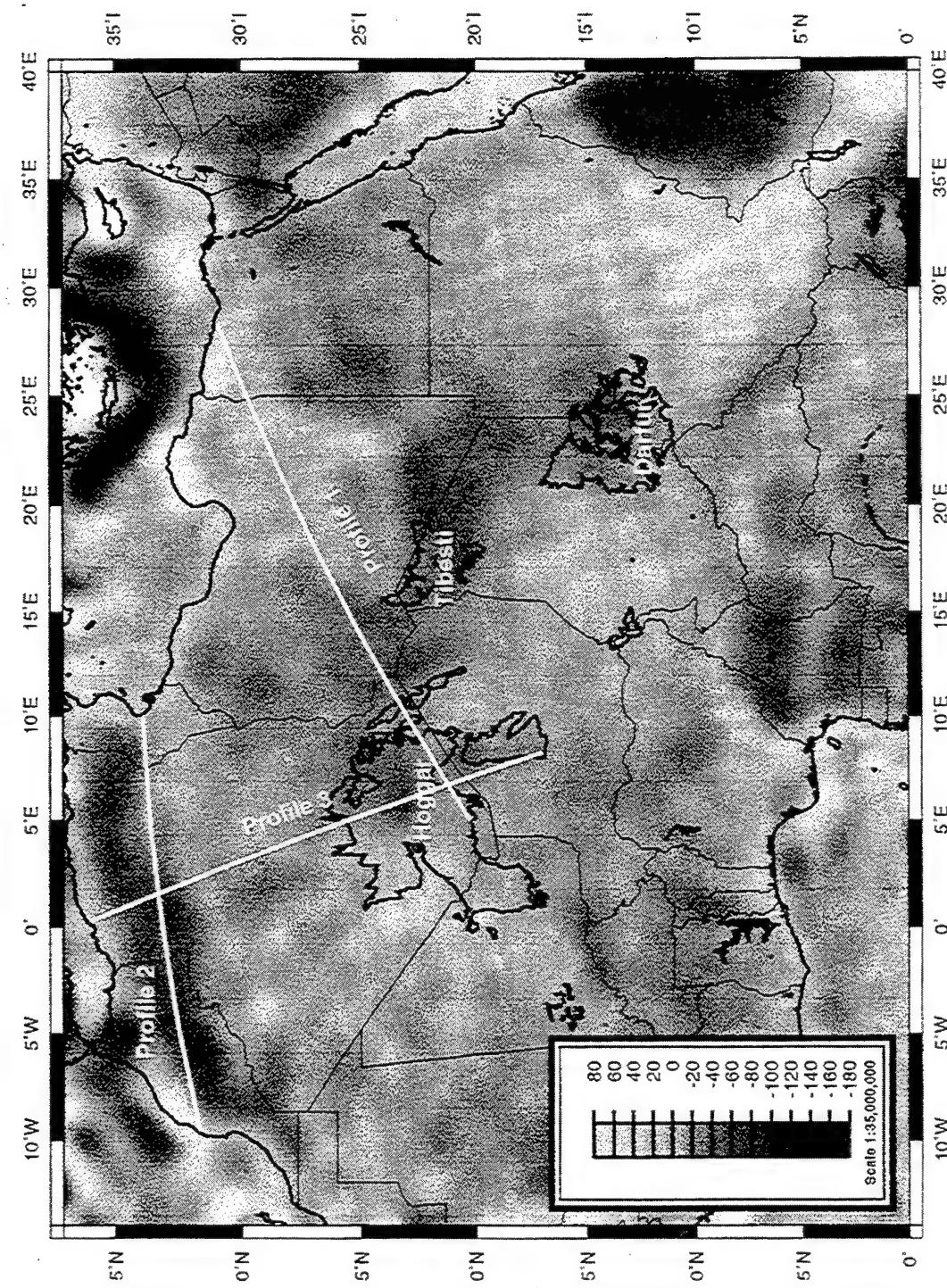
Figure 11. Filtered Bouguer gravity map of northern Africa. Wavelengths > 200 km passed.
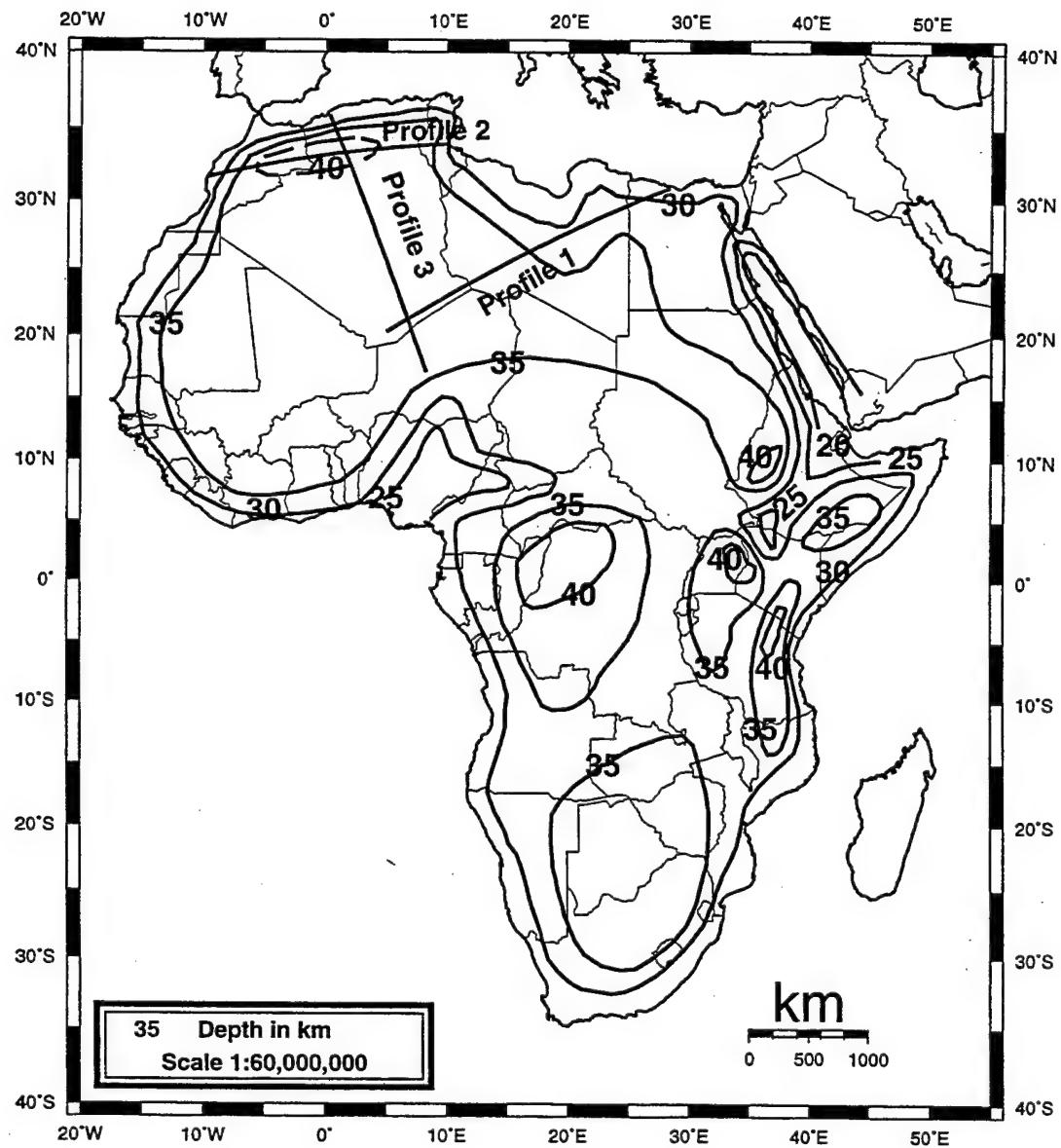
Figure 12. Crustal thickness map of Africa. Contour interval is 5 km.

Sirt Basin and the West and Central African rift system and the adjacent Cameroon line. The lack of a major crustal anomaly associated with the domal uplifts such as the Hoggar is surprising, and may suggest that the domal uplifts of Hoggar, Tibesti, and Darfur represent rising, less dense mantle more than crustal thickening. Locations of the three gravity profiles are shown in Figure 12. Note that they span the approximate northern third of the African continent. Crustal thickness determination in this area is our main contribution to this map. The thinnest crust of the African continent lies along the Red Sea rift (about 20 km). The thickest areas of North African crust appear to be in the WAC area surrounding the Hoggar. Since none of our profiles cross the WAC, we can only say that the crustal thickness of this region should be greater than 40 km, based on our modeling across the Hoggar region where some crustal thinning has probably taken place. Gravity profiles 2 and 3 indicate that the Atlas Mountains may have a root extending to a depth of 41 km.

Modeling of Regional Seismic Waveforms

Our seismic waveform modeling has included modeling of the entire regional wavetrain from P through to S waves. We have collected over 300 records and digitized over 200 records of seismic events occurring from 1963 to 1988 which were recorded at 12 WWSSN seismic stations (Figure 3). We are using older events in our study in order to focus on areas with little recent seismicity (post-1985) and/or to gain propagation paths not covered by more recent digital stations. The events selected were all above magnitude 5.0 and most contained numerous aftershock sequences. Many of the mainshocks have focal mechanisms determined from teleseismic waveform modeling or first motion studies (Table 2).

In order to model regional waveforms we first developed a preliminary 1-D velocity model (Figure 13) based upon our gravity modeling studies and previous geophysical studies (Seber et al., 1996; Sakia et al., 1996). The preliminary 1-D model was input into a reflectivity code (Randall, 1989) to produce synthetic seismograms which could be compared to the observed seismograms. Through a trial and error approach, the best 1-D model was developed to create synthetic seismograms similar to the observed seismograms. At this point in our study we are trying to get the best match to the full regional waveform from our 1-D models.

Our initial modeling results are for 88 observed seismograms at WWSSN stations TOL, MAL and PTO located on the Iberian Peninsula. These events are all part of the 1980 El Asnam, Algeria aftershock sequence (see Appendix D for waveforms). MAL is located ~500 km from the seismic events, while TOL and PTO are located 650 to 1000 km for the epicenters. Over 90% of the synthetic seismograms required a shift of less than 10 seconds to match the initial portion of the waveform. Our initial model contained four layers and a total crustal thickness of 35 km (Figure 13, top). For station MAL we have revised this 1-D model to have 4 layers with a total crustal thickness of 30 km (Figure 13, bottom). Models for stations TOL and PTO still seem to be best modeled with a total crustal thickness of 35 km. We have been able to match the early part of the waveform (P,PL) well, but the models severely mismatch the surface wave amplitudes. Much of this problem is related to the oceanic Mediterranean crust blocking surface wave propagation. We have also noticed large amounts of energy on the tangential component. This probably reflects backscattering from structural changes along the propagation path and/or dipping layers.

We will continue to revise these 1-D velocity models and begin investigating other propagation paths across the Mediterranean and North Africa. We will use events from the Hoggar region (including French nuclear tests) recorded at stations bordering the Red Sea to investigate the structure of gravity Profile 1. We will also investigate
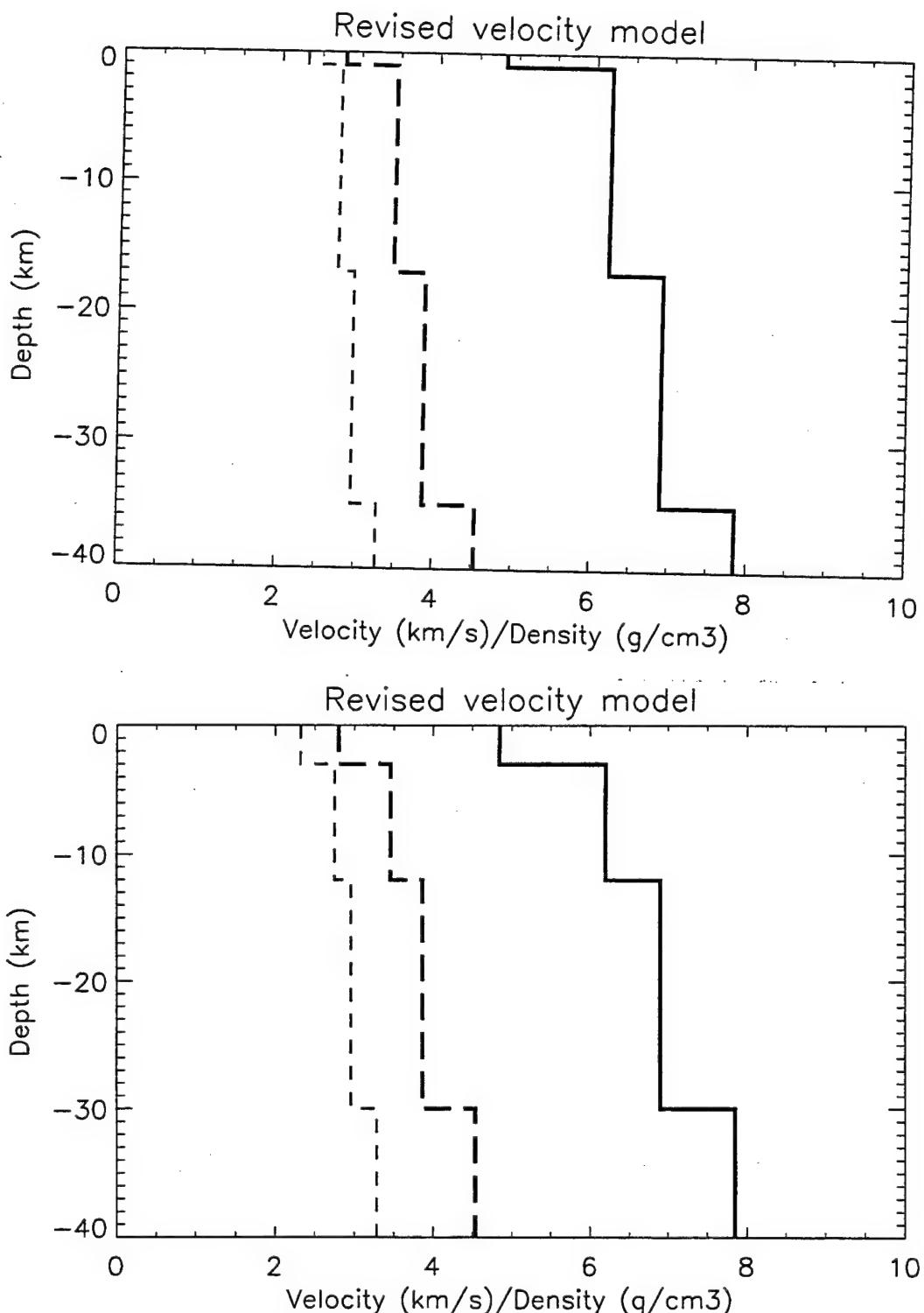
Figure 13. One-dimensional velocity models for TOL and PTO (top) and MAL (bottom). Bold dashed line is S-wave velocity, bold solid line is P-wave velocity. Fainter dashed line is density.

21

propagation paths near gravity profile 3 to test the structure modeled there. We have records from some events in northern Libya and in the Mediterranean Sea north of Libya which were recorded at stations on the Iberian Peninsula to the west and near the Red Sea to the east. We plan to investigate these paths for 2-D structure using a finite-difference code (Sandmeier, 1990) after we have determined the best averaged 1-D structure for this region.

Conclusions

Modeling of regional seismic phases will continue throughout the next year, as P. Dial, who is currently supported as a teaching assistant, completes the modeling as part of his dissertation research. Geophysical and geological data bases that we have collected for North Africa are available via our internet web site: http://www.geo.utep. edu/nafr/nafr.html.

References

Ansorge, J., D. Blundell, and St. Mueller, 1992. Europe's lithosphere-seismic structure, in A Continent Revealed: The European Geotraverse, D. Blundell, R. Freeman and St. Mueller (eds.), Cambridge University Press, 33-69.

Ben-Menahem, A., A. Nur, and M. Vered, 1976. Tectonics, seismicity and structure of the Afro-Eurasian junction - the breaking of an incoherent plate, Phys. Earth and Planet. Inter. 12, 1-50.

Black et al., 1994. Pan-African displaced terranes in the Tuareg shield (central Sahara), Geology 22, 641-644.

Dautria, J. M., and A. Lesquer, 1989. An example of the relationship between rift and dome: recent geodynamic evolution of the Hoggar swell and its nearby regions (Central Sahara, Southern Algeria and Eastern Niger), Tectonophysics 153, 45-61.

Deschamps, A., Y. Gaudemer, and A. Cisternas, 1982. The El Asnam, Algeria, earthquake of 10 October 1980: multiple-source mechanism determined from long-period records, Bull. Seismol. Soc. Am., 72, 1111-1128.

Exxon Basin Analysis Section, 1985. Tectonic Map of the World, 1:10,000,000.

Fairhead, D. 1992. A plate tectonic setting for Mesozoic rifts of west and central Africa, Tectonophysics 213, 141-151.

Genik, G. J., 1992. Regional framework, structural and petroleum aspects of rift basins in Niger, Chad and the Central African Republic (C.A.R.). In: P.A. Ziegler (ed.), Geodynamics of Rifting, Vol. II. Case History Studies on Rifts: North and South America and Africa, Tectonophysics 213, 169-185.

Goudarzi, G. H., 1980. Structure-Libya, in The Geology of Libya, Volume III, 879-892.

Guirard, R. and J.-C. Maurin, 1992. Early Cretaceous rifts of western and central Africa: an overview, in P.A. Ziegler (ed.), Geodynamics of Rifting, Volume II, Case History Studies on Rifts: North and South America and Africa, Tectonophysics 212, 153-168.

Kirton, M., and A. Bourennani, 1984. Geophysics as an aid to geological mapping - a case history from the Hoggar region of Algeria, Exploration Geophysics 15, 179-186.

Lesquer, A., A. Bourmatte, and J. M. Dautria, 1988. Deep structure of the Hoggar domal uplift (central Sahara, south Algeria) from gravity, thermal and petrological data, Tectonophysics, 152, 71-87.

Lesquer, A., D. Takherist, J. M. Dautria, and O. Hadiouche, 1990. Geophysical and petrological evidence for the presence of an "anomalous" upper mantle beneath the Sahara basins (Algeria), Earth and Planet. Sci. Lett. 96, 407-418.

McKenzie, D., 1972. Active tectonics of the Mediterranean region, Geophys. J. Roy. Astron. Soc. 30, 109-185.

McKenzie, D.P., D. Davies, and P. Molnar, 1980. Plate tectonics of the Red Sea and East Africa, Nature 226, 242-248.

McNamara, D. E., W.R. Walter, C. Schultz and G. Goldstein, 1996. Regional phase propagation in Northern Africa and the Mediterranean (abstract), Seismol. Res. Lett. 67, 47.

Nyblade, A.A., I.S. Suleiman, R. Roy, B. Pursell, A.S. Suleiman, D.I. Doser, and G.R. Keller, 1996, Terrestrial heat flow in the Sirt Basin, Libya, J. Geophys. Res. 101, 17,737-17,746.

Outtani, F., B. Adoum, E. Mercier, D. Frizon de Lamotte, and J. Andrieux, 1995, Geometry and kinematics of the South Atlas Front, Algeria and Tunisia, Tectonophysics 249, 233-248.

Ouyed, M., G. Yielding, D. Hatzfeld, and G. King, 1983. An aftershock study of the El Asnam (Algeria) earthquake of 1980 October 10, Geophys J. Roy. Astr. Soc. 73, 605-639.

Pearce, R. G., 1977. A study of earthquake modelling with applications to the East African Rift System, Ph.D. Dissert., University of Newcastle upon Tyne.

Pearce, R. G., 1980. Fault plane solutions using relative amplitudes of P and surface reflections: Further studies, Geophys. J. Roy. Astr. Soc. 60, 459-487.

Randall, G.E., 1989. Efficient calculation of differential seismograms for lithospheric receiver function, Geophys. J. Int. 99, 469-481.

Research Group for Lithospheric Structure in Tunisia, 1992. The EGT'85 seismic experiment in Tunisia: a reconnaissance of the deep structure. In: R. Freeman and S.T. Mueller (eds.), the European Geotraverse, Part 8, Tectonophysics 207, 245-267.

Saikia, S.C., H.K. Thio, B.B. Woods, X. Song, and D.V. Helmberger, 1996, Path calibration, source estimation and regional discrimination for the Middle East and western Mediterranean, Scientific Rept. No. 2, Phillips Laboratory, Air Force Material Command, 205 pp, PL-TR-96-2307, ADA323774.

Sandemeir, K.-J., 1990. Untersuchung der Ausbreitungseigenschaften seismischer Wellen in geschichteten und streuenden Medien, Ph.D. Dissert., Karlsruhe University.

Schurmann, H.M.E., 1974, The Precambrian in North Africa, E.J. Brill, Leiden, The Netherlands, 351 pp.

Seber, D., E. Sandoval, M. Wallve, G. Brew, and M. Barazangi, 1996, Development of a geological and geophysical information systems and seismological studies in the Middle East and North Africa, Proceedings of the 18th Annual Seismic Research Symposium on Monitoring a CTBT, 1026-1035, PL-TR-96-2153, ADA313692.

Suleiman, A.S., 1993. Geophysics of the rifts associated with the Sirt Basin (North Africa) and the Anadarko Basin (North America), Ph.D. Dissertation, The University of Texas at El Paso, 150 pp.

Sweeney, J.J., 1995. Preliminary maps of crustal thickness and regional seismic phases for the Middle East and North Africa, Lawrence Livermore Lab. Rept. UCRL-ID-122080, 13 pp.

UNESCO, 1971. Tectonics of Africa, UNESCO, Paris, 602 pp.

UNESCO, 1986. Carte geologique internationale de l'Afrique, scale 1:5,000,000.

van der Meer, F., and S. Cloetingh, 1993. Intraplate stresses and the subsidence history of the Sirte Basin (Libya), Tectonophysics 226, 37-58.

Van Houten, F.B., 1983. Sirte Basin, north-central Libya: Cretaceous rifting above a fixed mantle hotspot?, Geology 11, 115-118.

Westaway, R. , 1990. The Tripoli, Libya, earthquake of September 4, 1974: Implications for the active tectonics of the central Mediterranean, Tectonics 9, 231-248.

Wigger, P., G. Asch, P. Giese, W.D. Heinsohn, S. Othman El Alami, and F. Ramdani, 1992, Crustal structure along a traverse across the Middle and High Atlas Mountains of Morocco derived from seismic refraction studies, Geologische Rundschau 81(1), 237-248.

Yielding, G., M. Ouyed, G.C.P. King and D. Hatzfeld, 1989. Active tectonics of the Algerian Atlas Mountains - evidence from aftershocks of the 1980 El-Asnam earthquake, Geophys. J. Int. 99, 761-788.

Appendix A - Documentation of Geological Data Base

Maps of North African geological features that we have digitized are available at the UTEP Department of Geological Sciences' web site under the North Africa Project subheading (http://www.geo.utep.edu/nafr/ nafr.html). The sources of data used for the maps we have generated are given below, along with information on the scales of the original maps. Because the maps on the web site are in color, we have chosen not to reproduce them for this appendix.

Figure 2 shows the outlines of exposed Precambrian rocks in the Hoggar, Tibesti and Darfur uplifts (heavy, dark lines). These exposures were taken from UNESCO (1986) (1:5,000,000).

The website http://www.geo.utep.edu/nafr/nafrgeo.html contains a color topographic map with structural features shown in white. Early Cretaceous basins and faults taken from Guirard and Maurin (1992) (~1:55,000,000). Basement faults in north-central Libya are from van der Meer and Cloetingh (1993). Structural features of central Libya are from Goudarzi (1980) (~1:1,500,000). Structure in Algeria and Chad is from Dautria and Lesquer (1989) (1:10,500,000). Early Cretaceous basins in the northeastern portion of North Africa are from Van Houten (1983) (~1:1,500,000). Lines in western portion of North Africa are structures shown in Kirton and Bourennani (1984) (~1:3,000,000). Well locations used in our gravity analysis and in construction of the structural contours are shown on this map by red circles. Major geotectonic units of West Africa (Lesquer et al., 1990) are also shown. Green contours on the map indicate the depth to the Paleozoic based on Goudarzi, (1980; ~1:1,500,000).

The website htpp://www.geo.utep.edu/nafr/nafrgeo1.html shows a color topographic map with the location of our gravity profiles in white. The Central and West African rift system is shown in red. Rift basins in Niger, Chad and the central African Republic have been digitized from Genik (1992) (~1:2,500,000). Precambrian exposures of the Hoggar, Tibesti and Dafur uplifts (UNESCO, 1986) are also shown.

We have also digitized a Moho contour map from Research Group for Lithospheric Structure in Tunisia (1992) (~1:600,000) that was used to help constrain our gravity models.

27

Appendix B - Documentation of Gravity Data Base

Two gravity data bases have been compiled for public use in North Africa. The first of these in the Defense Mapping Agency (DMA) data base that includes 36,410 gravity points distributed over North Africa north of 10 degrees north. These data include principal facts and are in the following format: field #1 - latitude in decimal degrees, field #2 - longitude in decimal degrees, field #3 - Bouguer anomaly in milligals using a 2.67 g/cc reduction density, field #4 - inner zone terrain correction, Hammer zones (A-F), in milligals, field #5 - outer zone terrain correction, Hammer zones G and beyond, in milligals, field #6 - elevation above sea level in feet, field #7 - observed gravity in milligals, and field #8 - source number indicating the origin of the data point. A value of -99.99 milligals in the terrain correction fields means that the terrain correction for that point has not been made. This data base is available on the UTEP web page under "DMA gravity".

The second data base available is more detailed data for an area surrounding the Gulf of Sirt. Except for 92 points in this data set principal facts are not available for these data. This data set includes 5531 gravity points. The format is the same as for the DMA gravity data described above, except that only the first three fields of data are given. This data base is available on the UTEP web page under "Sirt gravity".

A third proprietary data base was used to prepare the maps in this report and those available on the UTEP web page. This data base contains 477,298 gravity points, including those virtually all of the data points in the two data sets mentioned above and has been gridded at 5 minute intervals. Neither the data points nor the gridded data are available to the public. Individuals with specific interest in these data should contact G. Randy Keller at UTEP.

28

Appendix C - Documentation of Seismic Data Base

We have collected earthquake listings from the bulletins of the International Seismological Centre and the U.S. Geological Survey's Earthquake Data Reports for earthquakes of M≥5.0 and associated aftershocks occurring between 1963 and 1988 within North Africa. These data have been organized into a data base using the PC based program EXCEL, as well as available through our Internet site through the ORACLE data base management program. Diskettes of the EXCEL formatted data base are available upon request.

Figure C1 shows an example of the main spread sheet we have created for all events of interest (example in EXCEL). The spread sheet contains information on the date, time, latitude (lat), longitude (lon), depth, magnitude (Ms, mb or other), and location.

For each earthquake for which we have obtained a listing, we have created the spreadsheet (example in EXCEL) shown in Figure C2. The first line of the spreadsheet contains header information on the earthquake itself. Then we list all stations within 20° of the earthquake and note the station distance, station time, P-wave arrival time, S-wave arrival time, and arrival time of other phases, if given. We also record the delay time (observed arrival time minus predicted time). Magnitude information (usually log A/T) is also noted, when available.

We have used the data contained in the spreadsheet data base to generate plots showing travel time delay information for earthquakes occurring in areas of Algeria and Egypt. Using plane-parallel coordinate projections we displayed data base information including earthquake parameters such as distance, azimuth, travel time delay and magnitude for WWSSN stations of interest. For events occurring in Egypt we used travel time delays for the following WWSSN stations: JER, AAE, HLW and IST. The stations of interest for Algerian events were: LOR, MAL, TOL, AGU, TRI and PTO. Examples of these plots are shown in Figure C3 and C4.

In addition to creating these plane-parallel coordinate plots we have also displayed delay information in map view. Examples of these maps are shown in Figures C5 and C6 for HLW and PTO.

Digitized seismograms are shown in Figures C7 to C40. For each figure a label is shown at the upper right of each seismogram. The first numbers represent the start time (hour and minute UT) of the seismogram. This time is followed by the 3 character WWSSN station code and a 1 character component type (r=radial, t=tangential, z=vertical). Seismograms are available upon request from P. Dial (dial@geo.utep.edu) and are written in SAC (seismic analysis code) format.

29

DATE	TIME	LAT	LON	DEPTH	Ms	Mb	MAGNITUDE	LOCATION	*	LISTING
4/16/69	8:12:56	27.3	33.9	33.0			5.0	Egypt		x
4/17/69	8:01:04	27.5	33.8	42.0			4.8	Egypt		x
4/23/69	13:37:17	27.5	33.7	18.0			5.0	Egypt		x
9/2/72	14:53:38	31.3	16.0	6.0		5.1	5.3	Sidra		x
9/4/74	6:29:14	33.0	13.5	0.0		5.2	5.5	Sidra		x
12/19/76	21:21:52	33.0	13.9	10.0		4.5	4.5	Sidra		x
1/19/77	20:46:53	36.5	8.4	21.0		4.9	5.7	A'in Soltane		x
2/9/77	13:55:00	36.4	8.4	41.0		4.5	4.9	A'in Soltane		x
10/10/80	12:25:17	36.1	1.4	0.0	7.2	6.3	5.5	El Asnam		x
10/10/80	12:37:08	36.3	1.5	0.0		5.6		El Asnam		x
10/10/80	14:12:27	36.1	1.3	16.0		4.7	4.6	El Asnam		x
10/10/80	14:44:51	36.3	1.4	0.0		5.4	5.3	El Asnam		x
10/10/80	15:18:46	36.0	1.5	10.0		3.8	4.0	El Asnam		x
10/10/80	15:25:36	36.0	1.3	10.0		4.6	4.6	El Asnam		x
10/10/80	15:36:52	36.4	1.7	10.0		4.8	4.9	El Asnam		x
10/10/80	15:39:06	36.2	1.6	3.0	6	6	6.1	El Asnam		x
10/10/80	17:15:17	36.3	1.6	10.0		3.9	4.0	El Asnam		x
10/10/80	17:32:59	36.1	1.4	10.0	4.7	5.4	5.2	El Asnam		x
10/10/80	19:07:59	36.4	1.6	0.0	4.5	5.4	5.0	El Asnam		x
10/10/80	20:22:41	36.5	1.5	10.0		4.5	4.3	El Asnam		x
10/10/80	21:21:18	36.2	1.7	10.0		4.1	4.2	El Asnam		x
10/10/80	23:55:33	36.2	1.8	10.0	3.4	4.2	3.2	El Asnam		x
10/10/80	23:59:58	36.2	1.3	10.0	3.4	3.9	3.4	El Asnam		x
10/11/80	1:29:16	36.3	1.5	10.0		4.1	4.2	El Asnam		x
10/11/80	5:40:48	36.3	1.6	10.0	3.9	4.6	4.6	El Asnam		x
10/11/80	19:30						4.3	El Asnam		
10/11/80	21:26:13	36.4	1.5	10.0	3.4	4.6	4.7	El Asnam		x
10/12/80	0:36:49	36.3	1.6	10.0		3.9	4.2	El Asnam		x
10/12/80	4:02:15	36.3	1.5	0.0	3.4	4.2	4.2	El Asnam		x
10/13/80	6:37:36	36.3	1.5	2.0	5.2	5.2	5.0	El Asnam		x
10/13/80	14:33:37	36.3	1.6	0.0	3.4	5	4.6	El Asnam		x
10/13/80	20:26:41	36.0	1.4	10.0		3.9	4.0	El Asnam		x
10/14/80	1:07:39	36.3	1.4	10.0		4	4.1	El Asnam		x
10/14/80							4.5	Algeria		
10/14/80	17:34:55	36.3	1.6	0.0	4.3	5.1	5.0	El Asnam		x

Figure C1. Example of page from master event spreadsheet that contains information on all earthquakes we plan to study.

Egypt	3/24/69	11:54:14	27.47N	33.87E	16km	Mag=4.9		
Station	Distance	Azimuth	P arrival	P delay	S arrival	S delay	PP arrival	PP delay
HLW	361.38	318	11:55:05	-0.06	11:55:50	5		
JER	493.70	15	11:55:20	-2.5	11:55:20	4		
CIN	1246.49	336	11:56:57	0.1	11:58:56	-7		
KSA	730.55	15	11:55:56	3.5	11:57:20	11		
VAM	1283.19	317	11:56:57	-4.3	-	-		
KER	1475.55	56	11:57:26	1.5	-	-		
ATH	1501.13	323	11:57:28	0.4	-	-		
TAB	1652.35	42	11:57:46	0.5	12:00:36	-		
VLS	1715.73	317	11:57:50	-2.8	-	-	11:58:04	12
PLG	1722.41	329	11:57:57	3.4	-	-		
GRS	1762.44	38	11:57:58	-0.3	-	-		
JAN	1809.14	322	11:58:08	4.4	-	-		
BKR	1810.25	27	11:58:01	-2.7	-	-		
SHI	1839.16	78	11:58:07	-0.1	-	-		
KRV	1855.84	35	11:58:09	0	-	-		
TIF	1868.07	29	11:58:10	-0.3	12:01:12	-4		
TEH	1893.65	57	11:58:15	1.7	-	-		
TIR	2000.39	324	-	-	12:01:50	6		
BUC	2003.73	342	11:58:18	-7.6	-	-		
AAE	2103.80	165	11:58:40	3.7	-	-		
CMP	2124.93	341	11:58:39	0.2	-	-		
VRI	2137.16	345	11:58:42	2.4	-	-		
KIS	2212.78	350	11:58:46	-1.9	-	-		

Figure C2: Example of spreadsheet data for an aftershock of the 1969 northern Red Sea earthquake sequence.

31
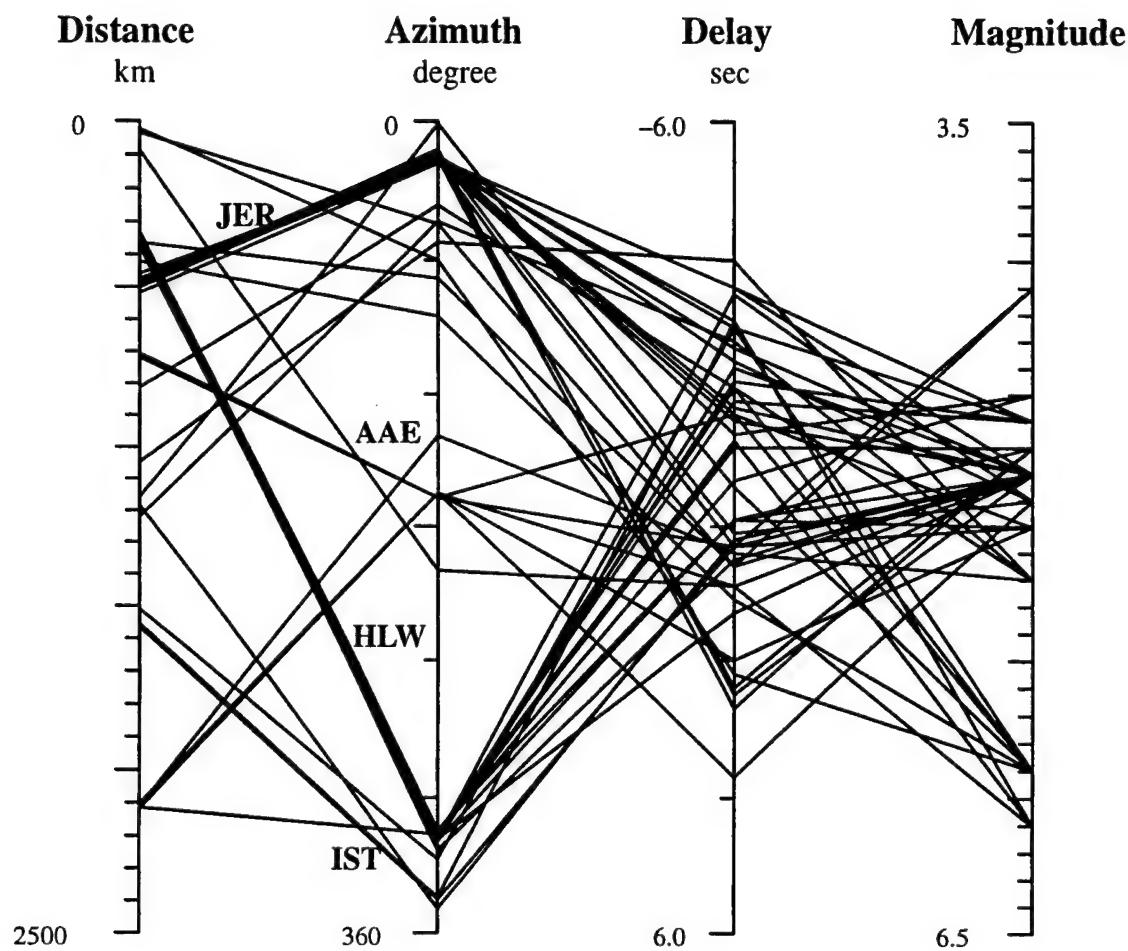
Figure C3. Plane-parallel coordinate projection showing earthquake parameters for Egyptian events recorded by WWSSN stations in 1969.
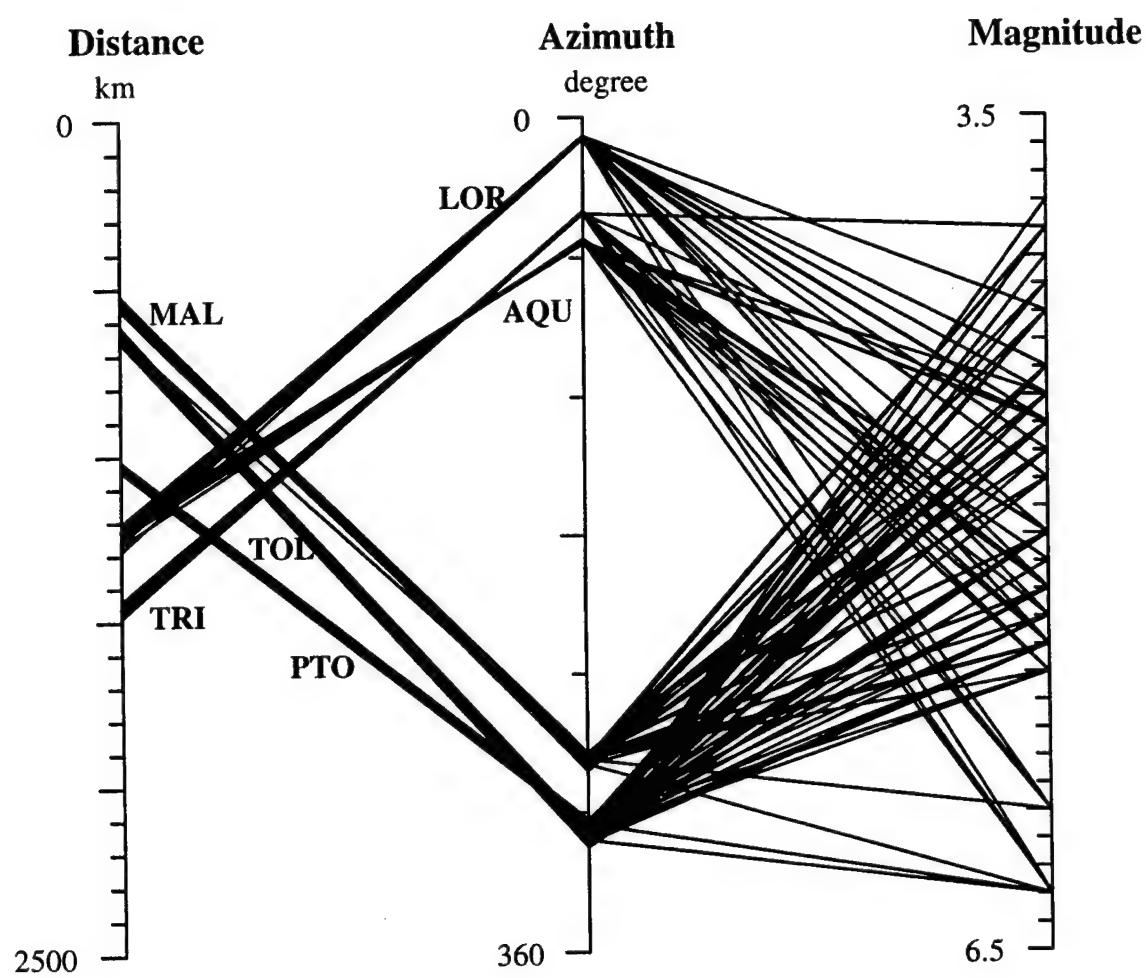
Figure C4. Plane-parallel coordinate projection showing earthquake parameter variations for WWSSN stations recording Algerian earthquakes between October 1980 and February 1981.

33
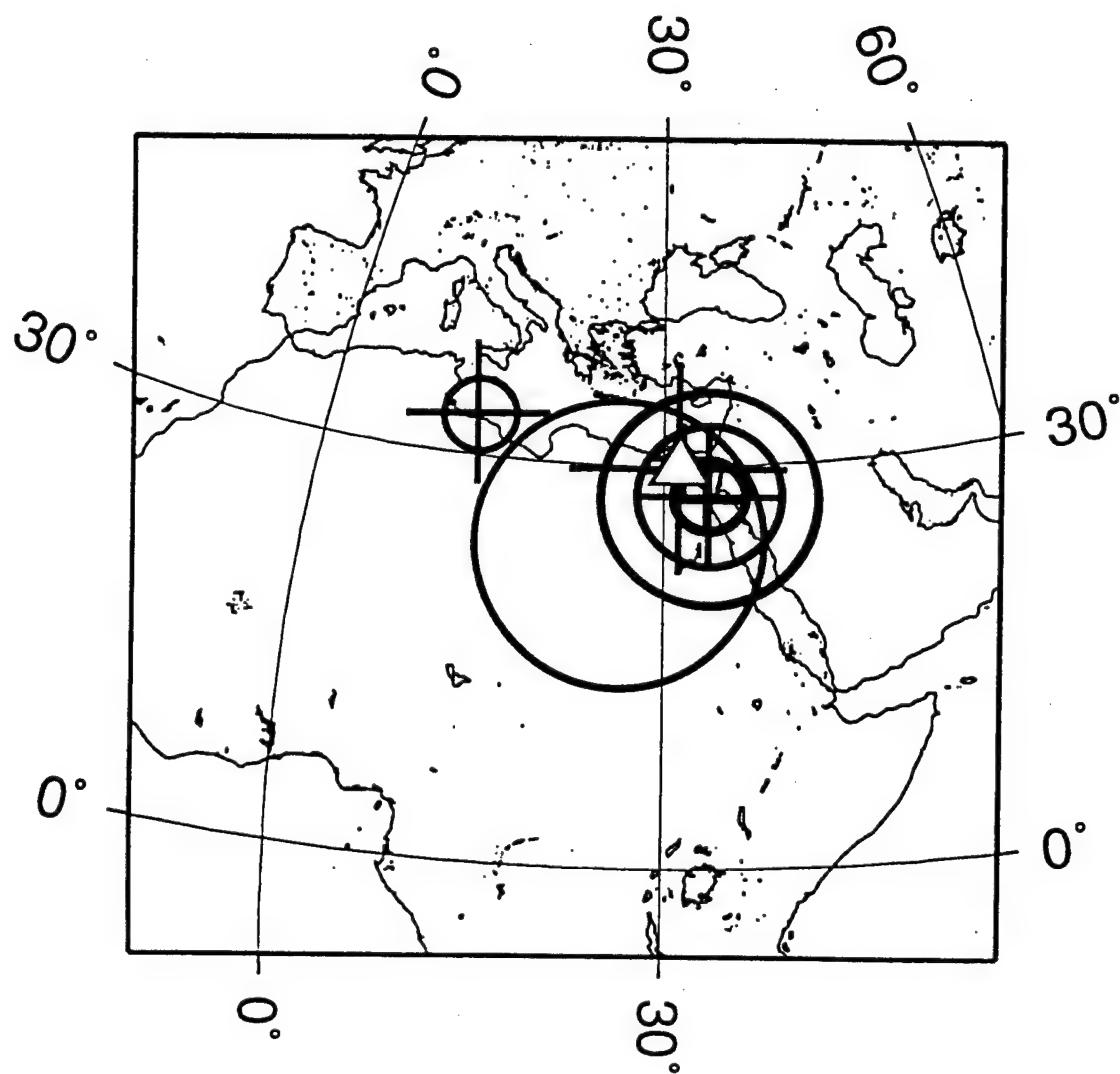
Figure C5. Azimuthal equal area projection showing travel time delays for the WWSSN station HLW (triangle). Circles denote negative delays and crosses indicate positive delays. Symbol size is scaled between +/- 6.0 seconds.

34
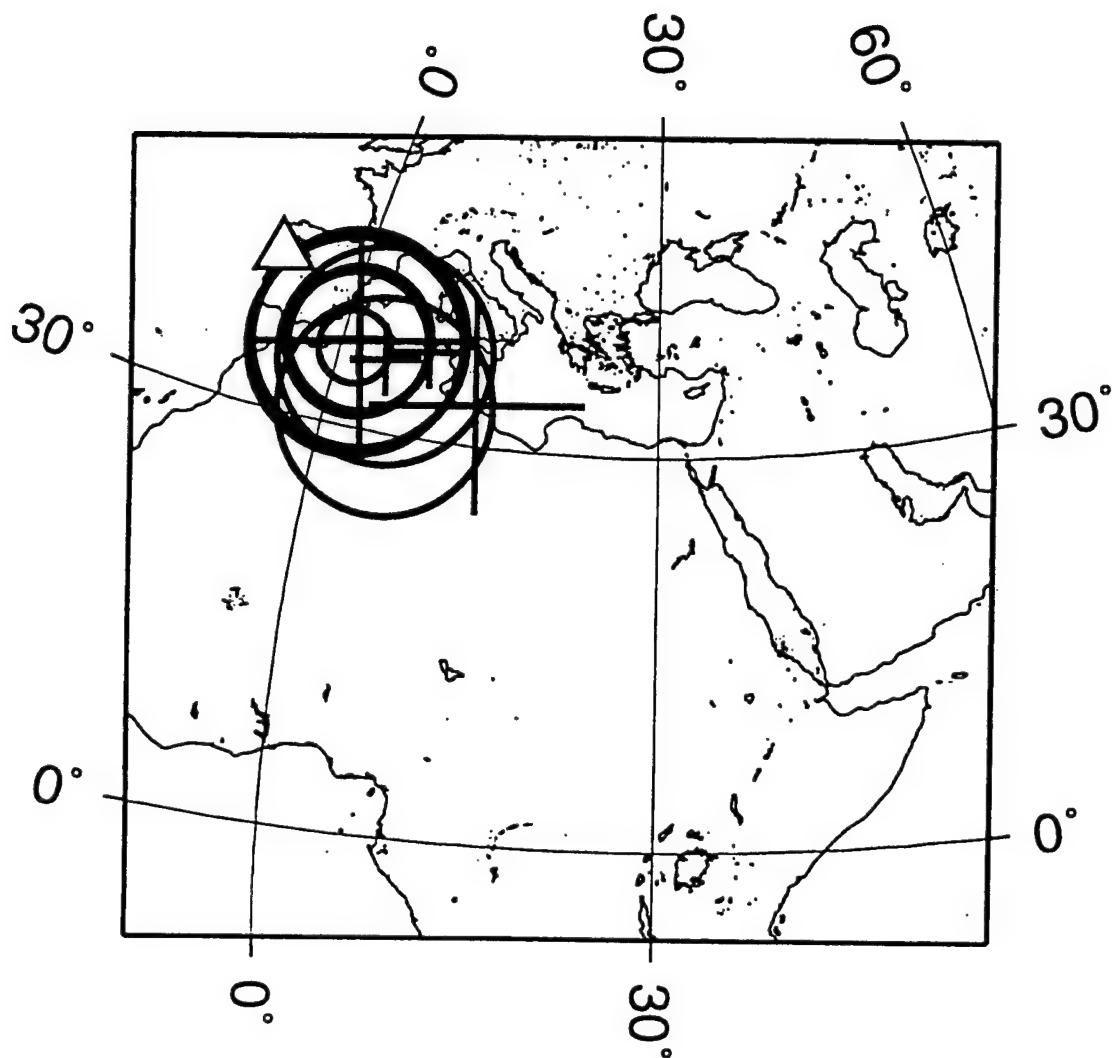
Figure C6. Azimuthal equal area projection showing travel time delays for Algerian earthquakes recorded at PTO (triangle). Circles and crosses are as in Figure C5.
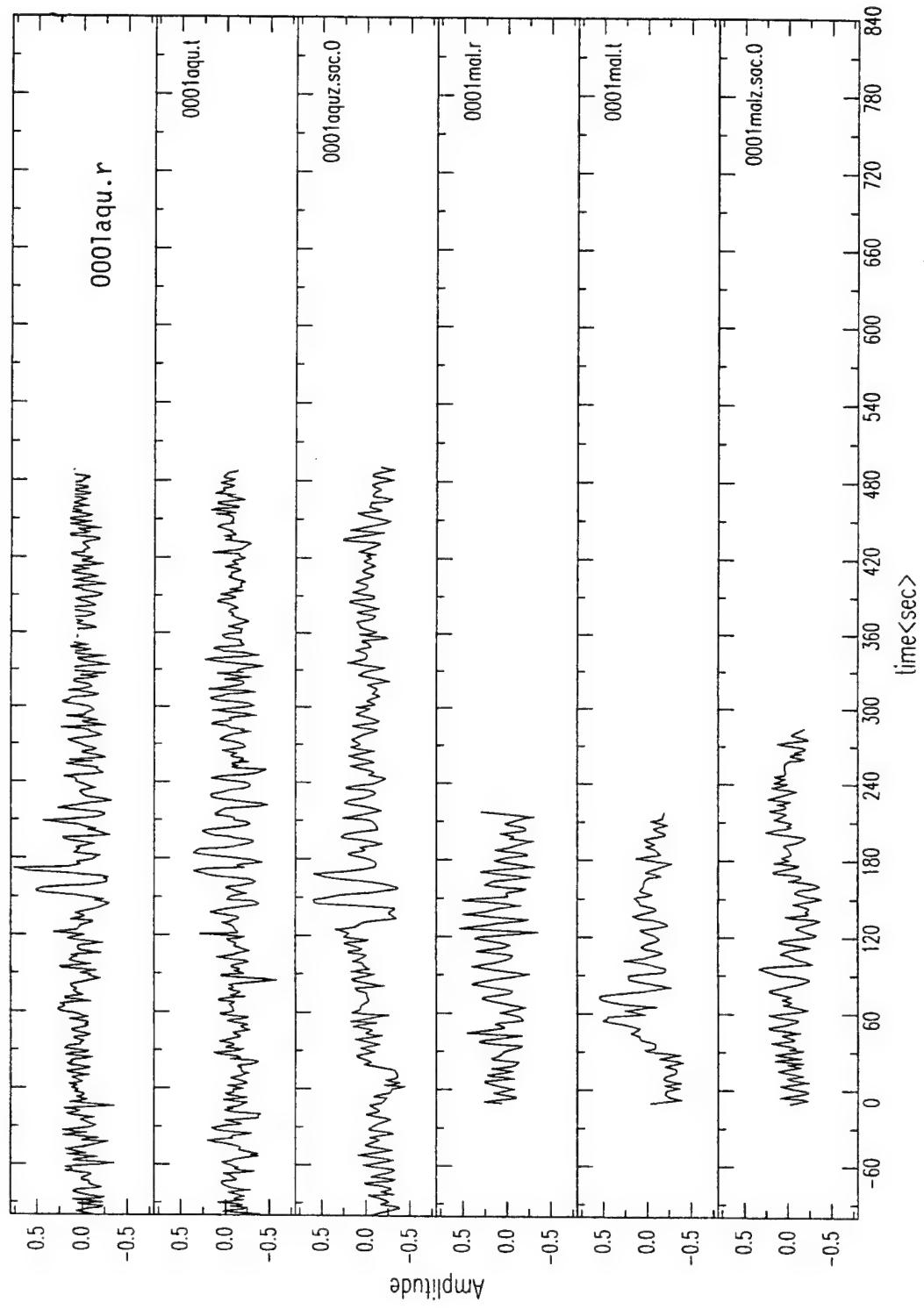
**Figure C7.** Seismograms of El Asnam aftershocks, October 10, 1980.
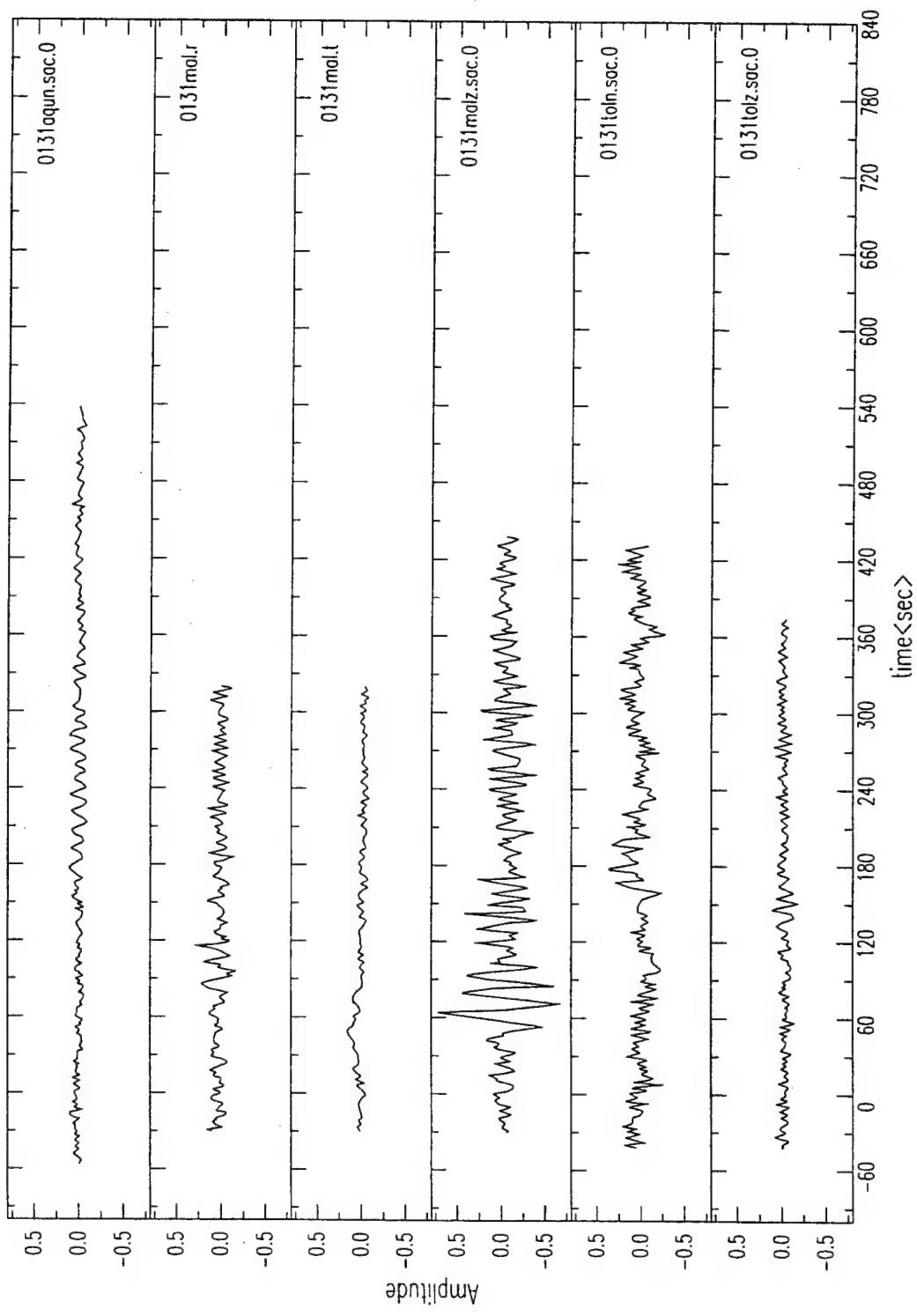
Figure C8. Seismograms of El Asnam aftershocks, October 10, 1980.

37
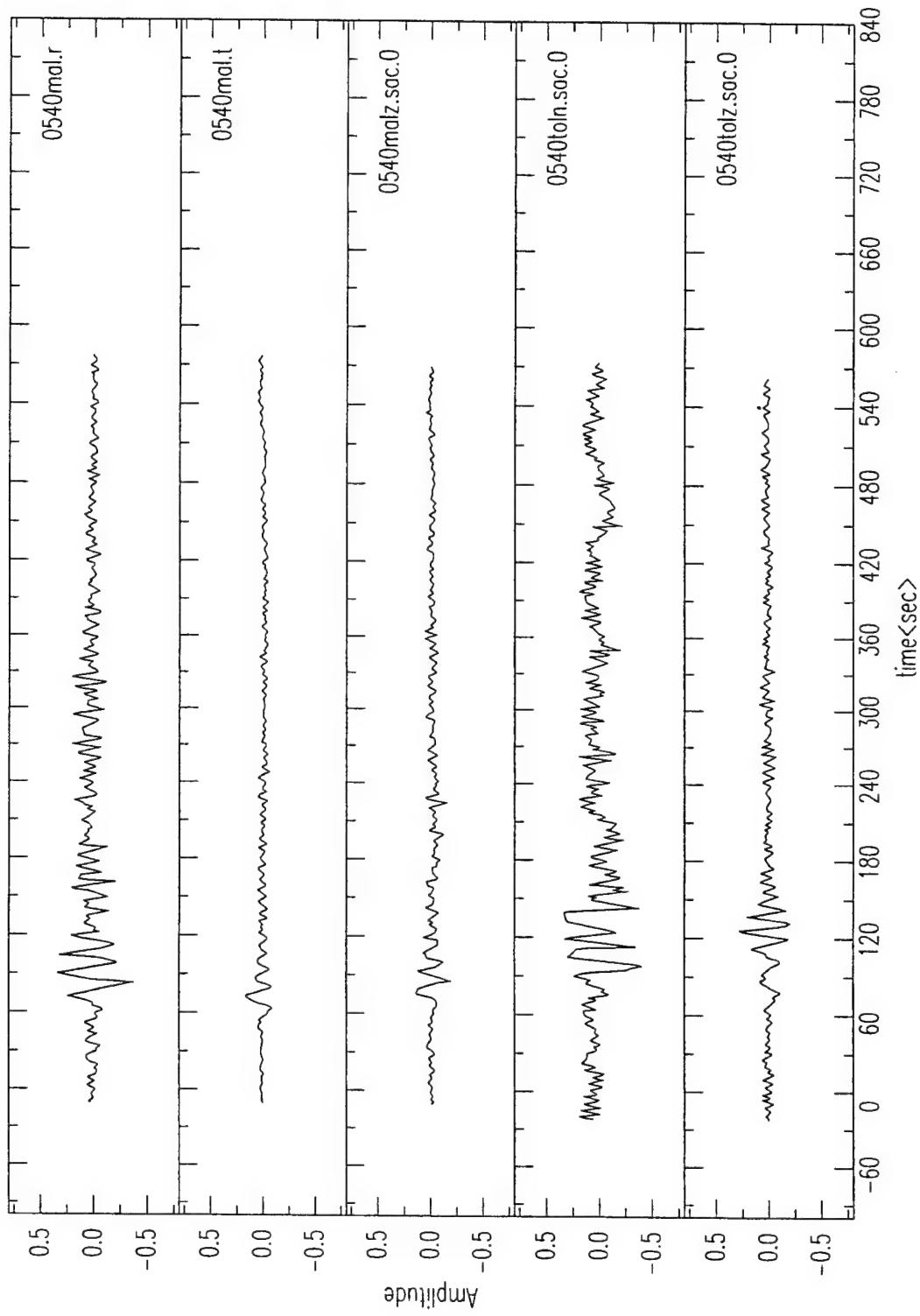
Figure C9. Seismograms of El Asnam aftershocks, October 10, 1980.
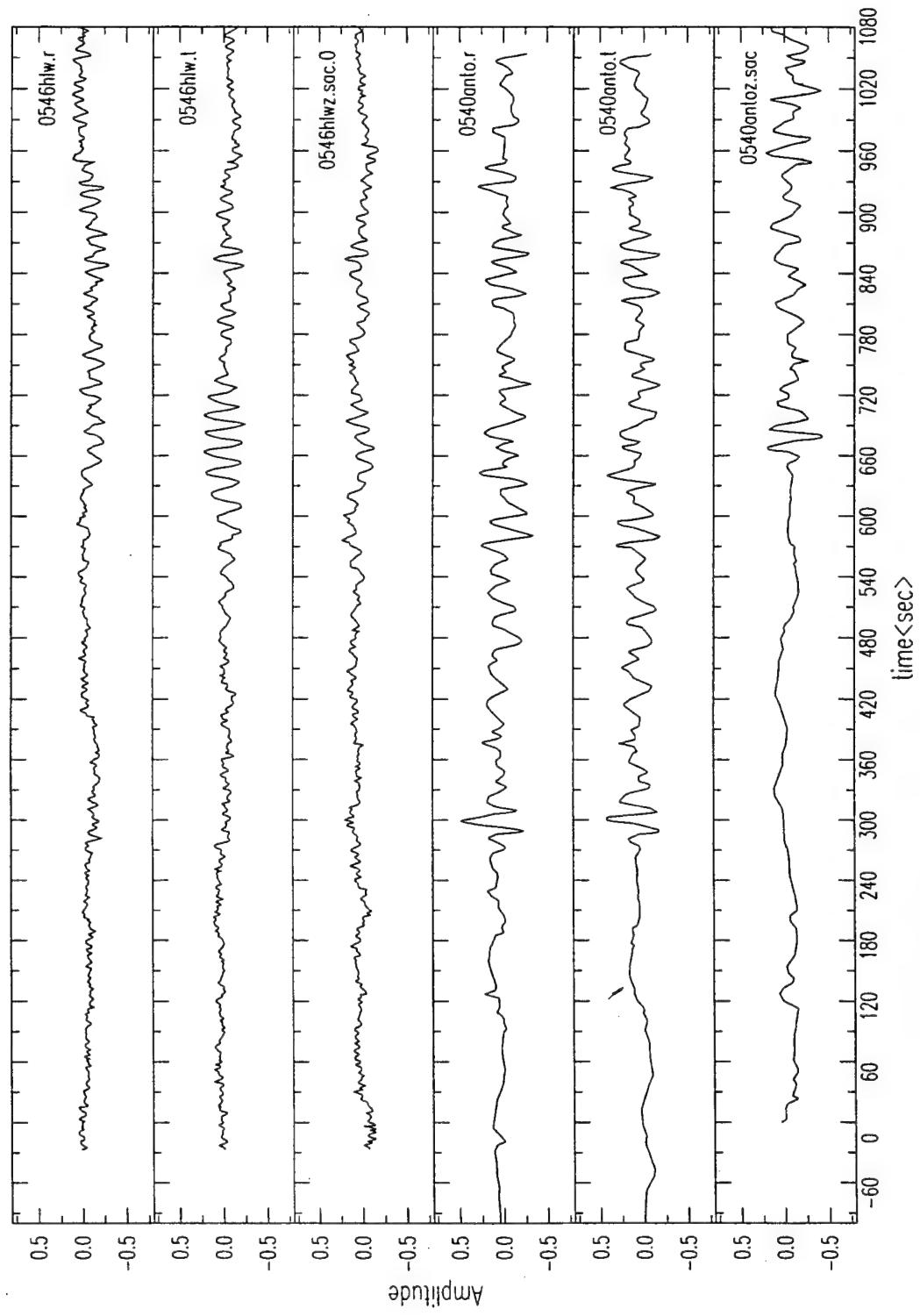
Figure C10. Seismograms of El Asnam aftershocks, October 10, 1980.
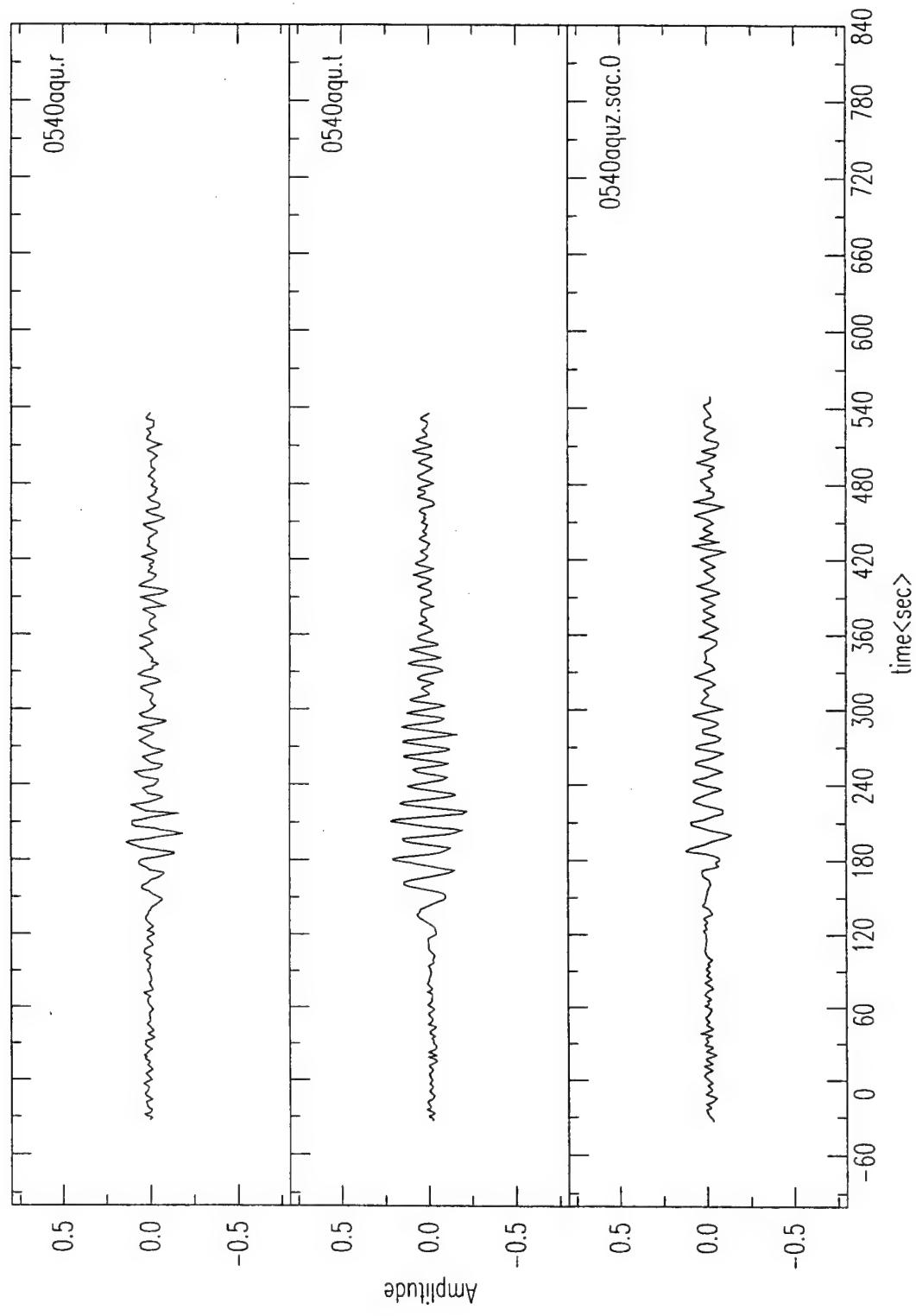
Figure C11. Seismograms of El Asnam aftershocks, October 10, 1980.
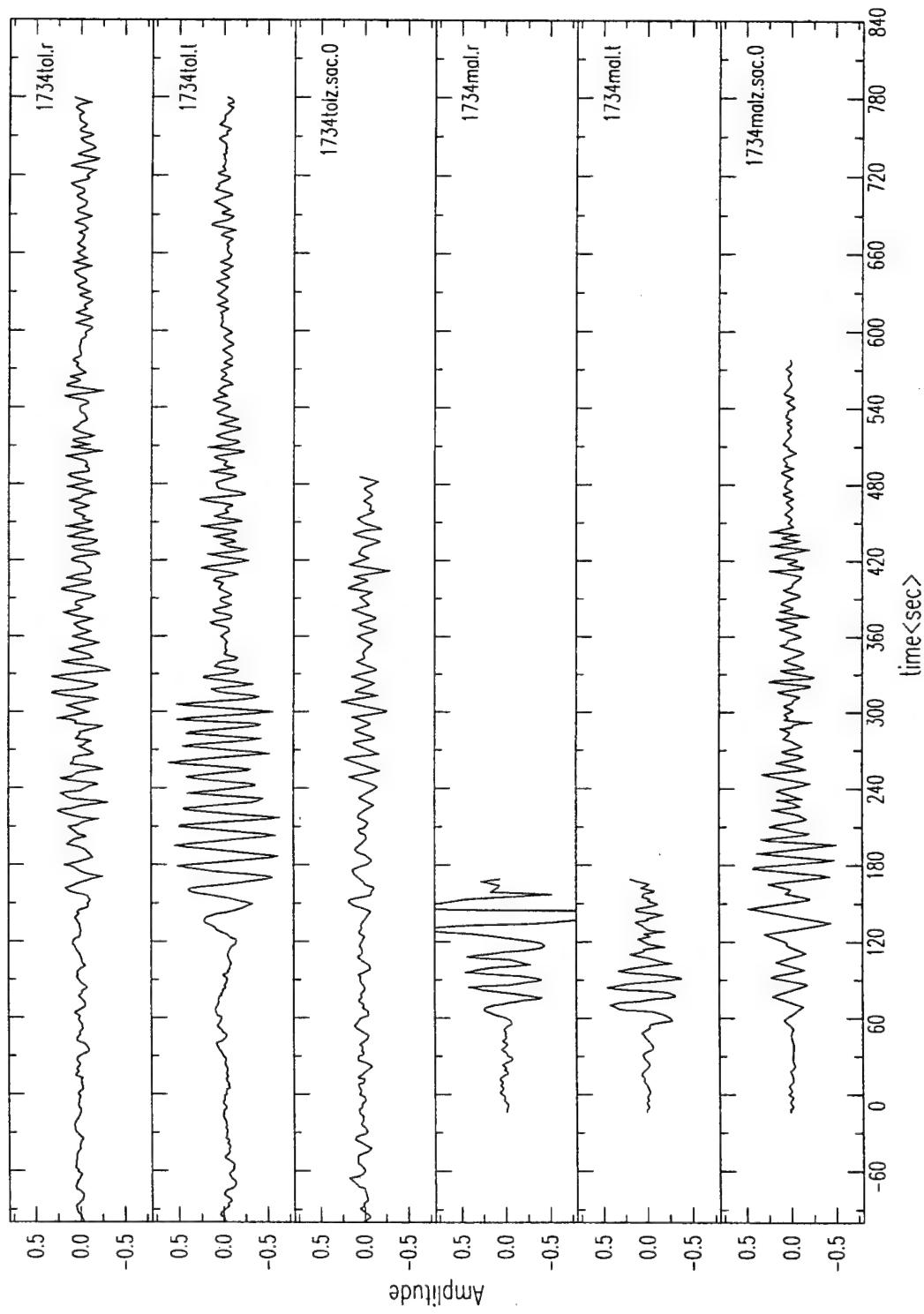
**Figure C12.** Seismograms of El Asnam aftershocks, October 10, 1980.

41
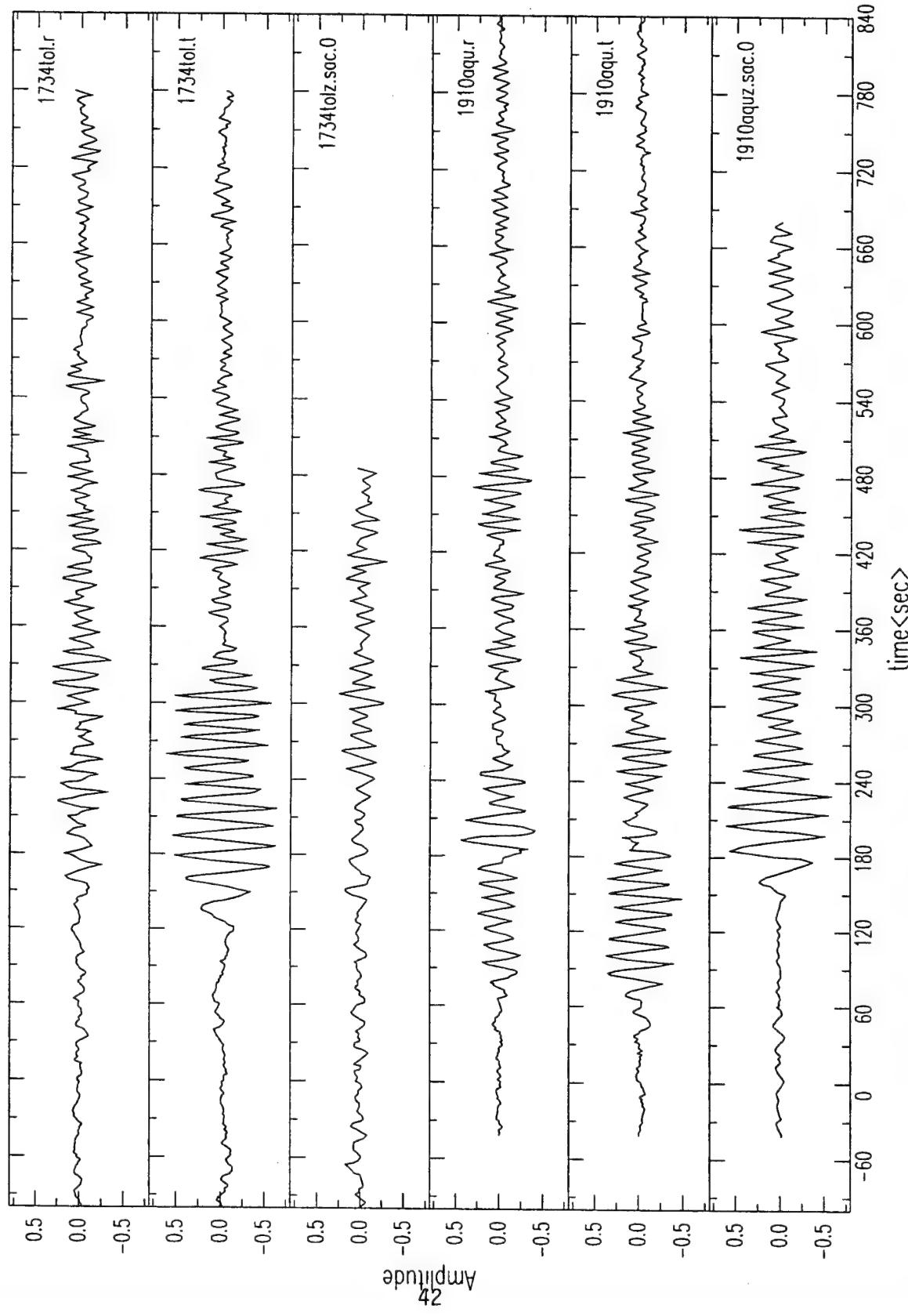
Figure C13. Seismograms of El Asnam aftershocks, October 10, 1980.

42
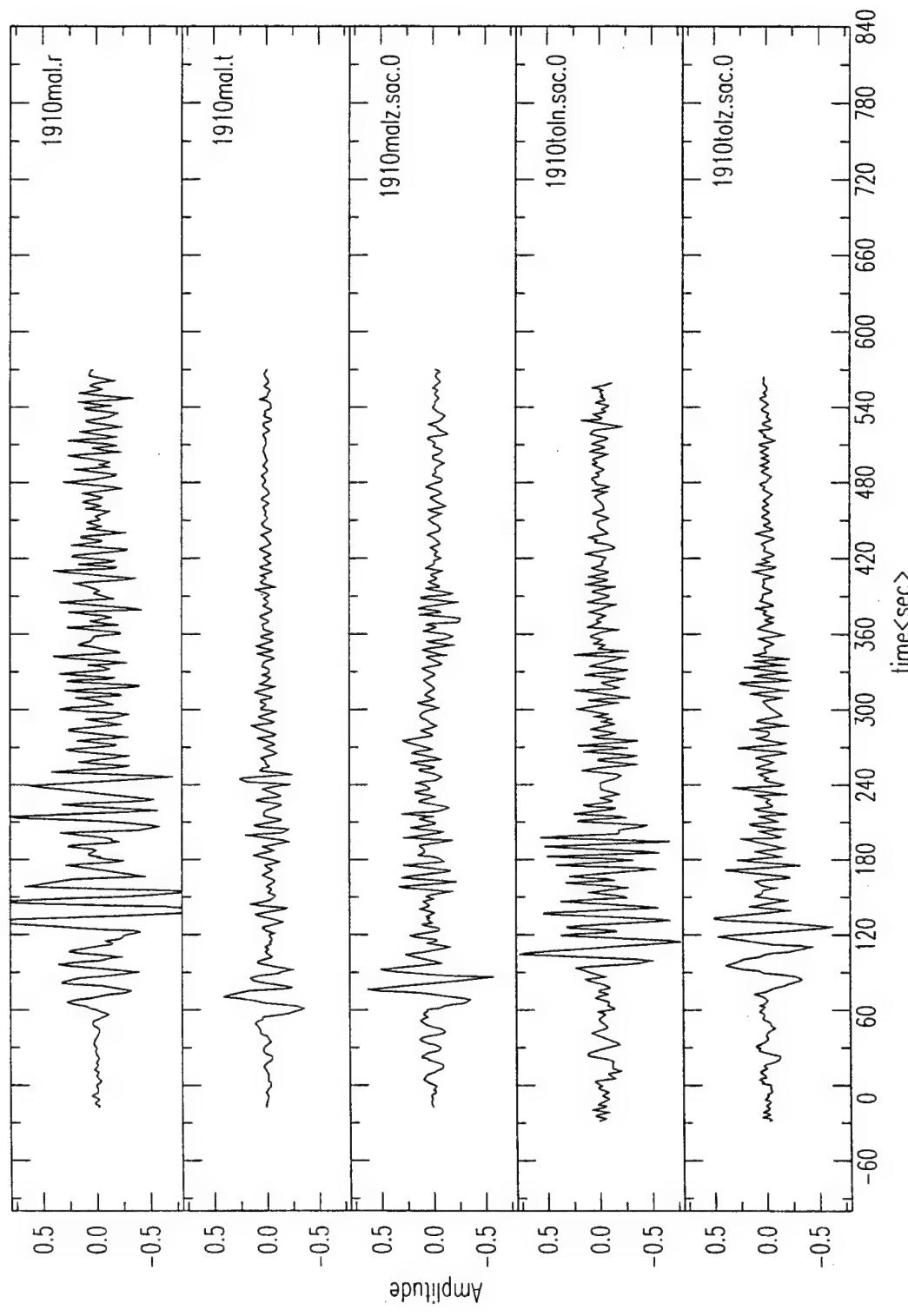
Figure C14. Seismograms of El Asnam aftershocks, October 10, 1980.
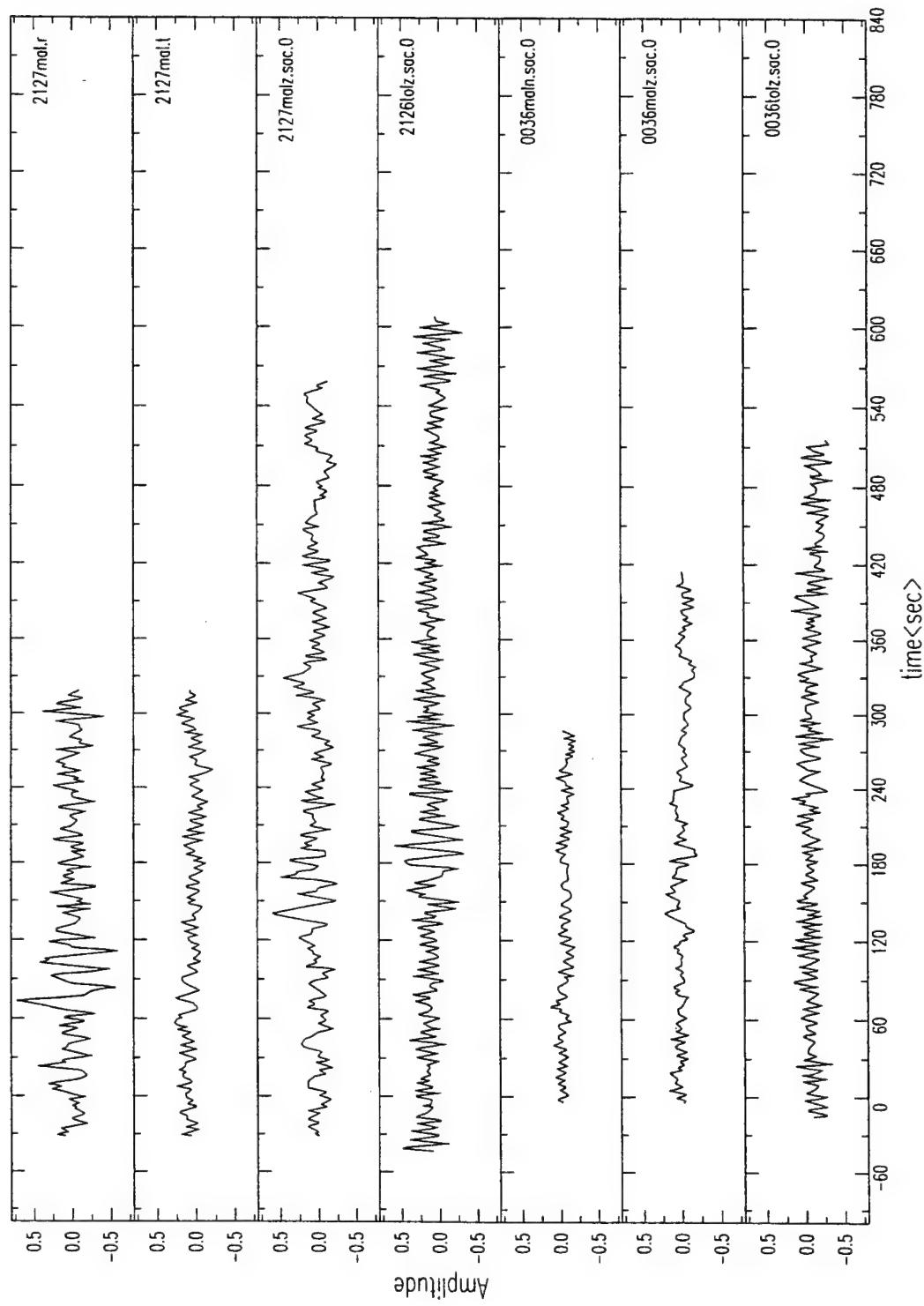
Figure C15. Seismograms of El Asnam aftershocks, October 10 (2127) and October 12 (0036), 1980.

44
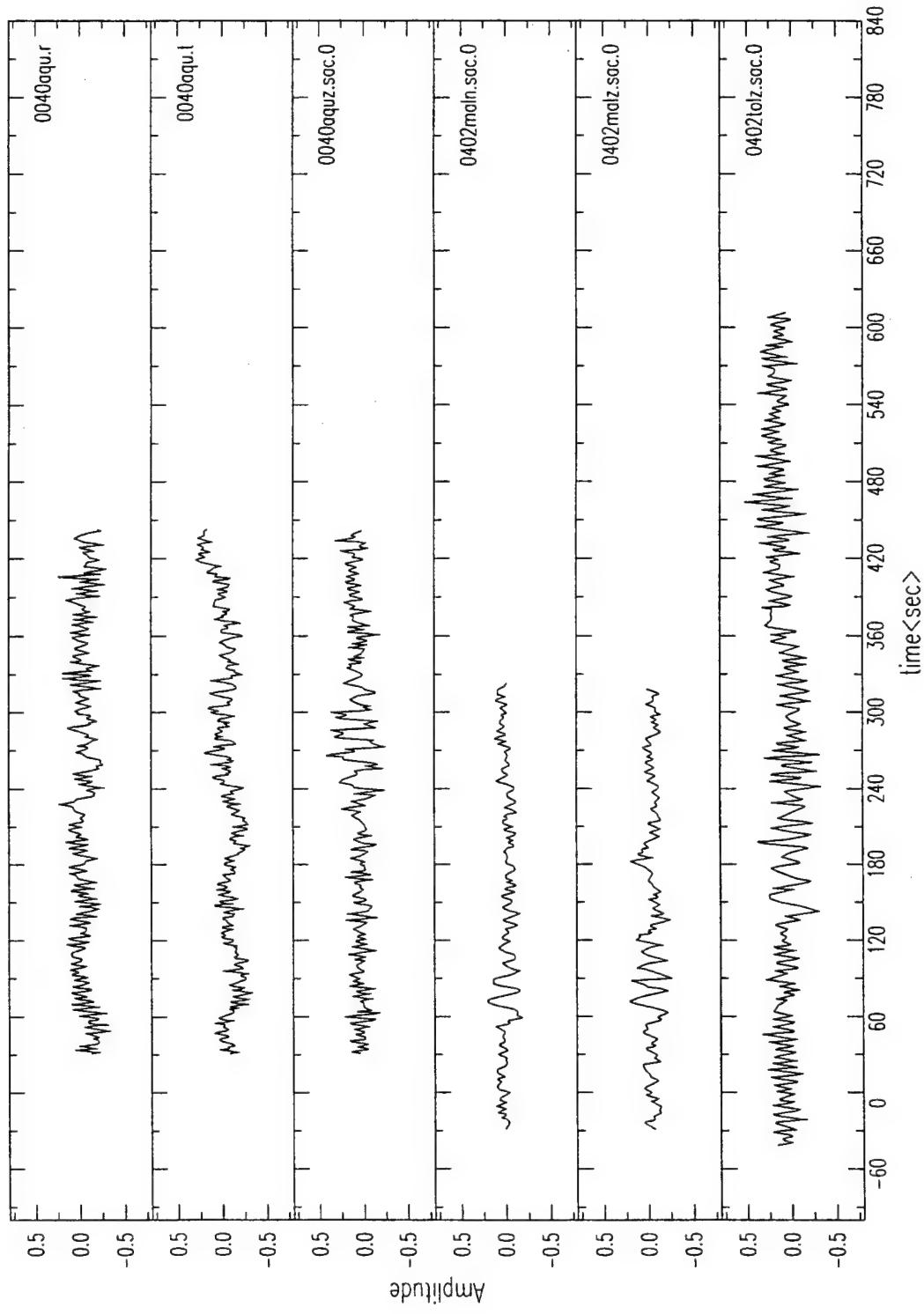
Figure C16. Seismograms of El Asnam aftershocks, October 12, 1980.
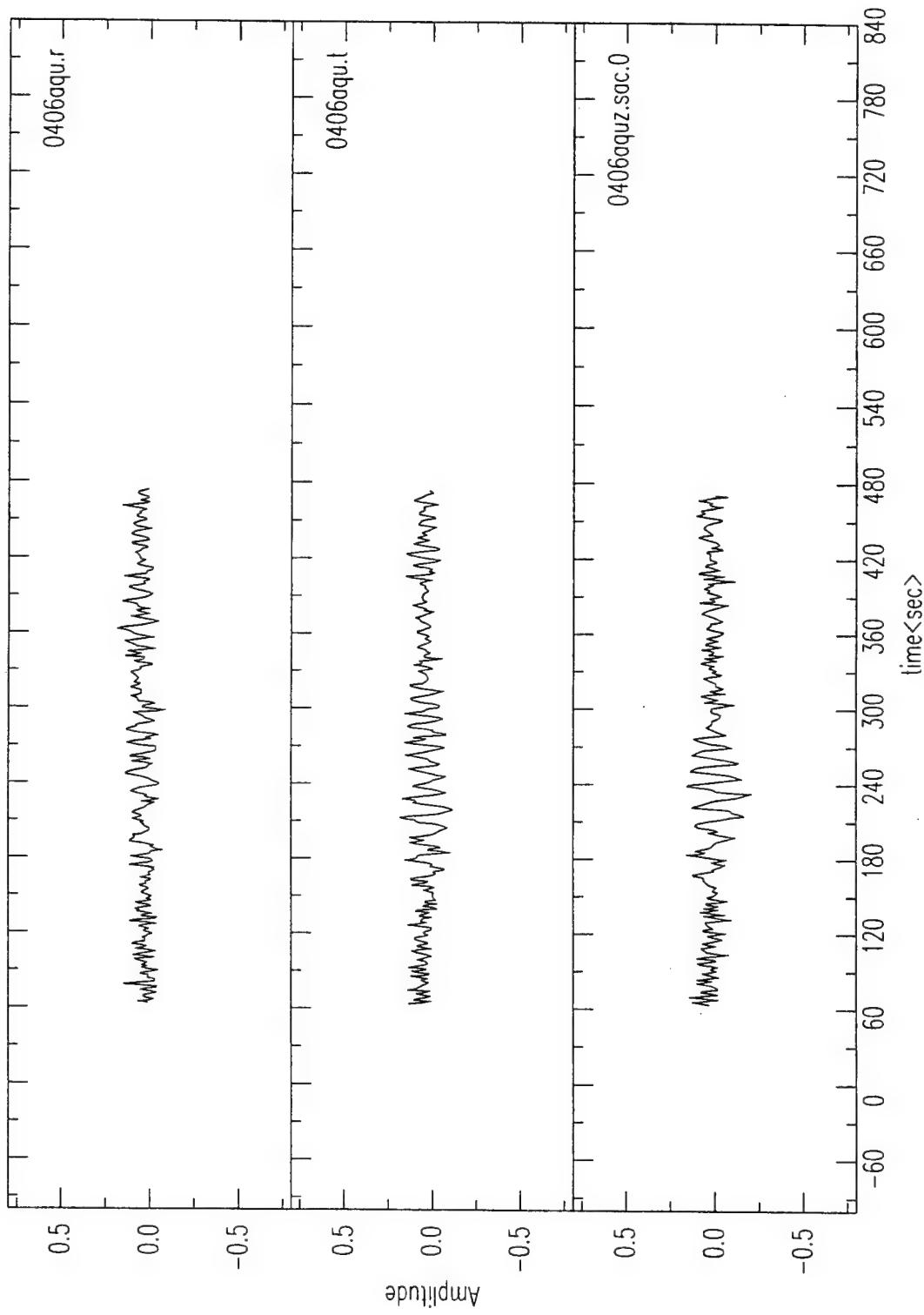
Figure C17. Seismograms of El Asnam aftershocks, October 12, 1980.

46
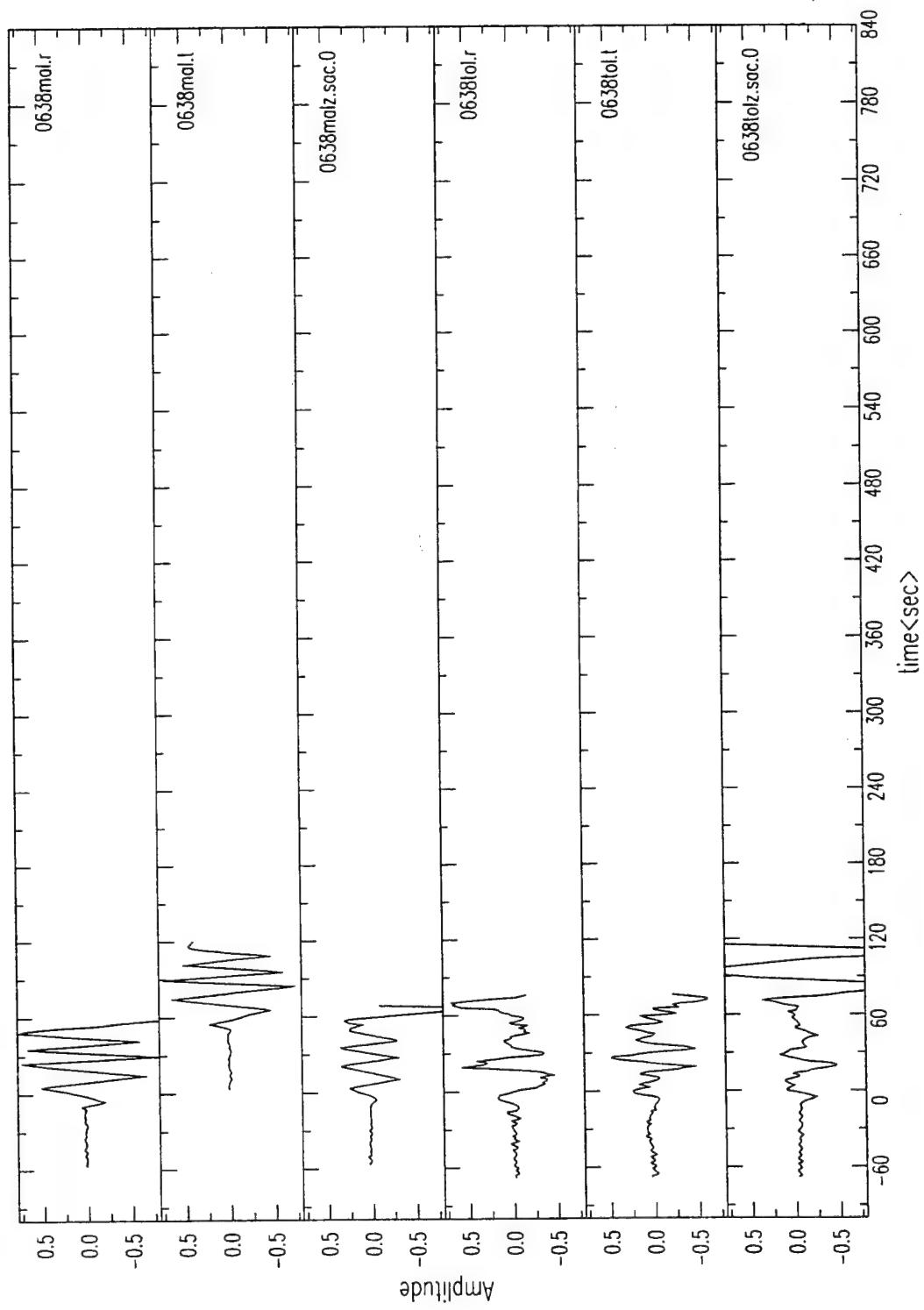
Figure C18. Seismograms of El Asnam aftershocks, October 13, 1980.

47
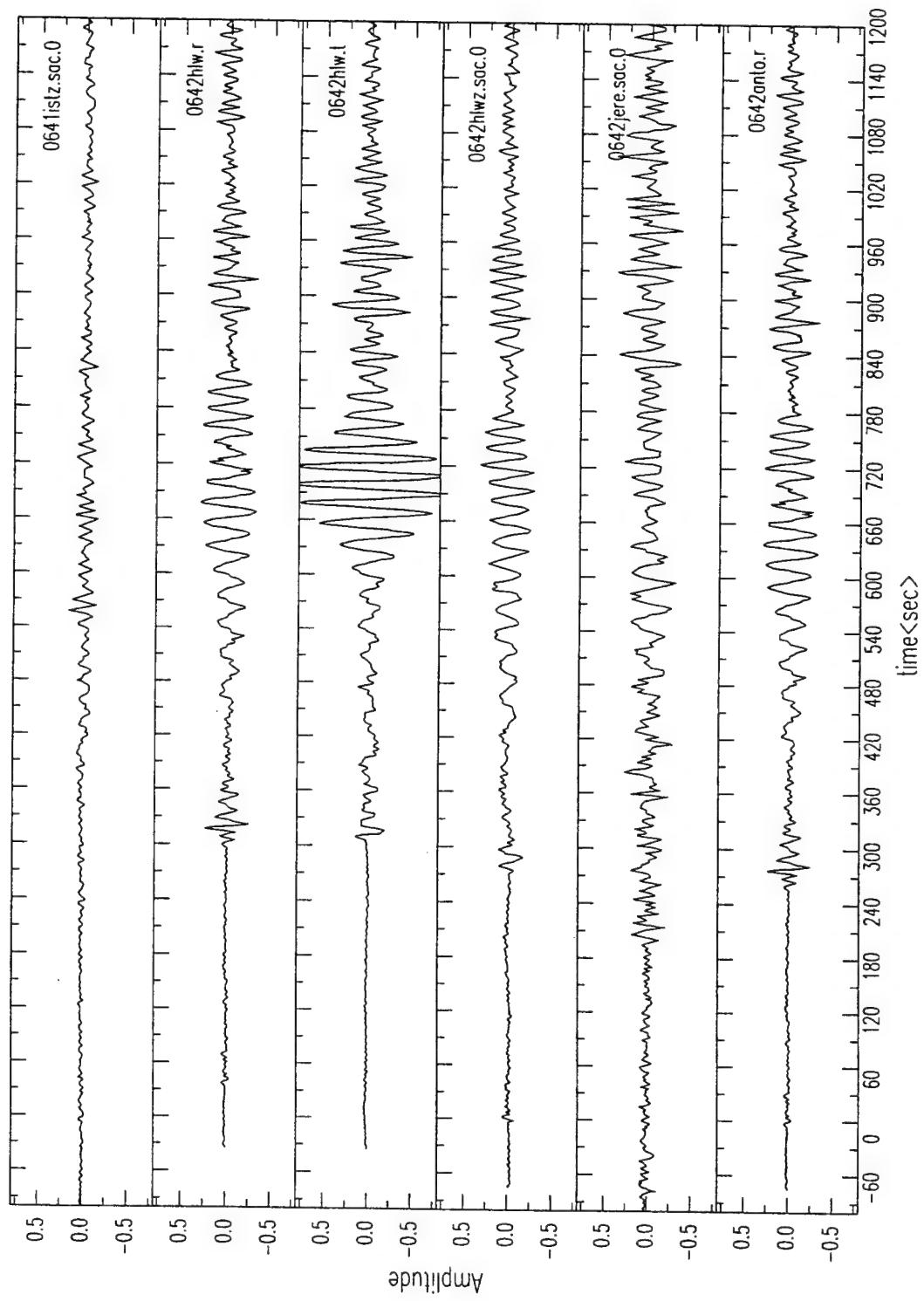
Figure C19. Seismograms of El Asnam aftershocks, October 13, 1980.

48
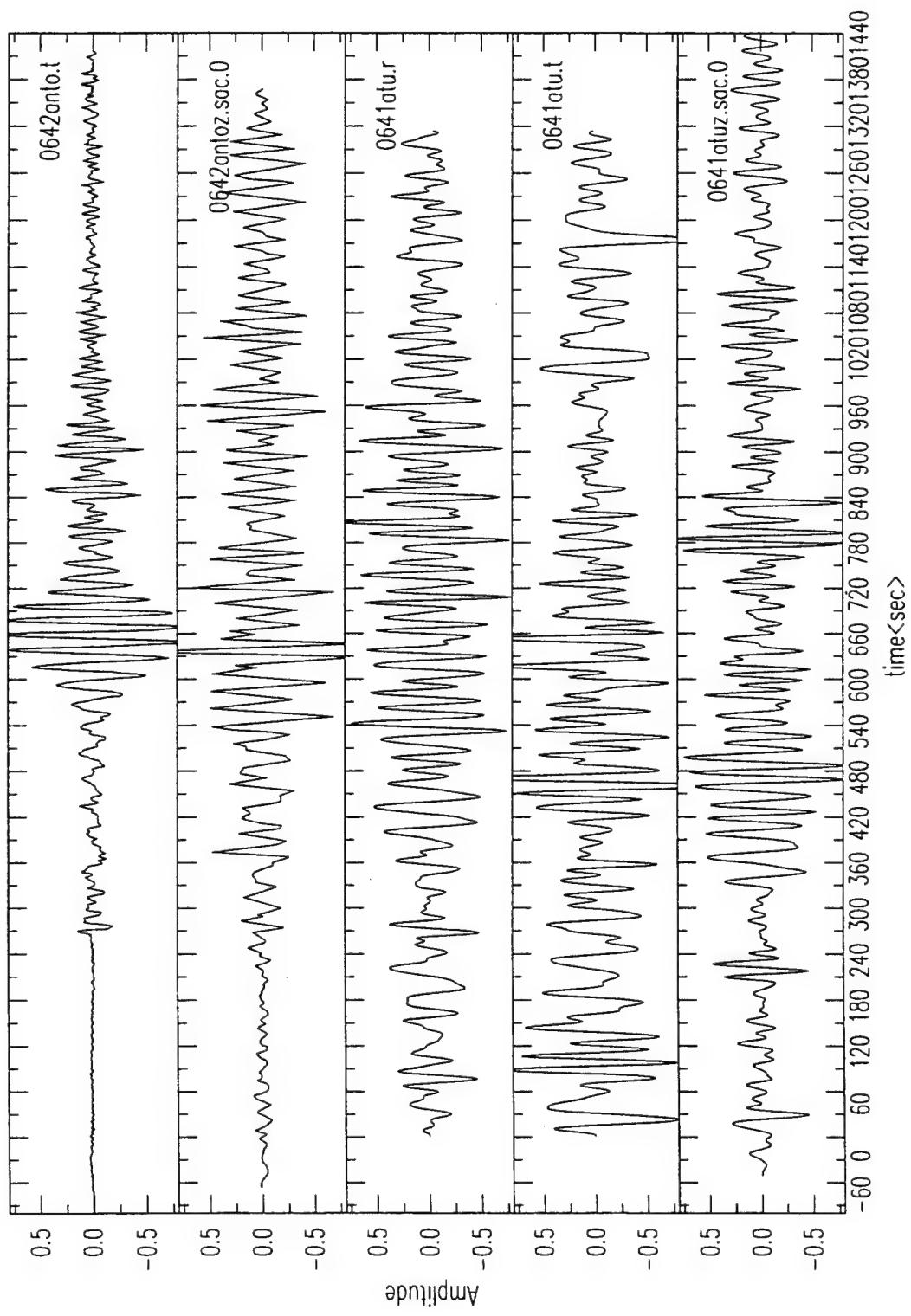
Figure C20. Seismograms of El Asnam aftershocks, October 13, 1980.

49
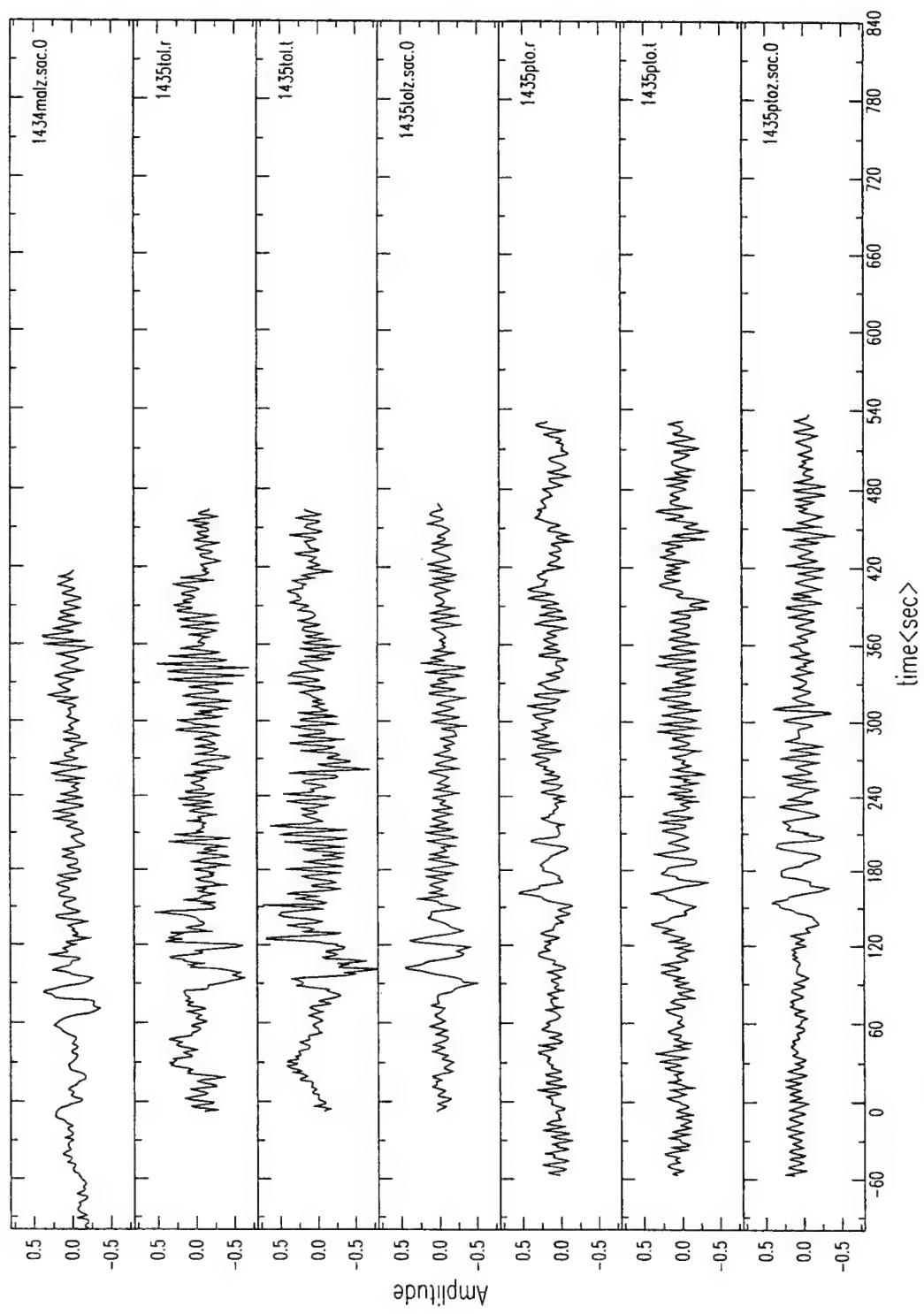
Figure C21. Seismograms of El Asnam aftershocks, October 13, 1980.

50
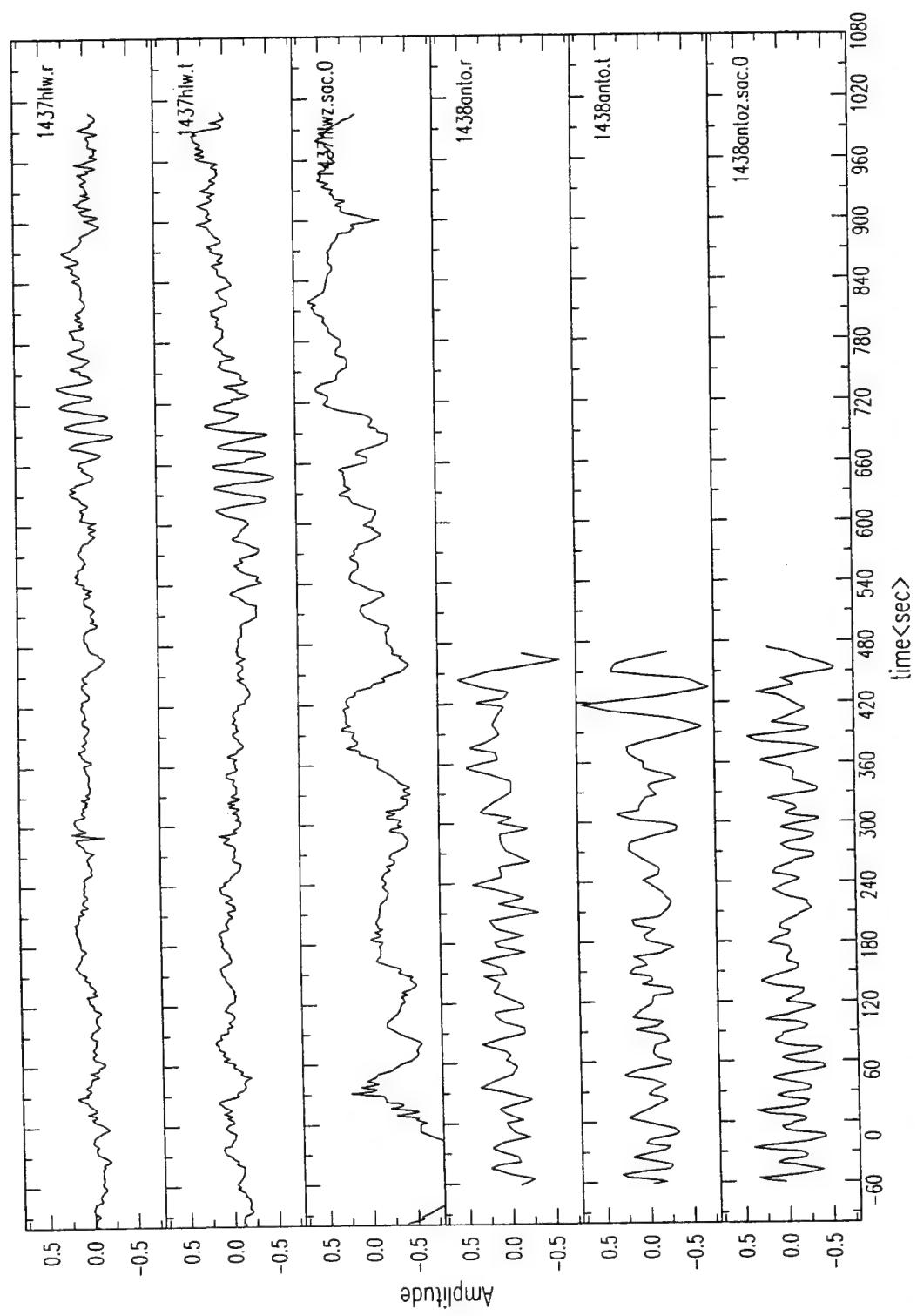
Figure C22. Seismograms of El Asnam aftershocks, October 13, 1980.
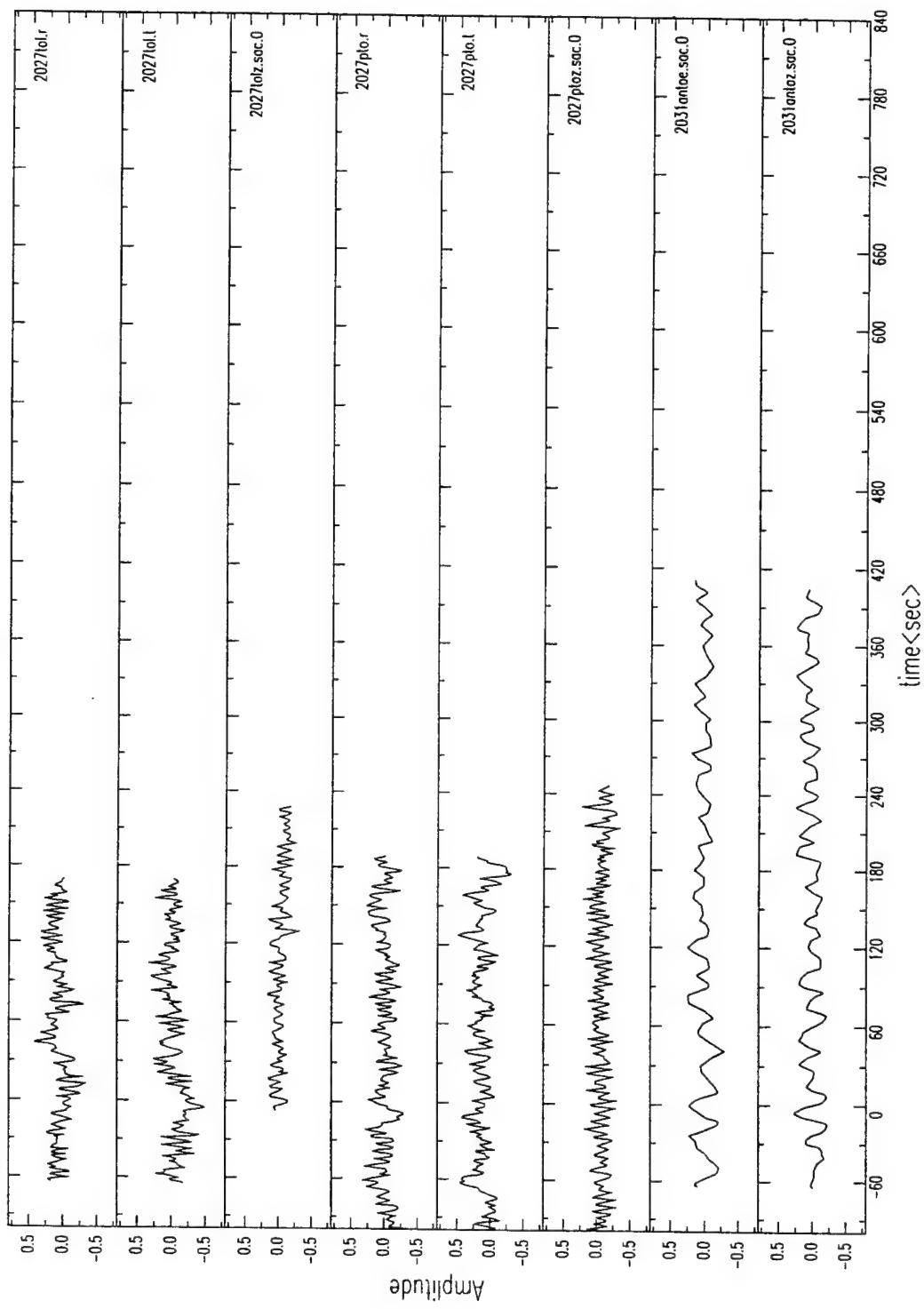
Figure C23. Seismograms of El Asnam aftershocks, October 13, 1980.
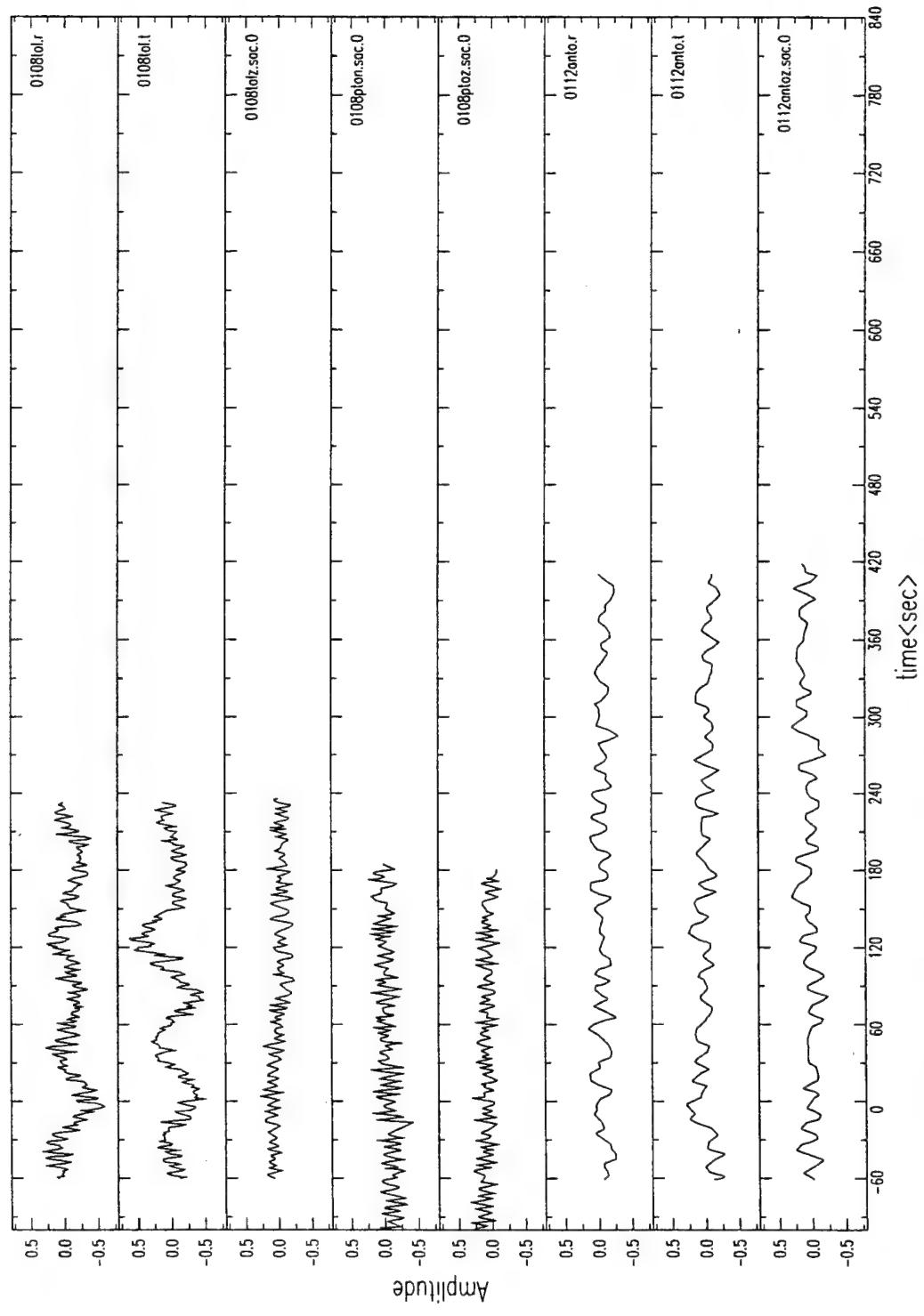
Figure C24. Seismograms of El Asnam aftershocks, October 14, 1980.

53
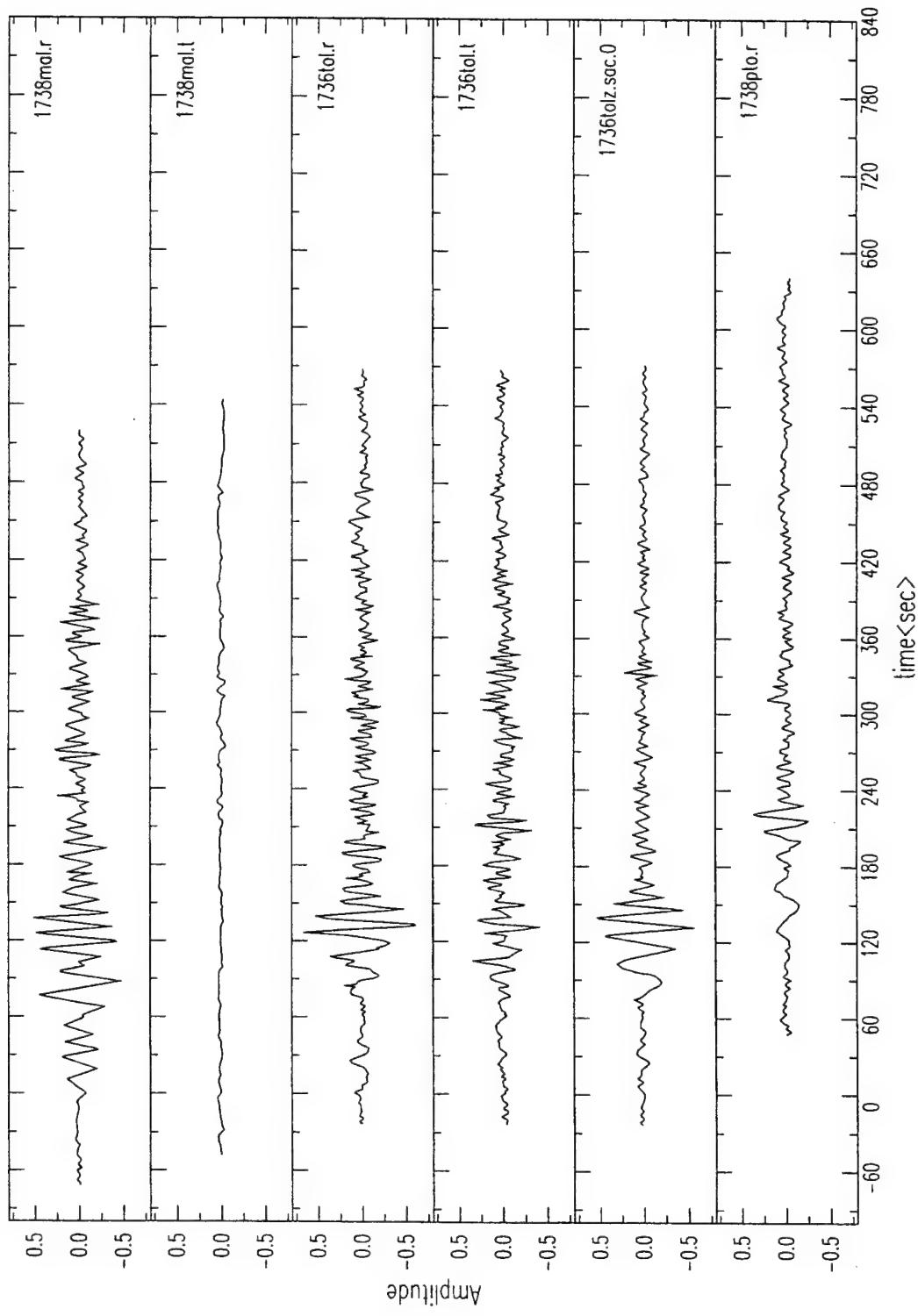
Figure C25. Seismograms of El Asnam aftershocks, October 14, 1980.

54
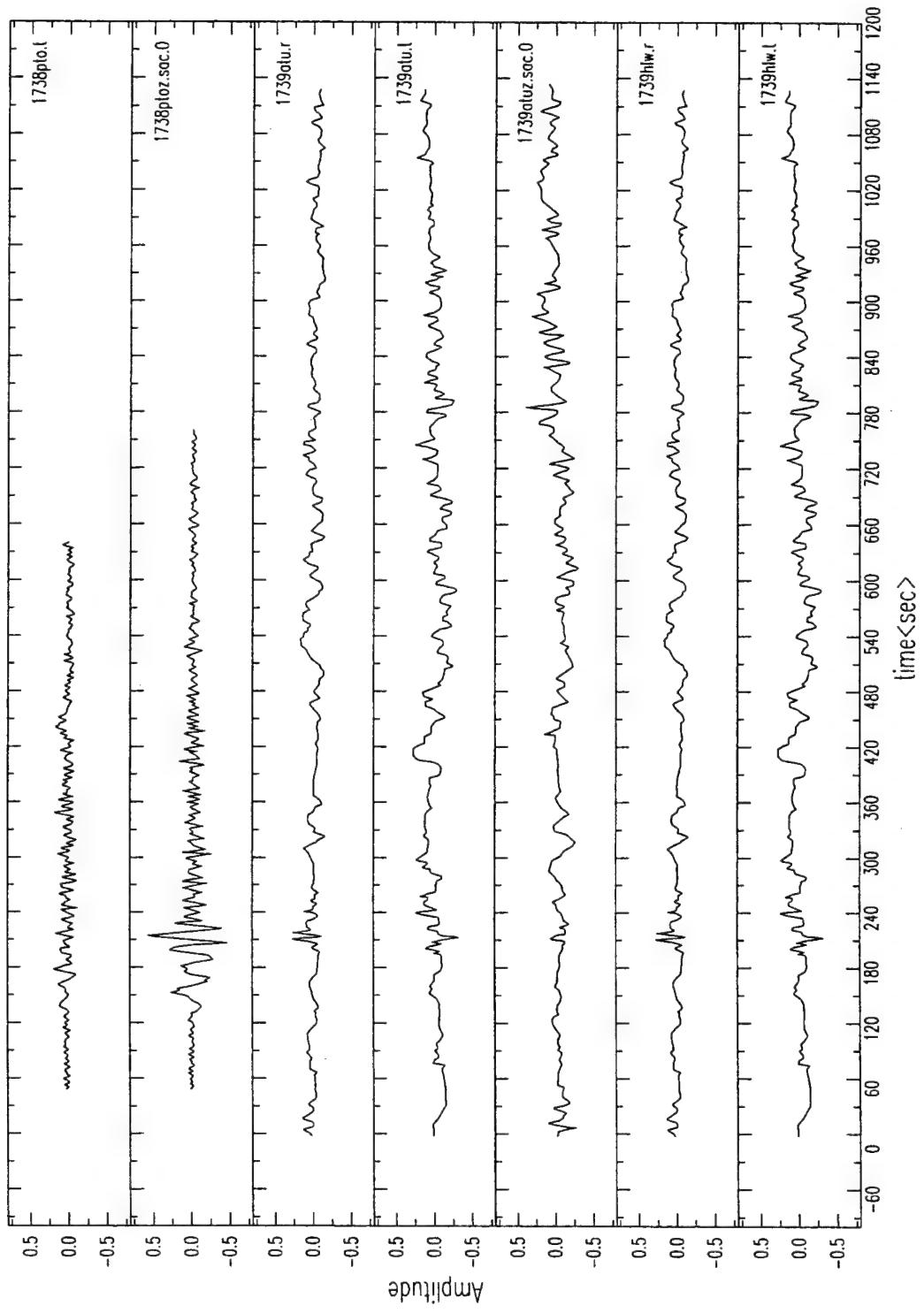
Figure C26. Seismograms of El Asnam aftershocks, October 14, 1980.
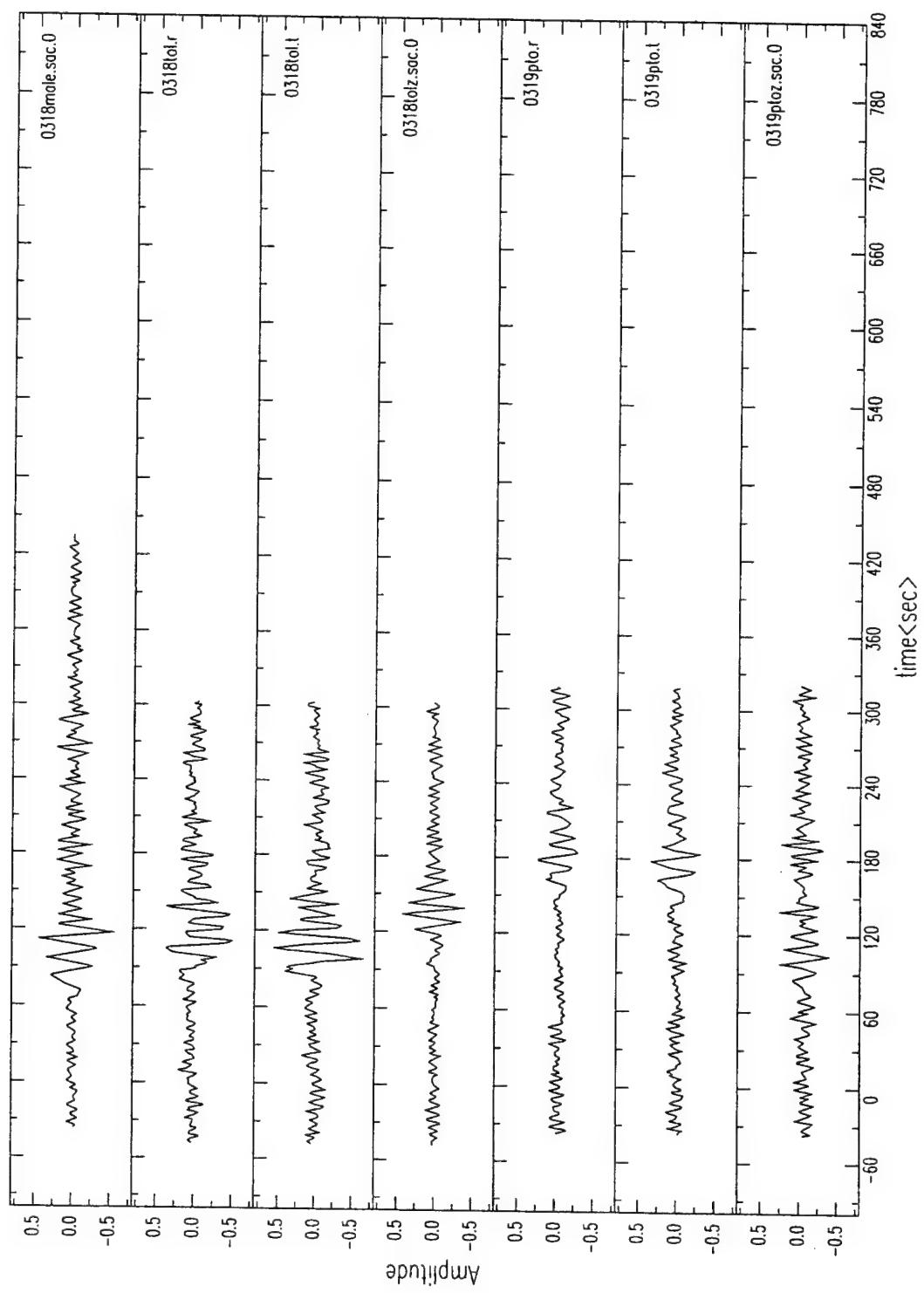
Figure C27. Seismograms of El Asnam aftershocks, October 15, 1980.
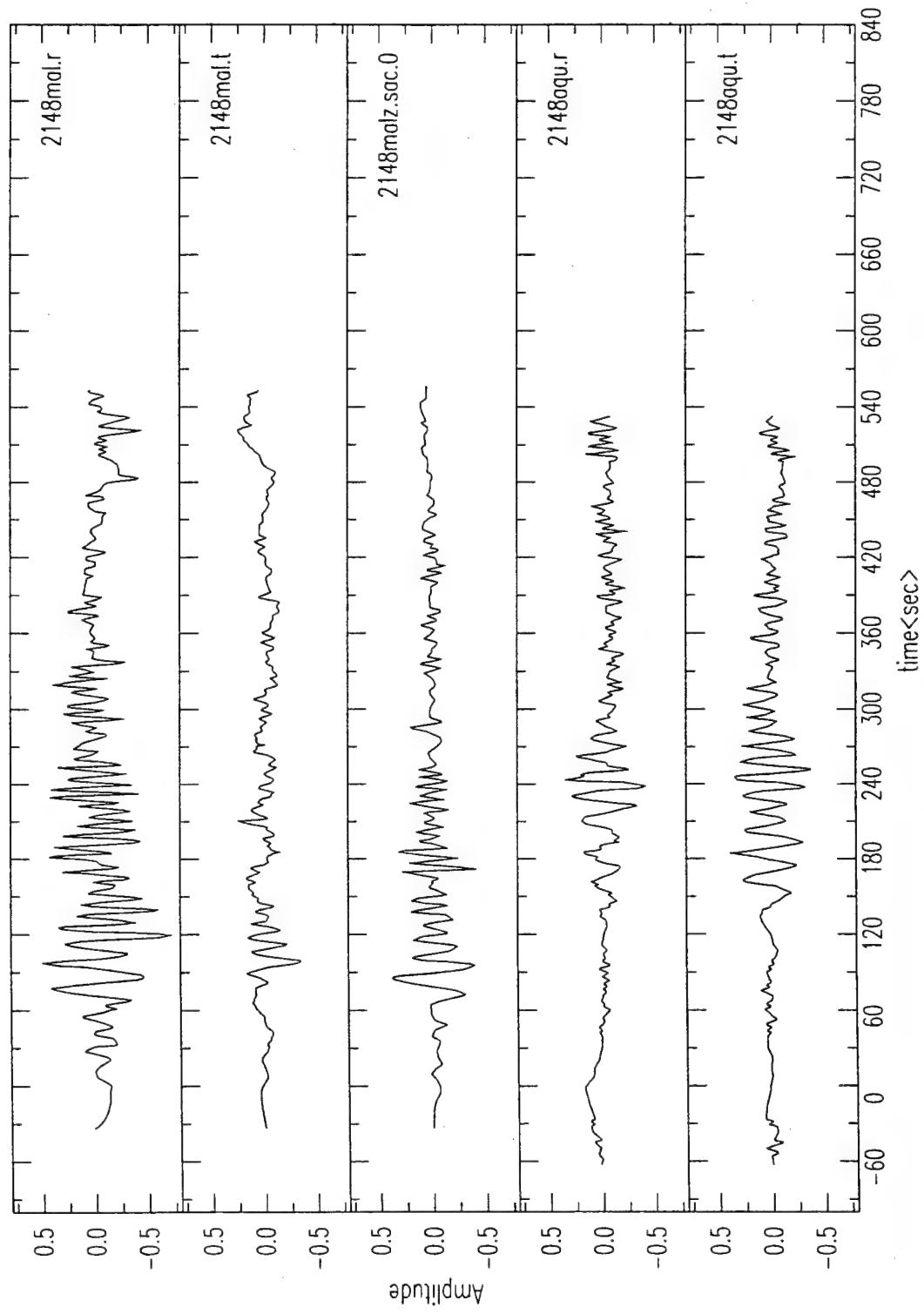
Figure C28. Seismograms of El Asnam aftershocks, October 19, 1980.
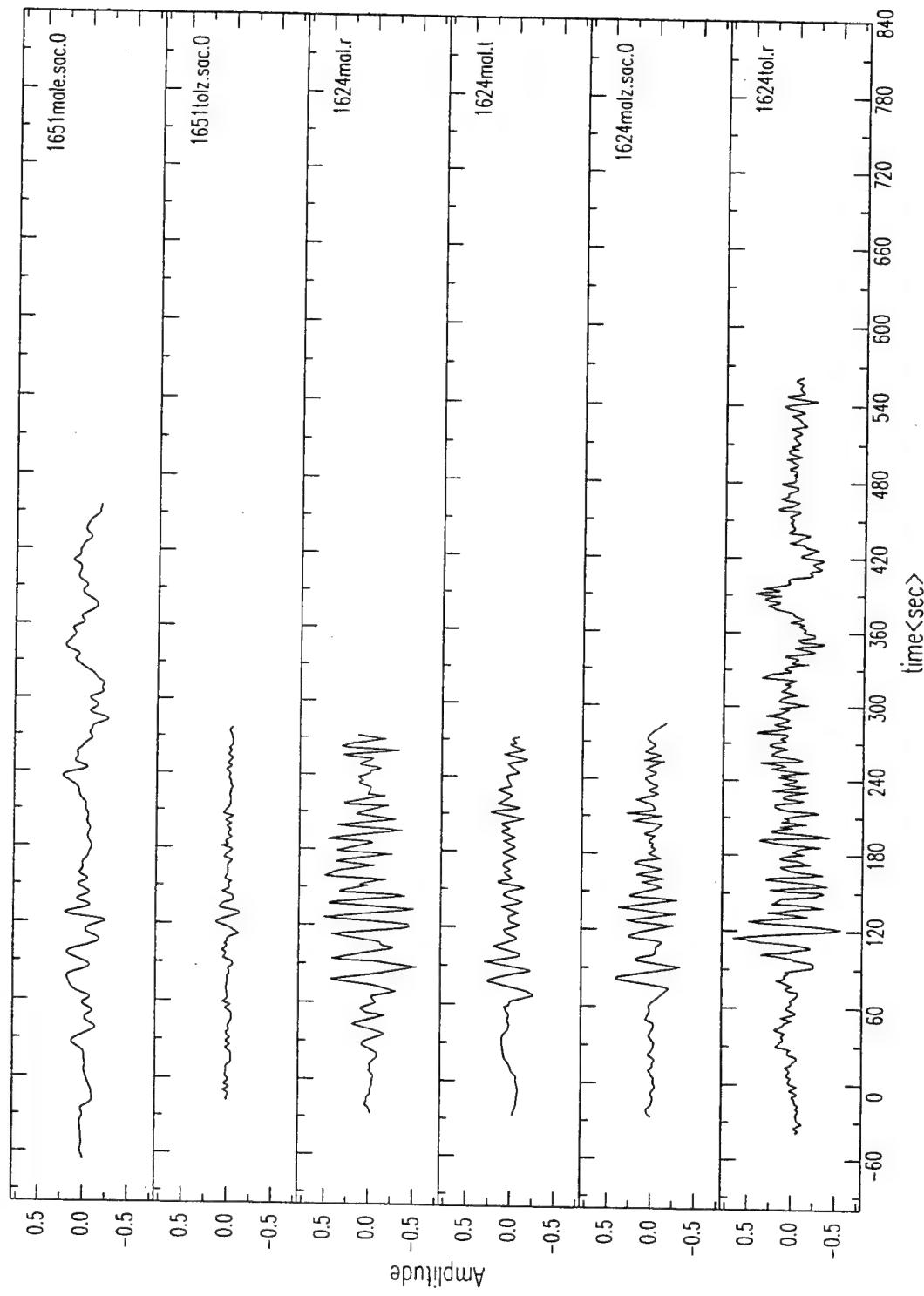
Figure C29. Seismograms of El Asnam aftershocks, October 21 (1651) and October 22 (1624), 1980.
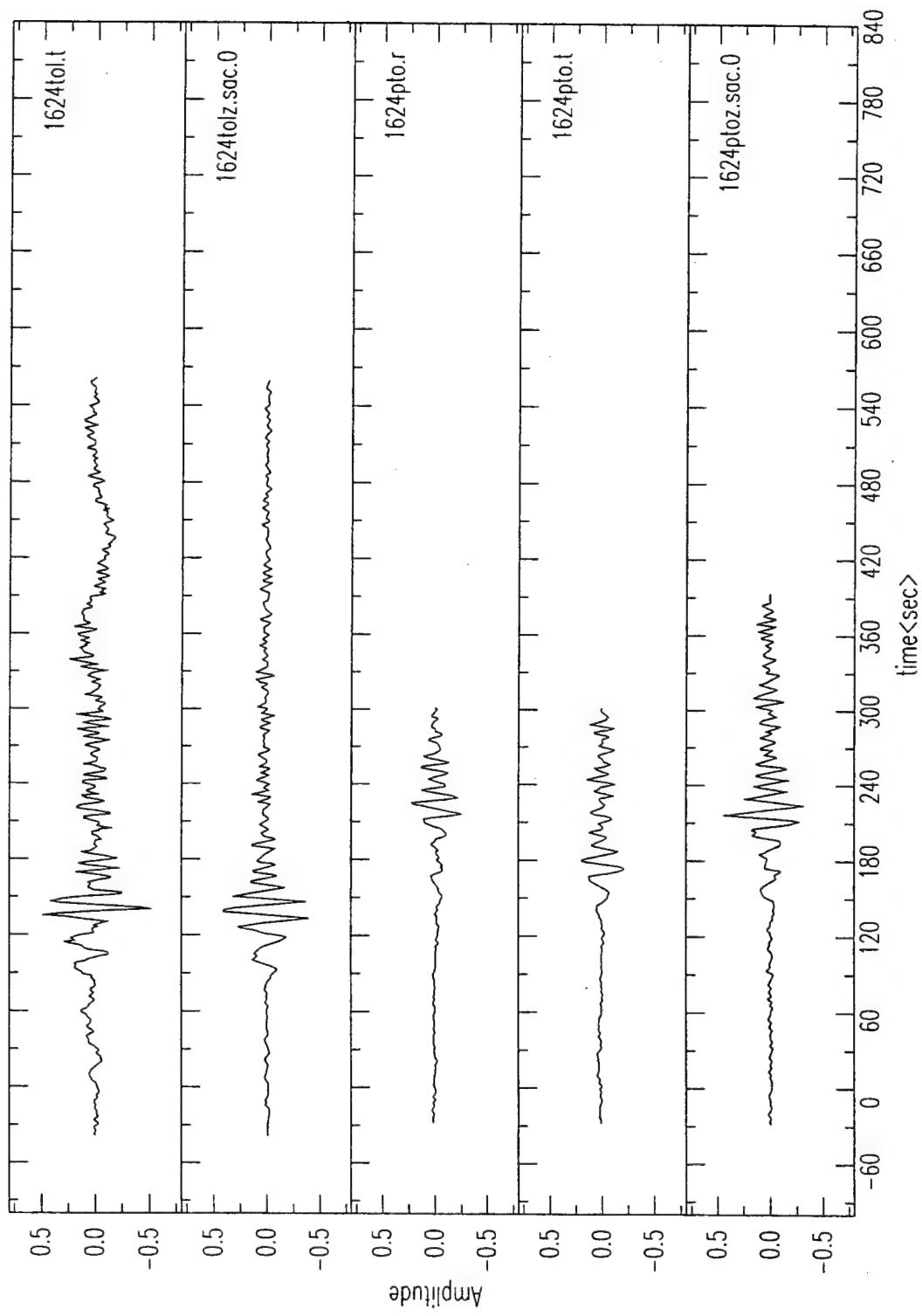
Figure C30. Seismograms of El Asnam aftershocks, October 22, 1980.
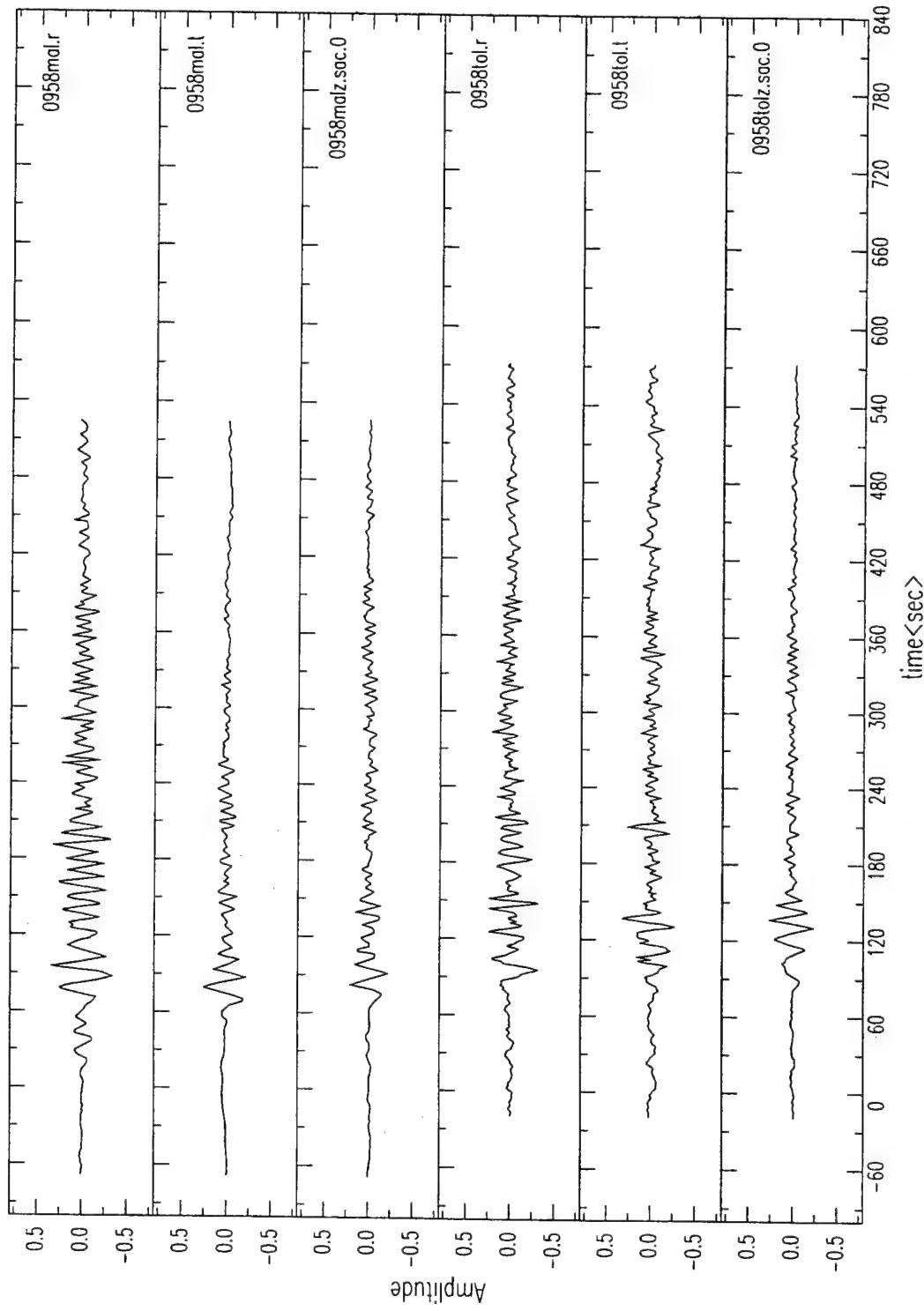
Figure C31. Seismograms of El Asnam aftershocks, October 23, 1980.

60
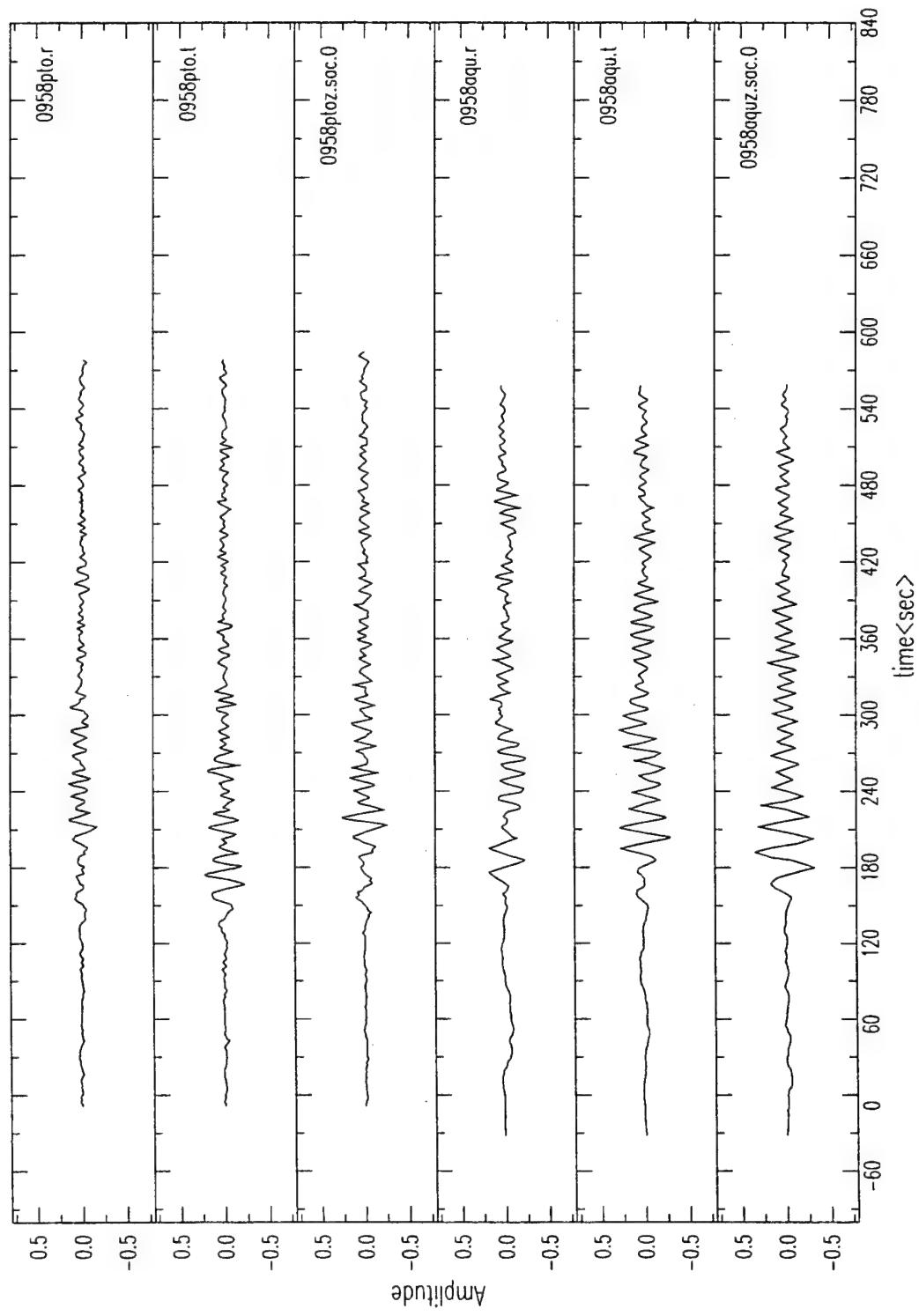
Figure C32. Seismograms of El Asnam aftershocks, October 23, 1980.

61
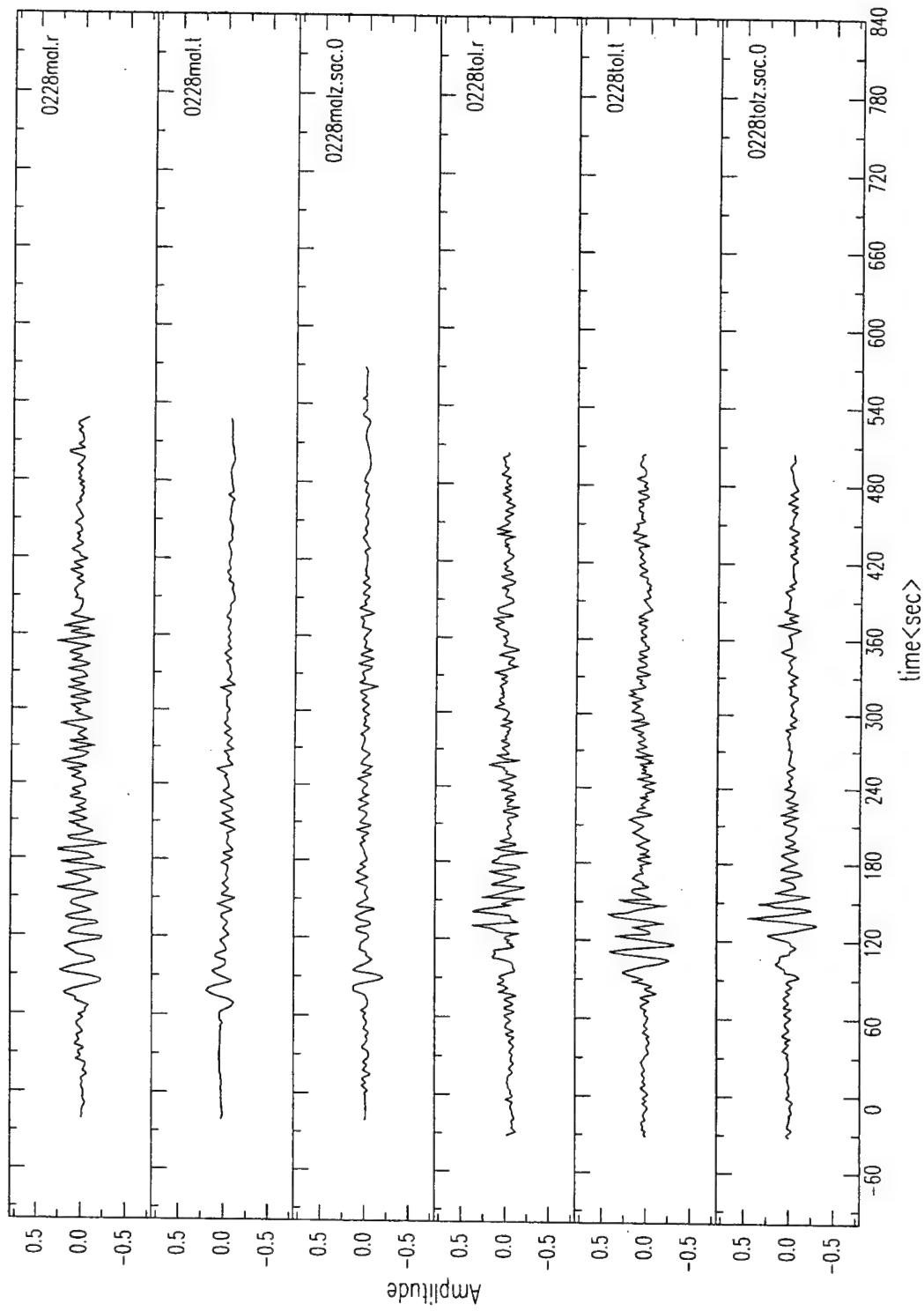
Figure C33. Seismograms of El Asnam aftershocks, October 26, 1980.

62
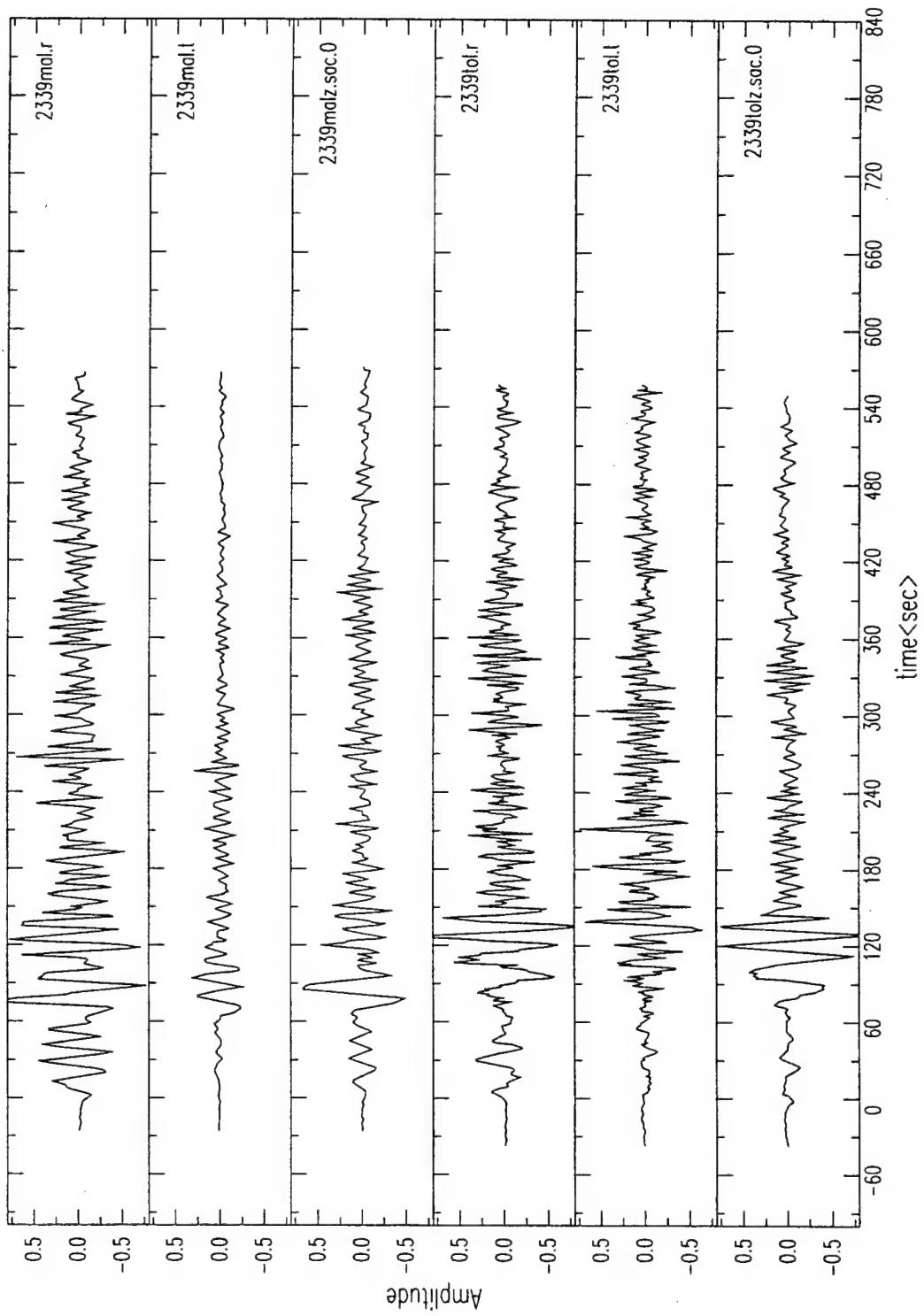
Figure C34. Seismograms of El Asnam aftershocks, October 30, 1980.
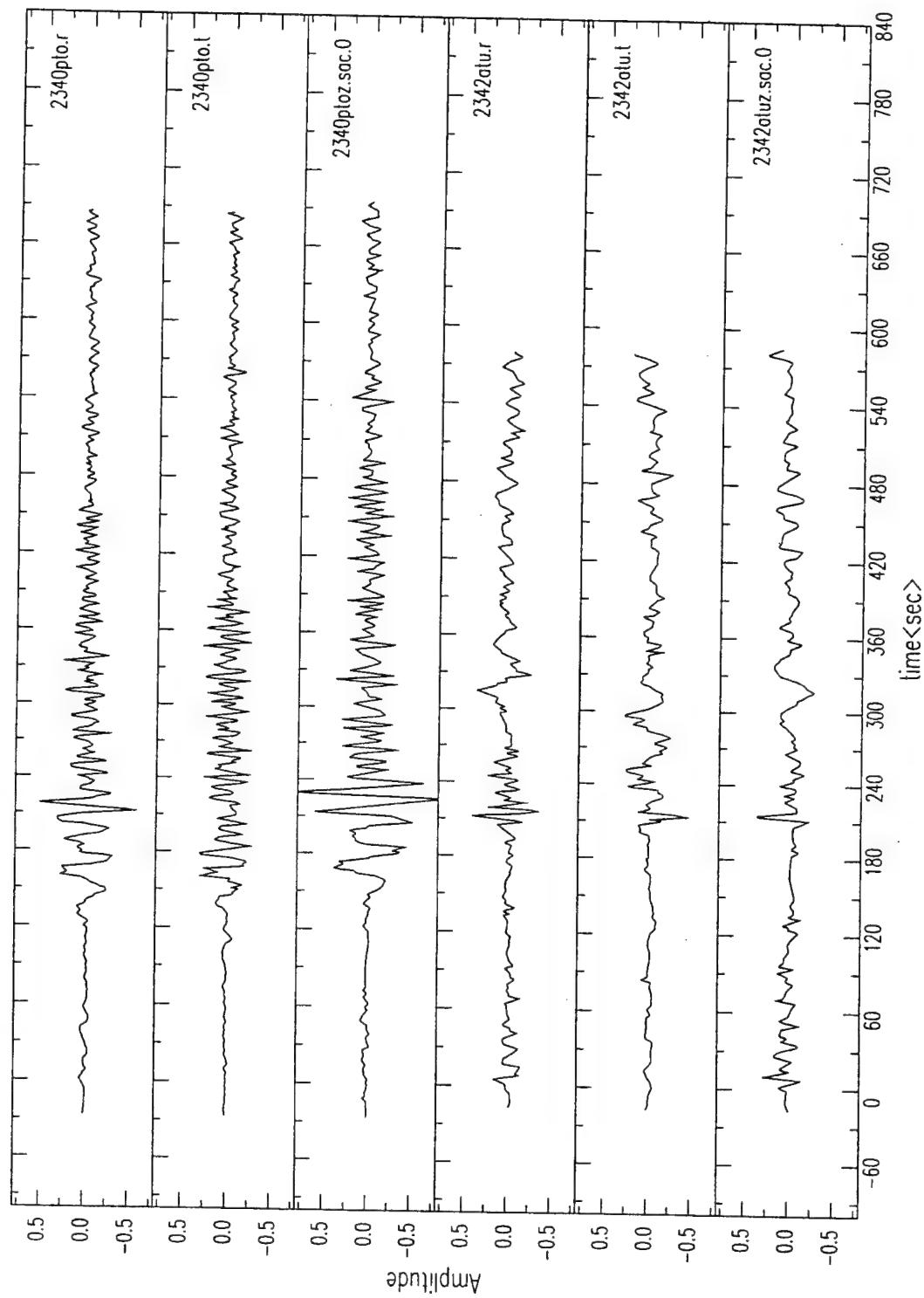
Figure C35. Seismograms of El Asnam aftershocks, October 30, 1980.

64
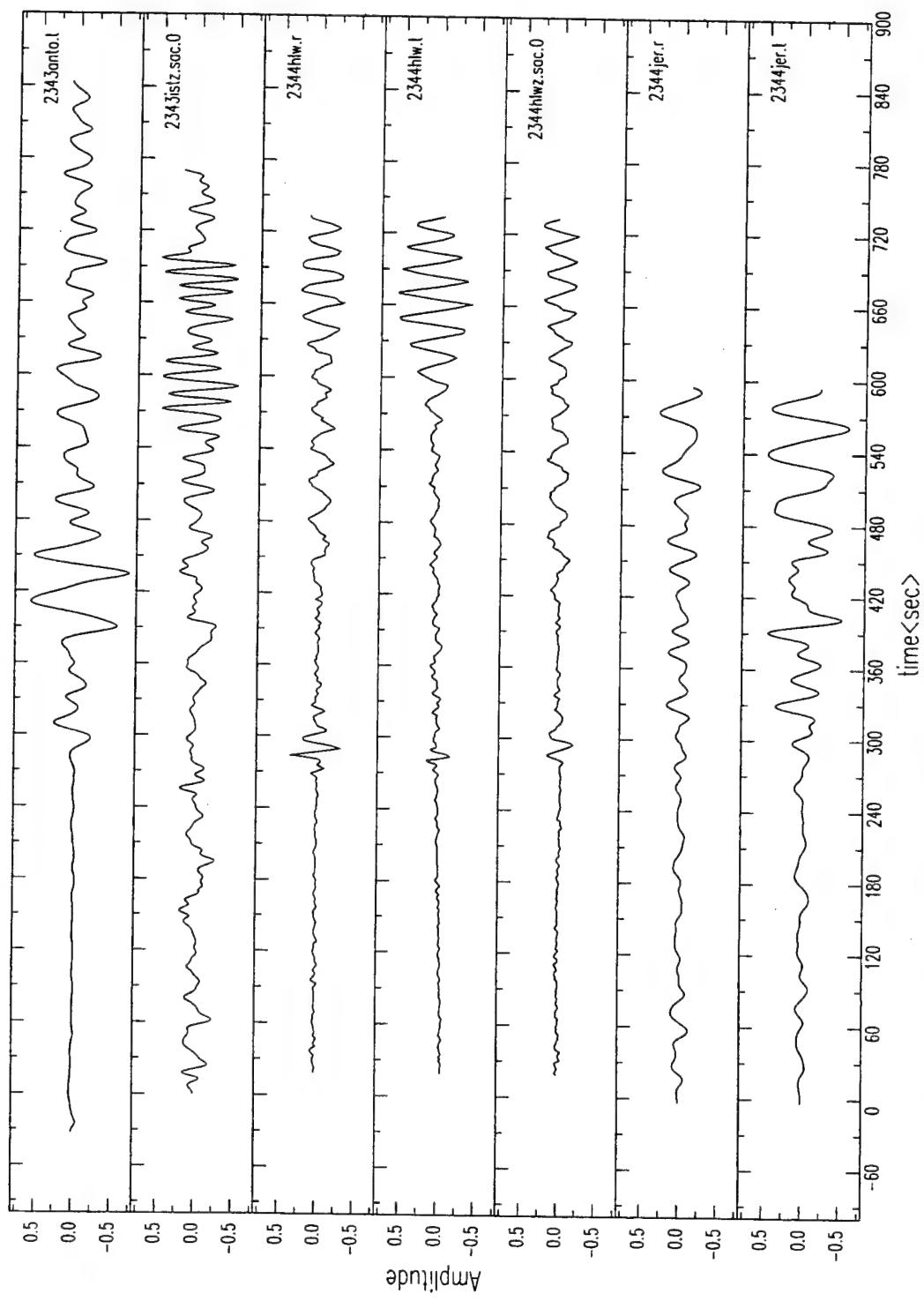
Figure C36. Seismograms of El Asnam aftershocks, October 30, 1980.

65
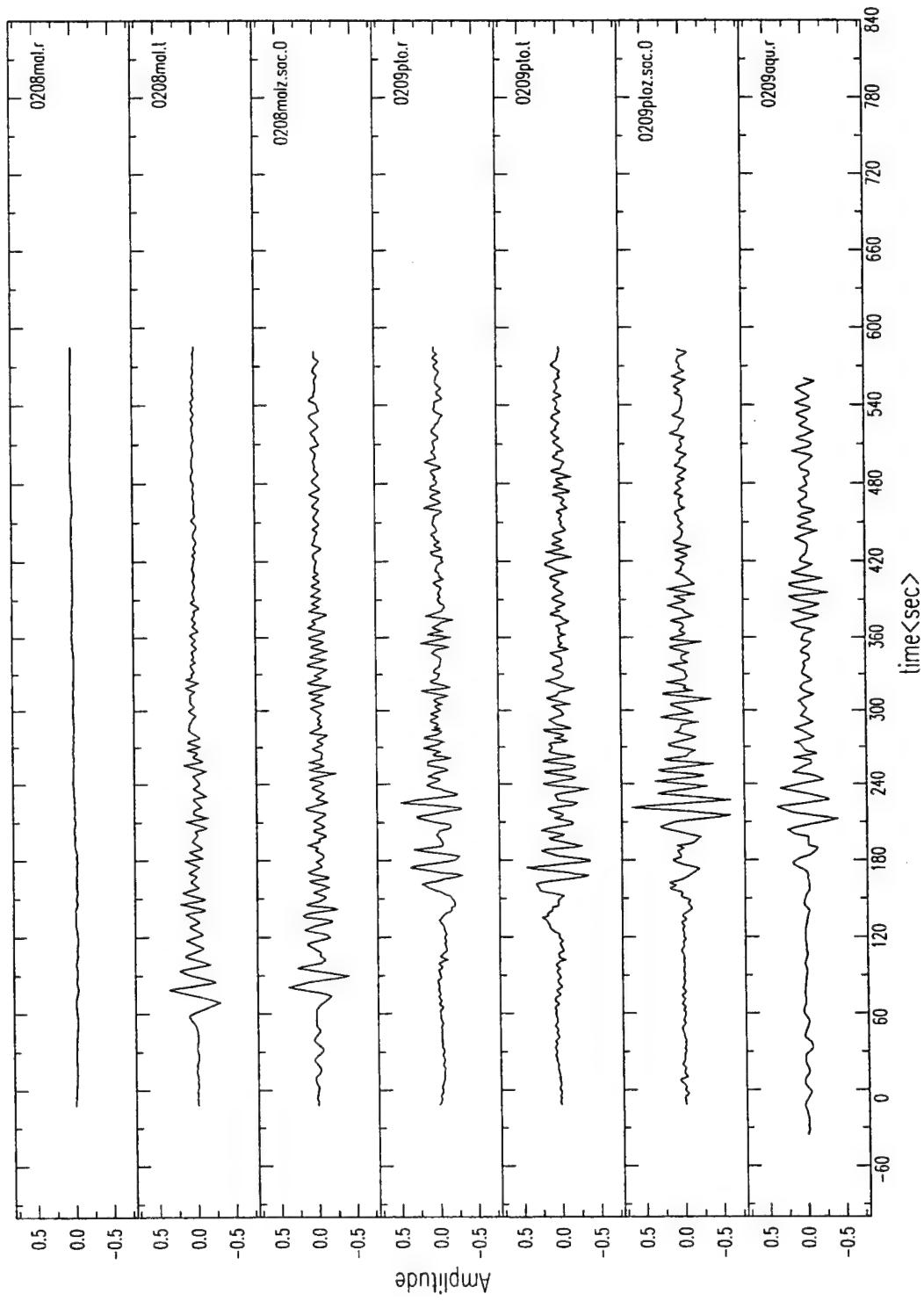
Figure C37. Seismograms of El Asnam aftershocks, November 8, 1980.
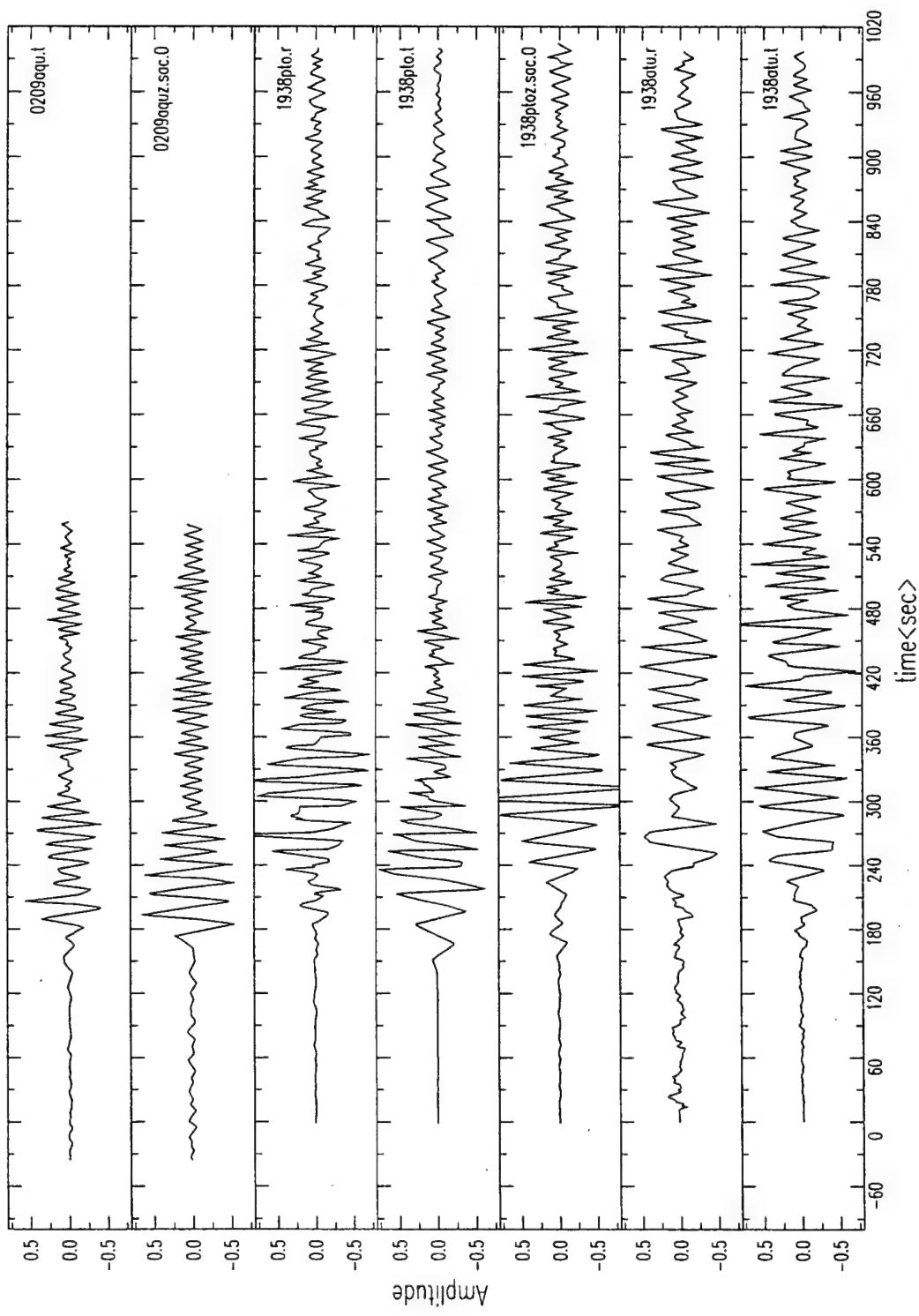
Figure C38. Seismograms of El Asnam aftershocks, November 8 (0209), 1980 and of Constantine aftershocks, October 27, 1985 (1938).
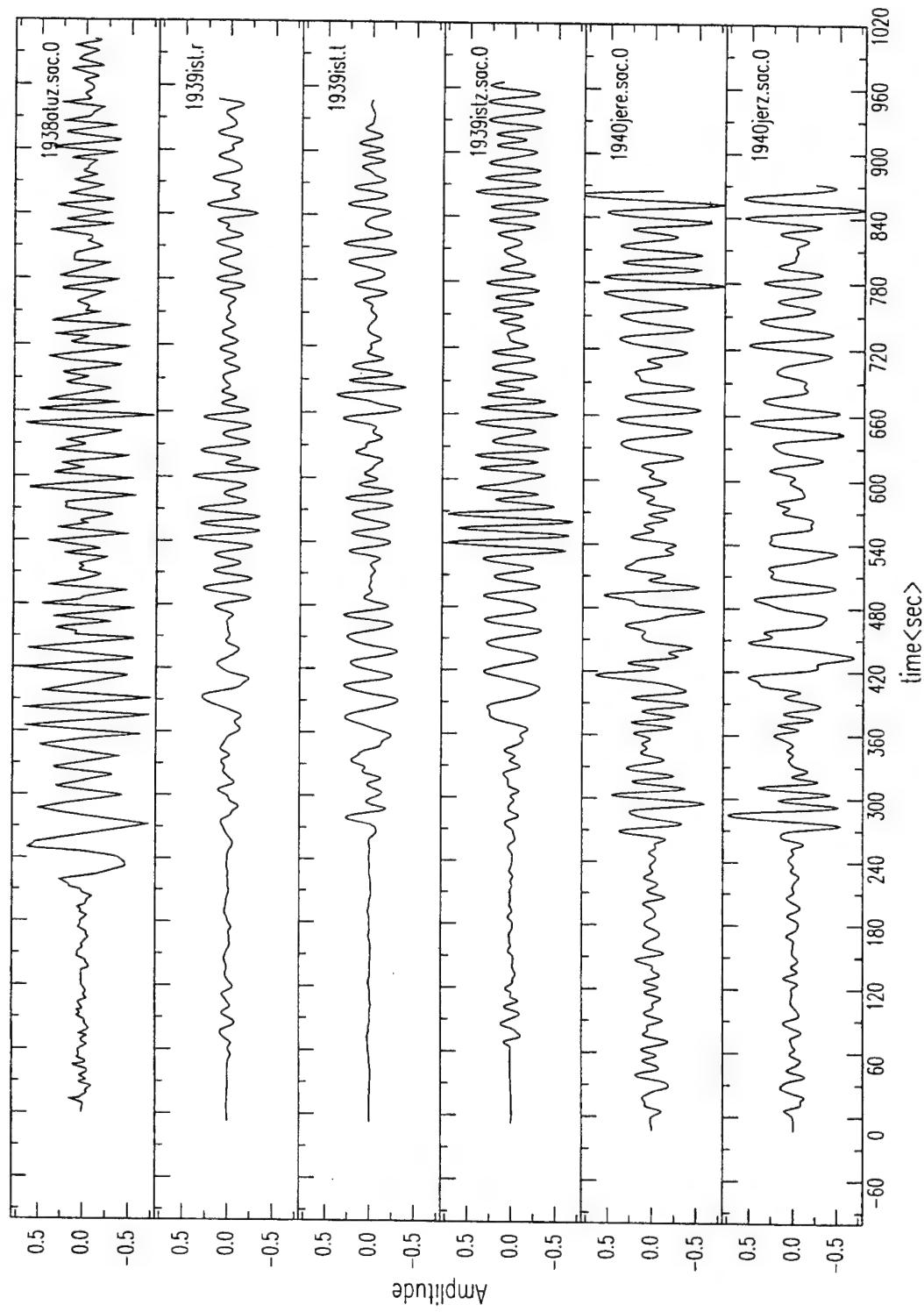
Figure C39. Seismograms of Constantine aftershocks, October 27, 1985.

68
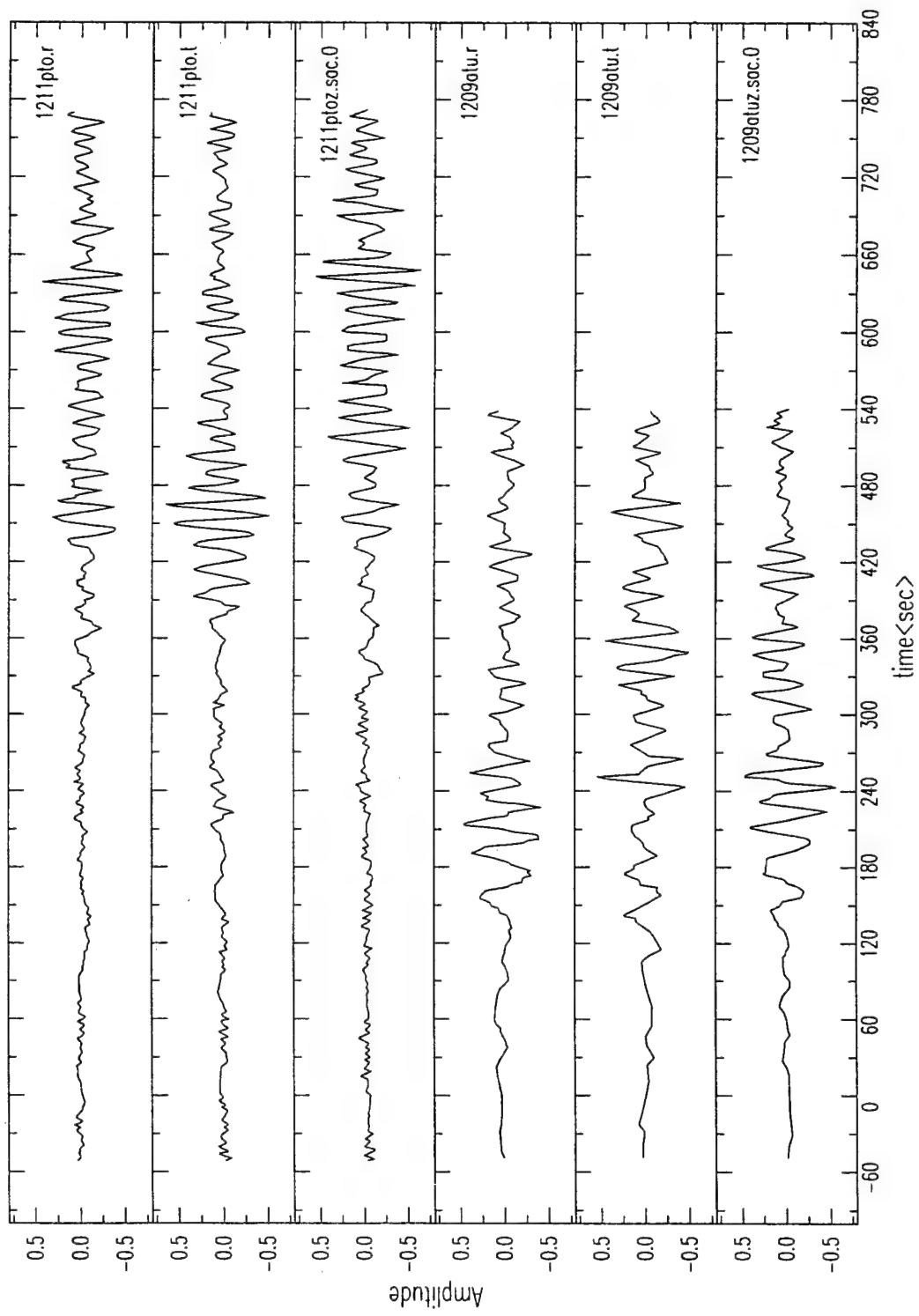
Figure C40. Seismograms of Gulf of Sirt earthquake, March 26, 1988.

THOMAS AHRENS
SEISMOLOGICAL LABORATORY 252-21
CALIFORNIA INSTITUTE OF TECHNOLOGY
PASADENA, CA 91125

AIR FORCE RESEARCH LABORATORY
ATTN: VSOE
29 RANDOLPH ROAD
HANSCOM AFB, MA 01731-3010   (2 COPIES)

AIR FORCE RESEARCH LABORATORY
ATTN: RESEARCH LIBRARY/TL
5 WRIGHT STREET
HANSCOM AFB, MA 01731-3004

AIR FORCE RESEARCH LABORATORY
ATTN: AFRL/SUL
3550 ABERDEEN AVE SE
KIRTLAND AFB, NM 87117-5776 (2 COPIES)

RALPH ALEWINE
NTPO
1901 N. MOORE STREET, SUITE 609
ARLINGTON, VA 22209

MUAWIA BARAZANGI
INSTITUTE FOR THE STUDY OF THE CONTINENTS
3126 SNEE HALL
CORNELL UNIVERSITY
ITHACA, NY 14853

T.G. BARKER
MAXWELL TECHNOLOGIES
8888 BALBOA AVE.
SAN DIEGO, CA 92123-1506

DOUGLAS BAUMGARDT
ENSCO INC.
5400 PORT ROYAL ROAD
SPRINGFIELD, VA 22151

THERON J. BENNETT
MAXWELL TECHNOLOGIES
11800 SUNRISE VALLEY DRIVE SUITE 1212
RESTON, VA 22091

WILLIAM BENSON
NAS/COS
ROOM HA372
2001 WISCONSIN AVE. NW
WASHINGTON DC 20007

JONATHAN BERGER
UNIVERSITY OF CA, SAN DIEGO
SCRIPPS INSTITUTION OF OCEANOGRAPHY IGPP, 0225
9500 GILMAN DRIVE
LA JOLLA, CA 92093-0225

ROBERT BLANDFORD
AFTAC
1300 N. 17TH STREET
SUITE 1450
ARLINGTON, VA 22209-2308

LESLIE A. CASEY
DEPT. OF ENERGY/NN-20
1000 INDEPENDENCE AVE. SW
WASHINGTON DC 20585-0420

CENTER FOR MONITORING RESEARCH
ATTN: LIBRARIAN
1300 N. 17th STREET, SUITE 1450
ARLINGTON, VA 22209

ANTON DAINTY
HQ DSWA/PMP
6801 TELEGRAPH ROAD
ALEXANDRIA, VA 22310-3398

CATHERINE DE GROOT-HEDLIN
UNIVERSITY OF CALIFORNIA, SAN DIEGO
INSTITUTE OF GEOPHYSICS AND PLANETARY PHYSICS
8604 LA JOLLA SHORES DRIVE
SAN DIEGO, CA 92093

DEFENSE TECHNICAL INFORMATION CENTER
8725 JOHN J. KINGMAN ROAD
FT BELVOIR, VA 22060-6218 (2 COPIES)

DIANE DOSER
DEPARTMENT OF GEOLOGICAL SCIENCES
THE UNIVERSITY OF TEXAS AT EL PASO
EL PASO, TX 79968

MARK D. FISK
MISSION RESEARCH CORPORATION
735 STATE STREET
P.O. DRAWER 719
SANTA BARBARA, CA 93102-0719

LORI GRANT
MULTIMAX, INC.
311C FOREST AVE. SUITE 3
PACIFIC GROVE, CA 93950

HENRY GRAY
SMU STATISTICS DEPARTMENT
P.O. BOX 750302
DALLAS, TX 75275-0302

I. N. GUPTA
MULTIMAX, INC.
1441 MCCORMICK DRIVE
LARGO, MD 20774

DAVID HARKRIDER
BOSTON COLLEGE
INSTITUTE FOR SPACE RESEARCH
140 COMMONWEALTH AVENUE
CHESTNUT HILL, MA 02167

THOMAS HEARN
NEW MEXICO STATE UNIVERSITY
DEPARTMENT OF PHYSICS
LAS CRUCES, NM 88003

MICHAEL HEDLIN
UNIVERSITY OF CALIFORNIA, SAN DIEGO
SCRIPPS INSTITUTION OF OCEANOGRAPHY IGPP, 0225
9500 GILMAN DRIVE
LA JOLLA, CA 92093-0225

DONALD HELMBERGER
CALIFORNIA INSTITUTE OF TECHNOLOGY
DIVISION OF GEOLOGICAL & PLANETARY SCIENCES
SEISMOLOGICAL LABORATORY
PASADENA, CA 91125

EUGENE HERRIN
SOUTHERN METHODIST UNIVERSITY
DEPARTMENT OF GEOLOGICAL SCIENCES
DALLAS, TX 75275-0395

ROBERT HERRMANN
ST. LOUIS UNIVERSITY
DEPARTMENT OF EARTH & ATMOSPHERIC SCIENCES
3507 LACLEDE AVENUE
ST. LOUIS, MO 63103

VINDELL HSU
HQ/AFTAC/TTR
1030 S. HIGHWAY A1A
PATRICK AFB, FL 32925-3002

RONG-SONG JIH
HQ DSWA/PMP/CTBT
6801 TELEGRAPH ROAD
ALEXANDRIA, VA 22310-3398

THOMAS JORDAN
MASSACHUSETTS INSTITUTE OF TECHNOLOGY
EARTH, ATMOSPHERIC & PLANETARY SCIENCES
77 MASSACHUSETTS AVENUE, 54-918
CAMBRIDGE, MA 02139

LAWRENCE LIVERMORE NATIONAL LABORATORY
ATTN: TECHNICAL STAFF (PLS ROUTE)
PO BOX 808, MS L-175
LIVERMORE, CA 94551

LAWRENCE LIVERMORE NATIONAL LABORATORY
ATTN: TECHNICAL STAFF (PLS ROUTE)
PO BOX 808, MS L-208
LIVERMORE, CA 94551

LAWRENCE LIVERMORE NATIONAL LABORATORY
ATTN: TECHNICAL STAFF (PLS ROUTE)
PO BOX 808, MS L-202
LIVERMORE, CA 94551

LAWRENCE LIVERMORE NATIONAL LABORATORY
ATTN: TECHNICAL STAFF (PLS ROUTE)
PO BOX 808, MS L-195
LIVERMORE, CA 94551

LAWRENCE LIVERMORE NATIONAL LABORATORY
ATTN: TECHNICAL STAFF (PLS ROUTE)
PO BOX 808, MS L-205
LIVERMORE, CA 94551

LAWRENCE LIVERMORE NAT'L LABORATORY
ATTN: TECHNICAL STAFF (PLS ROUTE)
PO BOX 808, MS L-200
LIVERMORE, CA 94551

LAWRENCE LIVERMORE NAT'L LABORATORY
ATTN: TECHNICAL STAFF (PLS ROUTE)
PO BOX 808, MS L-221
LIVERMORE, CA 94551

THORNE LAY
UNIVERSITY OF CALIFORNIA, SANTA CRUZ
EARTH SCIENCES DEPARTMENT
EARTH & MARINE SCIENCE BUILDING
SANTA CRUZ, CA 95064

2

ANATOLI L. LEVSHIN
DEPARTMENT OF PHYSICS
UNIVERSITY OF COLORADO
CAMPUS BOX 390
BOULDER, CO 80309-0309

JAMES LEWKOWICZ
WESTON GEOPHYSICAL CORP.
325 WEST MAIN STREET
NORTHBORO, MA 01532

LOS ALAMOS NATIONAL LABORATORY
ATTN: TECHNICAL STAFF (PLS ROUTE)
PO BOX 1663, MS F659
LOS ALAMOS, NM 87545

LOS ALAMOS NATIONAL LABORATORY
ATTN: TECHNICAL STAFF (PLS ROUTE)
PO BOX 1663, MS F665
LOS ALAMOS, NM 87545

LOS ALAMOS NATIONAL LABORATORY
ATTN: TECHNICAL STAFF (PLS ROUTE)
PO BOX 1663, MS D460
LOS ALAMOS, NM 87545

LOS ALAMOS NATIONAL LABORATORY
ATTN: TECHNICAL STAFF (PLS ROUTE)
PO BOX 1663, MS C335
LOS ALAMOS, NM 87545

GARY MCCARTOR
SOUTHERN METHODIST UNIVERSITY
DEPARTMENT OF PHYSICS
DALLAS, TX 75275-0395

KEITH MCLAUGHLIN
MAXWELL TECHNOLOGIES
8888 BALBOA AVE.
SAN DIEGO, CA 92123-1506

BRIAN MITCHELL
DEPARTMENT OF EARTH & ATMOSPHERIC SCIENCES
ST. LOUIS UNIVERSITY
3507 LACLEDE AVENUE
ST. LOUIS, MO 63103

RICHARD MORROW
USACDA/IVI
320 21ST STREET, N.W.
WASHINGTON DC 20451

JOHN MURPHY
MAXWELL TECHNOLOGIES
11800 SUNRISE VALLEY DRIVE SUITE 1212
RESTON, VA 22091

JAMES NI
NEW MEXICO STATE UNIVERSITY
DEPARTMENT OF PHYSICS
LAS CRUCES, NM 88003

ROBERT NORTH
CENTER FOR MONITORING RESEARCH
1300 N. 17th STREET, SUITE 1450
ARLINGTON, VA 22209

OFFICE OF THE SECRETARY OF DEFENSE
DDR&E
WASHINGTON DC 20330

JOHN ORCUTT
INSTITUTE OF GEOPHYSICS AND PLANETARY PHYSICS
UNIVERSITY OF CALIFORNIA, SAN DIEGO
LA JOLLA, CA 92093

PACIFIC NORTHWEST NATIONAL LABORATORY
ATTN: TECHNICAL STAFF (PLS ROUTE)
PO BOX 999, MS K6-48
RICHLAND, WA 99352

PACIFIC NORTHWEST NATIONAL LABORATORY
ATTN: TECHNICAL STAFF (PLS ROUTE)
PO BOX 999, MS K6-40
RICHLAND, WA 99352

PACIFIC NORTHWEST NATIONAL LABORATORY
ATTN: TECHNICAL STAFF (PLS ROUTE)
PO BOX 999, MS K6-84
RICHLAND, WA 99352

PACIFIC NORTHWEST NATIONAL LABORATORY
ATTN: TECHNICAL STAFF (PLS ROUTE)
PO BOX 999, MS K5-12
RICHLAND, WA 99352

FRANK PILOTTE
HQ AFTAC/TT
1030 S. HIGHWAY A1A
PATRICK AFB, FL 32925-3002

KEITH PRIESTLEY
DEPARTMENT OF EARTH SCIENCES
UNIVERSITY OF CAMBRIDGE
MADINGLEY RISE, MADINGLEY ROAD
CAMBRIDGE, CB3 OEZ UK

JAY PULLI
BBN
1300 NORTH 17TH STREET
ROSSLYN, VA 22209

DELAINE REITER
SENCOM CORP.
73 STANDISH ROAD
WATERTOWN, MA 02172

PAUL RICHARDS
COLUMBIA UNIVERSITY
LAMONT-DOHERTY EARTH OBSERVATORY
PALISADES, NY 10964

MICHAEL RITZWOLLER
DEPARTMENT OF PHYSICS
UNIVERSITY OF COLORADO
CAMPUS BOX 390
BOULDER, CO 80309-0309

DAVID RUSSELL
HQ AFTAC/TTR
1030 SOUTH HIGHWAY A1A
PATRICK AFB, FL 32925-3002

CHANDAN SAIKIA
WOOODWARD-CLYDE FEDERAL SERVICES
566 EL DORADO ST., SUITE 100
PASADENA, CA 91101-2560

SANDIA NATIONAL LABORATORY
ATTN: TECHNICAL STAFF (PLS ROUTE)
DEPT. 5704
MS 0979, PO BOX 5800
ALBUQUERQUE, NM 87185-0979

SANDIA NATIONAL LABORATORY
ATTN: TECHNICAL STAFF (PLS ROUTE)
DEPT. 9311
MS 1159, PO BOX 5800
ALBUQUERQUE, NM 87185-1159

SANDIA NATIONAL LABORATORY
ATTN: TECHNICAL STAFF (PLS ROUTE)
DEPT. 5704
MS 0655, PO BOX 5800
ALBUQUERQUE, NM 87185-0655

SANDIA NATIONAL LABORATORY
ATTN: TECHNICAL STAFF (PLS ROUTE)
DEPT. 5736
MS 0655, PO BOX 5800
ALBUQUERQUE, NM 87185-0655

THOMAS SERENO JR.
SCIENCE APPLICATIONS INTERNATIONAL CORPORATION
10260 CAMPUS POINT DRIVE
SAN DIEGO, CA 92121

AVI SHAPIRA
SEISMOLOGY DIVISION
THE INSTITUTE FOR PETROLEUM RESEARCH AND
GEOPHYSICS
P.O.B. 2286 NOLON 58122 ISRAEL

ROBERT SHUMWAY
410 MRAK HALL
DIVISION OF STATISTICS
UNIVERSITY OF CALIFORNIA
DAVIS, CA 95616-8671

DAVID SIMPSON
IRIS
1200 NEW YORK AVE., NW
SUITE 800
WASHINGTON DC 20005

JEFFRY STEVENS
MAXWELL TECHNOLOGIES
8888 BALBOA AVE.
SAN DIEGO, CA 92123-1506

BRIAN SULLIVAN
BOSTON COLLEGE
INSITUTE FOR SPACE RESEARCH
140 COMMONWEALTH AVENUE
CHESTNUT HILL, MA 02167

TACTEC
BATTELLE MEMORIAL INSTITUTE
505 KING AVENUE
COLUMBUS, OH 43201 (FINAL REPORT)

NAFI TOKSOZ
EARTH RESOURCES LABORATORY, M.I.T.
42 CARLTON STREET, E34-440
CAMBRIDGE, MA 02142

LAWRENCE TURNBULL
ACIS
DCI/ACIS
WASHINGTON DC 20505

GREG VAN DER VINK
IRIS
1200 NEW YORK AVE., NW
SUITE 800
WASHINGTON DC 20005

FRANK VERNON
UNIVERSITY OF CALIFORNIA, SAN DIEGO
SCRIPPS INSTITUTION OF OCEANOGRAPHY IGPP, 0225
9500 GILMAN DRIVE
LA JOLLA, CA 92093-0225

TERRY WALLACE
UNIVERSITY OF ARIZONA
DEPARTMENT OF GEOSCIENCES
BUILDING #77
TUCSON, AZ 85721

JILL WARREN
LOS ALAMOS NATIONAL LABORATORY
GROUP NIS-8
P.O. BOX 1663
LOS ALAMOS, NM 87545 (5 COPIES)

DANIEL WEILL
NSF
EAR-785
4201 WILSON BLVD., ROOM 785
ARLINGTON, VA 22230

RU SHAN WU
UNIVERSITY OF CALIFORNIA SANTA CRUZ
EARTH SCIENCES DEPT.
1156 HIGH STREET
SANTA CRUZ, CA 95064

JIAKANG XIE
COLUMBIA UNIVERSITY
LAMONT DOHERTY EARTH OBSERVATORY
ROUTE 9W
PALISADES, NY 10964

JAMES E. ZOLLWEG
BOISE STATE UNIVERSITY
GEOSCIENCES DEPT.
1910 UNIVERSITY DRIVE
BOISE, ID 83725